

→ EARTH OBSERVATION SUMMER SCHOOL

Earth System Monitoring & Modelling

Physics of Remote Sensing

Gastellu-Etchegorry Jean-Philippe
CESBIO

Paul Sabatier University, CNES, CNRS, IRD,
France

Outline

- Major remote sensing configurations and remote sensing (RS) images.
- Sun radiation reflexion: - Radiometric variables & Components of TOA radiance
- Hot spot, penumbra, 2D display of reflectance, albedo
- Thermal emission: Radiometric quantities and Components of TOA radiance
- Interpretation of VIS/IR/TIR satellite images: angular anisotropy, spectral wealth,...
- Hyperspectral remote sensing: mixels, end-members,...
- Satellite / airborne sensors with finite FOV
- LiDAR

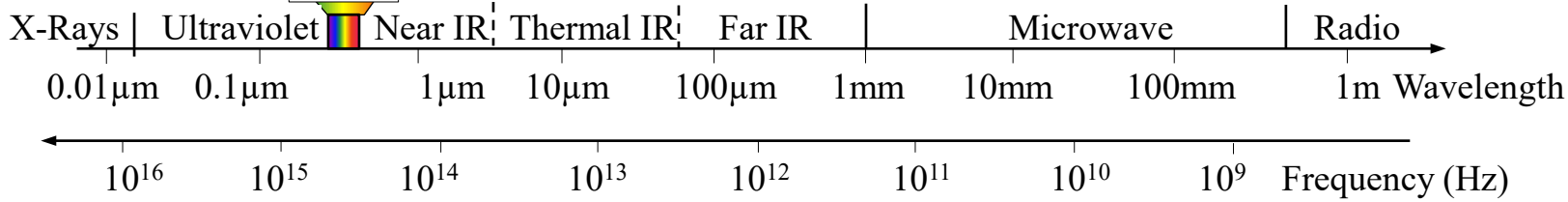
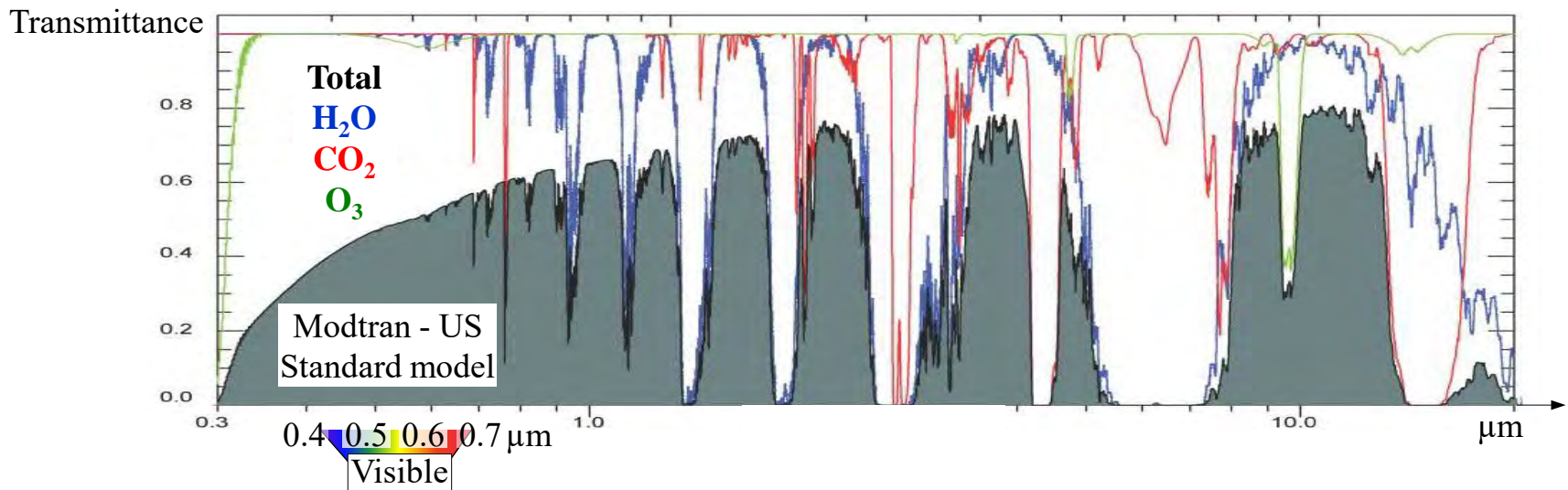
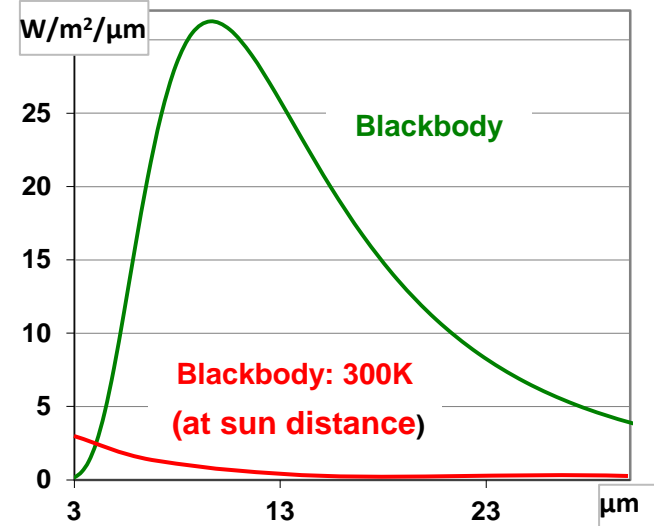
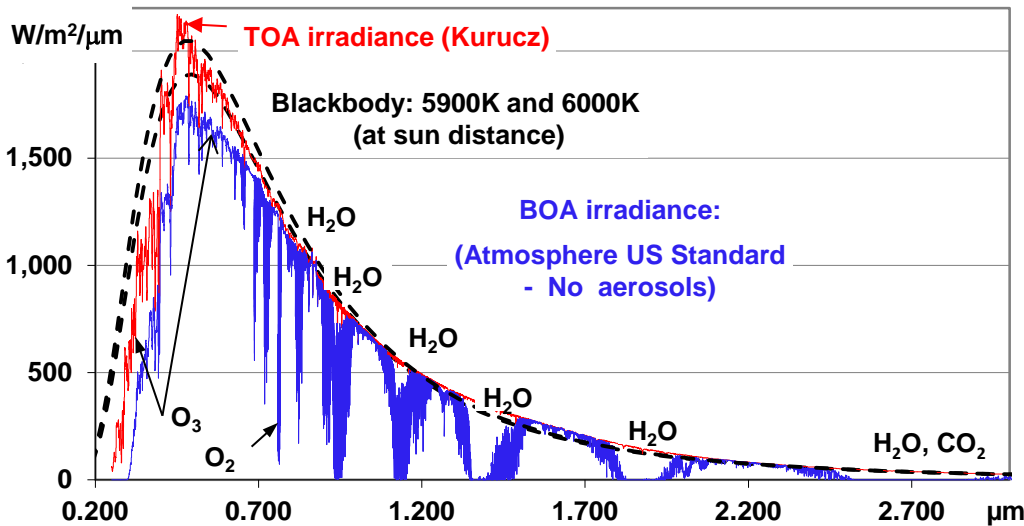
Very often, analysis of RS signal without any physics understanding is dangerous...

Approach:

- To introduce physics with examples
 - ⇒ simple questions not always so simple...
 - ⇒ thank you for participating
- To illustrate RS physics with RS model (DART)
(www.cesbio.ups-tlse.fr/dart)
 - ⇒ DART input parameters represent major RS atmosphere / Earth surface parameters

Objective: to explain remote sensing signals with physics, and remote sensing models

Spectrum, atmosphere transmittance and Sun / Earth thermal emission





Radiometer $L_\lambda(\Omega_s, \Omega_v)$



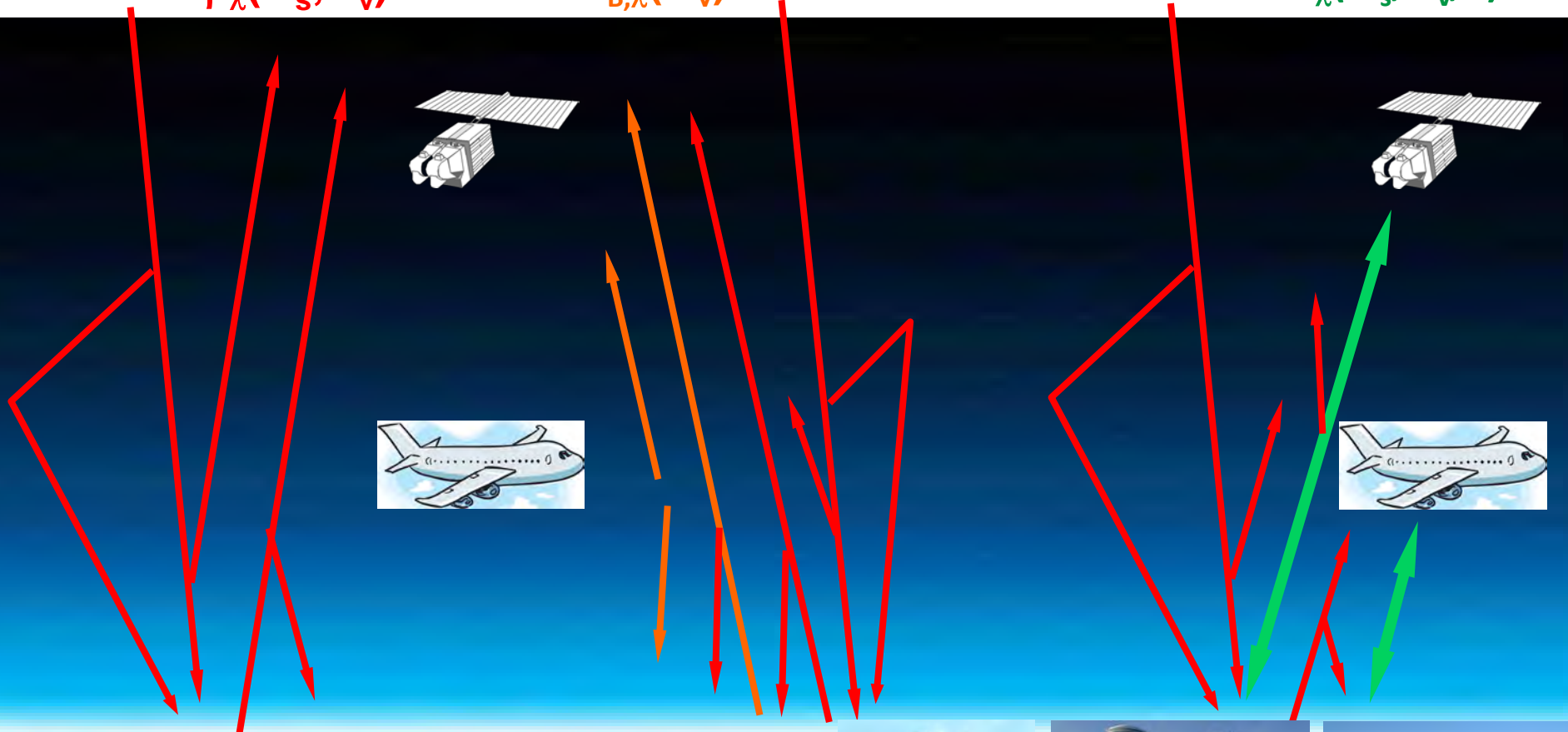
$\rho_\lambda(\Omega_s, \Omega_v)$

$T_{B,\lambda}(\Omega_v)$



Lidar (WF, PC)

$w_\lambda(\Omega_s, \Omega_v, t)$



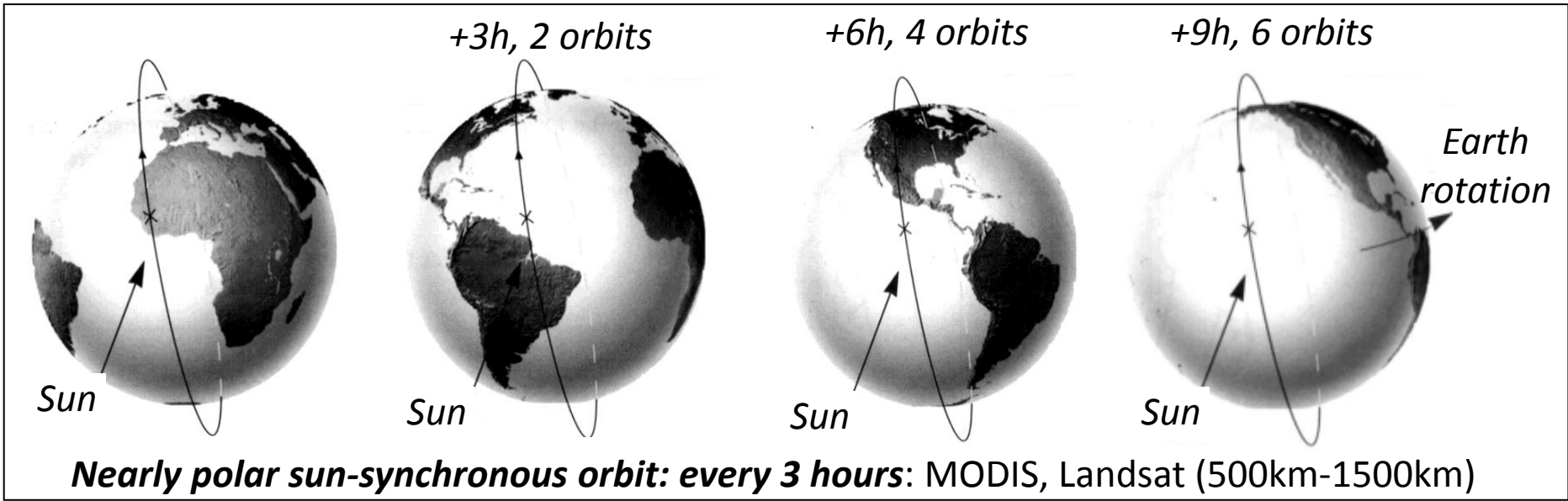
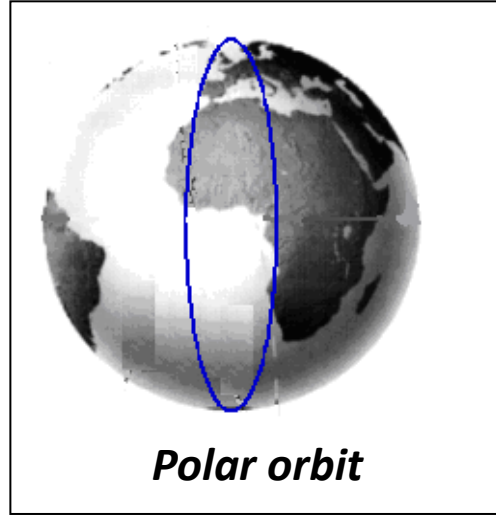
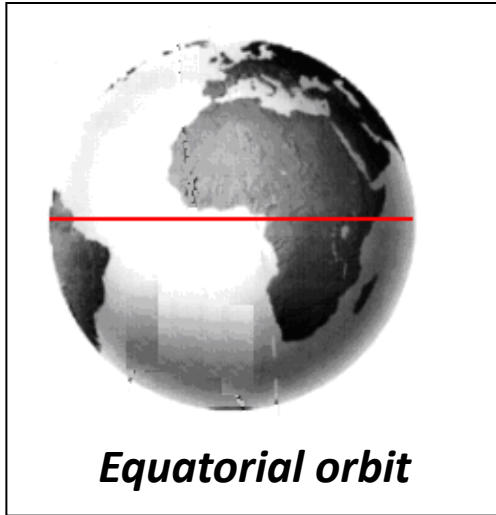
3D radiative budget



Any Earth landscape



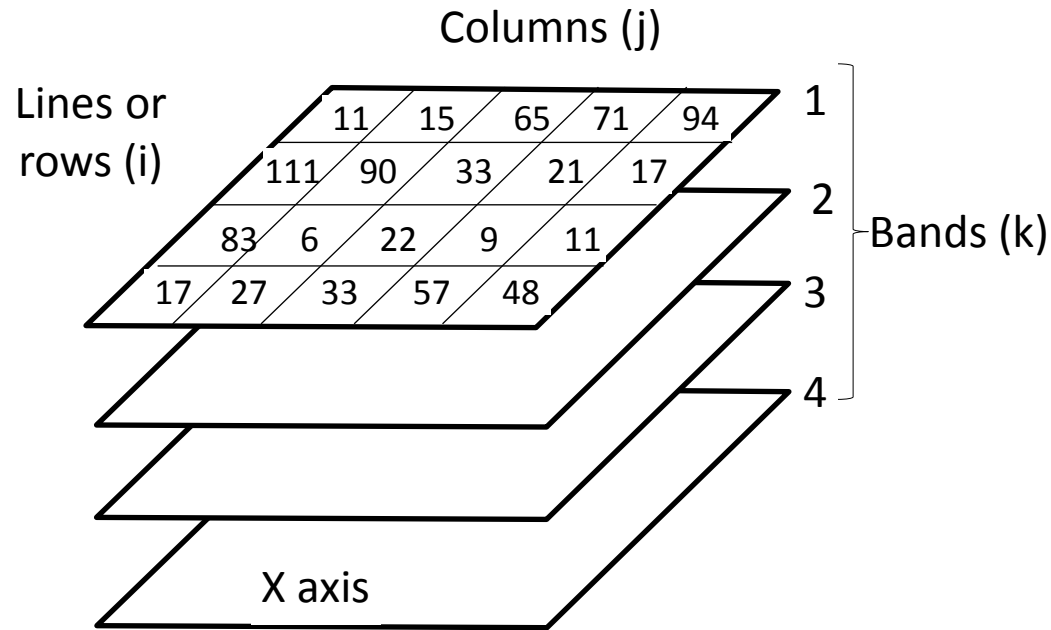
Orbits of Earth observation satellites



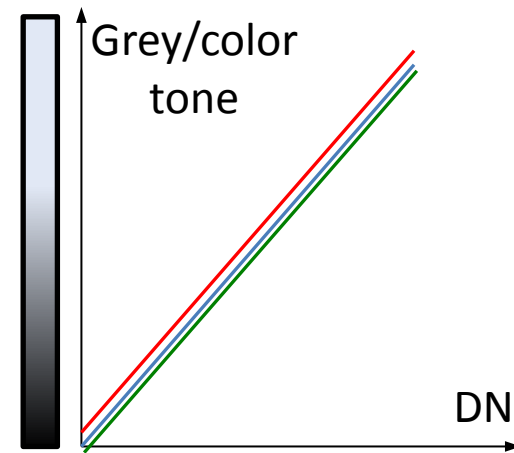
Non sun-synchronous orbit: IceSat (LiDAR)

Geostationary orbit: Meteosat, etc. (36 000km)

Remote sensing raster image



Multi-spectral image.
 $DN_k(i,j)$ is the digital number of pixel $P_k(i,j)$



Images (i.e., DNs) are displayed with LUTs: grey/color tone = $f(DN)$

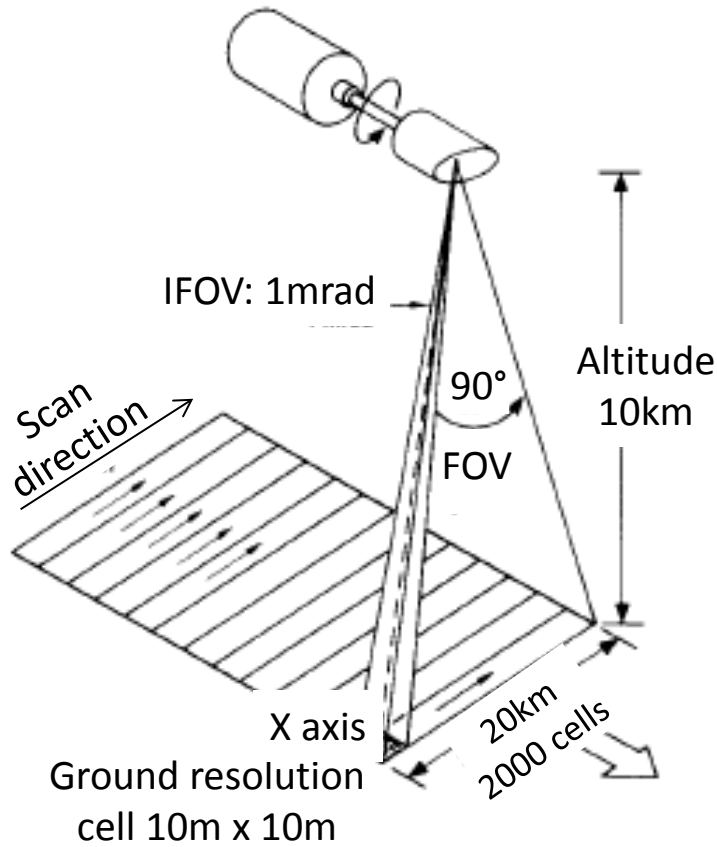
High res commercial data galleries

- <http://www.geoeye.com/CorpSite/gallery/Default.aspx>
- <http://www.digitalglobe.com/>
- <http://www.digitalglobe.com/index.php/27/Sample+Imagery+Gallery>

Signatures of Earth surfaces vs. Resolutions in remote sensing images

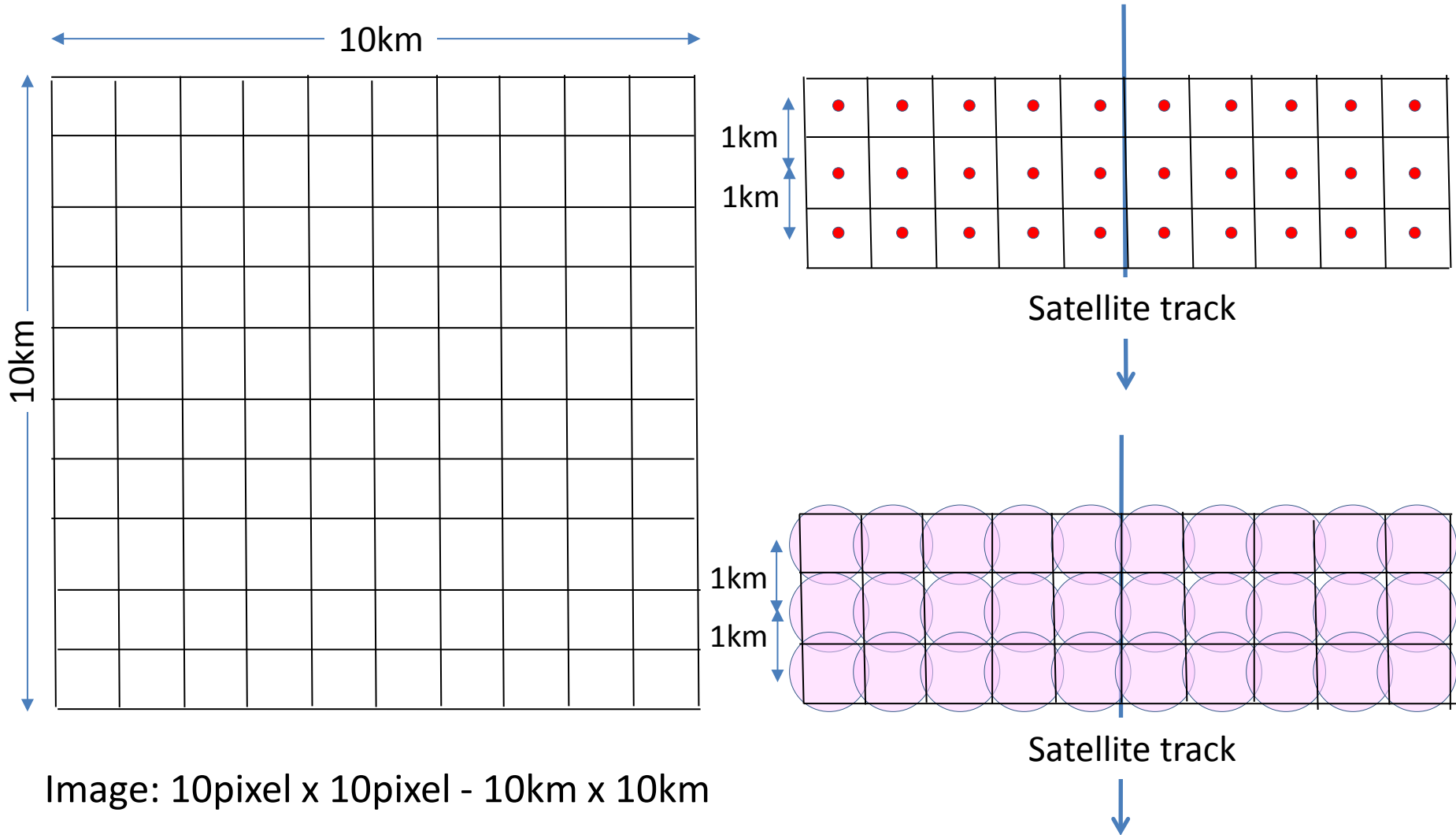
Cross track scanner: whiskbroom

Scan rate: $2 \cdot 10^{-2}$ s per scan line



Dwell time \Rightarrow Signal to noise ratio (SNR)

$$\Delta t = \frac{\text{Scan rate per line}}{\text{Number cells per line}} = \frac{2 \cdot 10^{-2}}{2000 \text{ cells}} = 10^{-5} \text{ s/cell} \quad \Delta t = \frac{\text{Cell dimension}}{\text{Velocity}} = \frac{10 \text{ m per cell}}{200 \text{ m/s}} = 5 \cdot 10^{-2} \text{ s per cell}$$



👉 **What is the spatial resolution (GIFOV) of the sensor?**



Variety of satellite / airborne sensors

- **Passive sensors (multi/hyper spectral radiometers):**
 - sun radiation reflected by Earth surfaces
 - radiation that is thermally emitted by Earth surfaces
- **Active sensors: LiDARs and Radars (not considered here)**

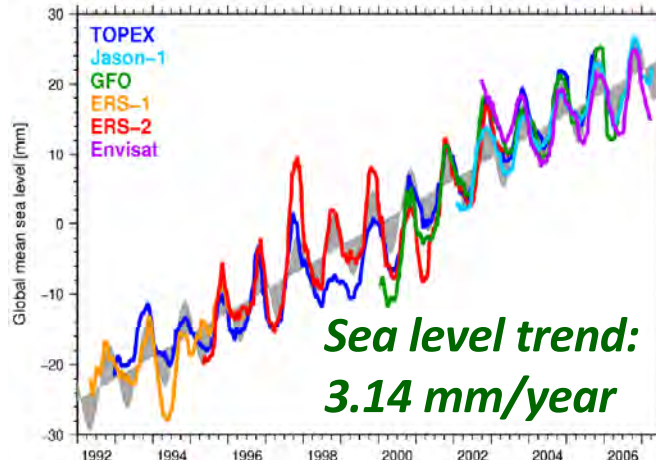
Very diverse information

- **Vegetation:** biochemistry (Chl, H₂O,...), spatial extent,...
- **Soil:** humidity, temperature, chemistry, altitude,...
- **Water:** temperature, salinity, roughness,...

Many applications: Biosphere functioning, Cartography & Topography, Agriculture (irrigation, crop forecast,...), Oceanography, Forestry, Environment (fires, floods,...),...



Seasonal evolution of vegetation



Sea level trend:
3.14 mm/year



Disks:
crops + circular irrigation

Information about Earth surfaces to derive from remote sensing signals:

- **Spectral signature**: signal variation with wavelength \Leftrightarrow spectrometers
- **Angular signature**: signal variation with view (sun) direction \Leftrightarrow multi-view sensor,...
- **Spatial signature**: signal variation with space \Leftrightarrow high / mid spatial resolution
- **Temporal signature**: signal variation with time \Leftrightarrow sensor acquisition repetitivity
- **Architecture** / distance signature: backscattering of LiDAR pulse
- **Fluorescence** emission (specific spectral bands), **polarization**, etc.

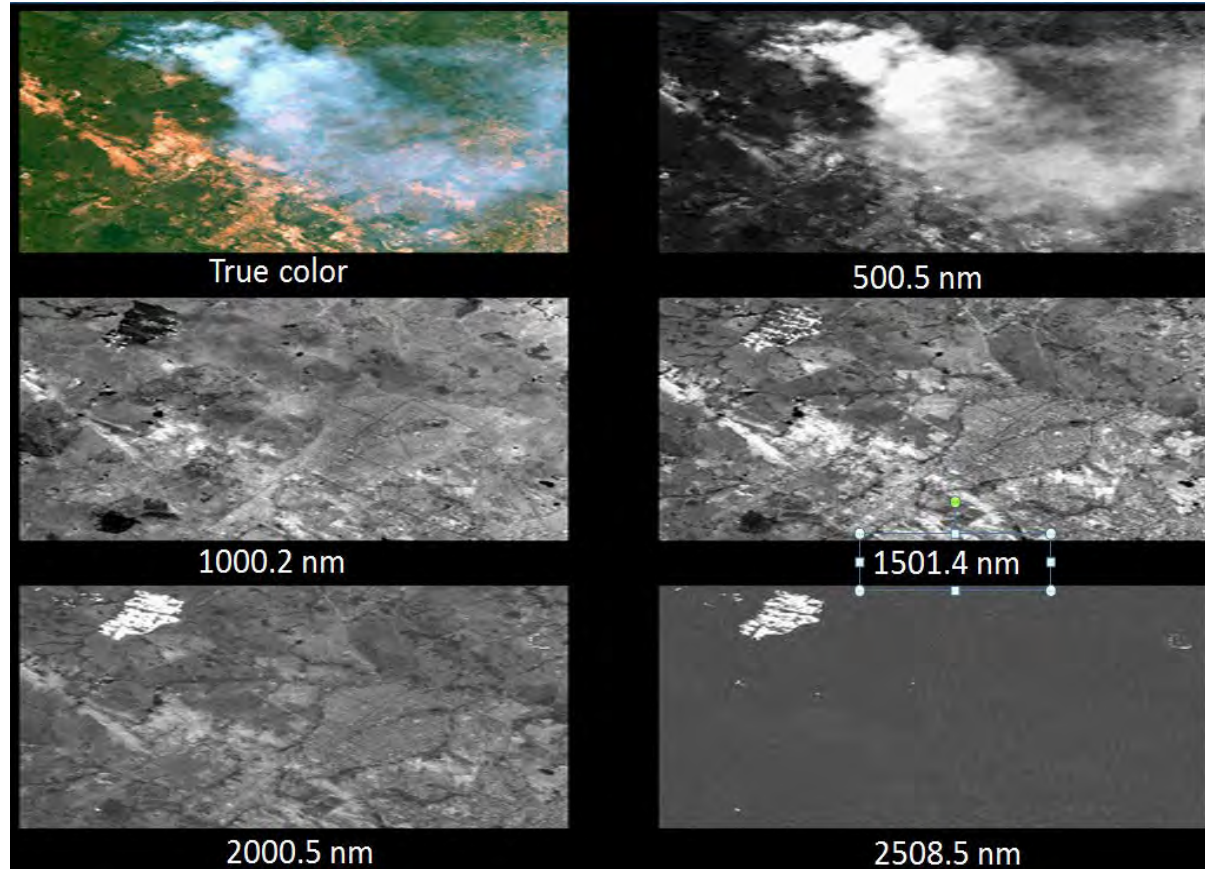
Several resolutions: - Radiometric resolution

- **Spatial resolution** GIFOV (IFOV + altitude) \neq pixel dimension
- **Spectral resolution**
- **Temporal resolution**

Importance of sensor characteristics and configuration

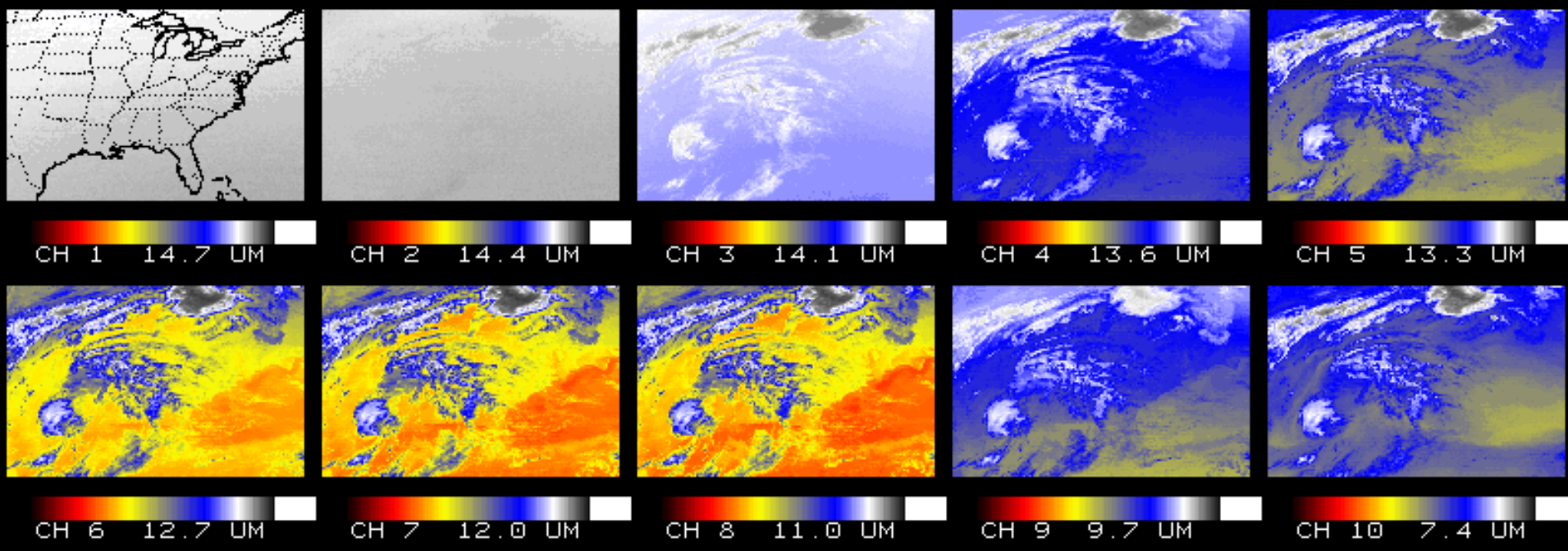
AVIRIS images: forest clearing fire (Cuiaba, Brazil, 25/08/1995)

- Radiometric resolution
- Sun / Sensor configuration
- Spatial resolution,
- Spectral domain/resolution,
- Time resolution.

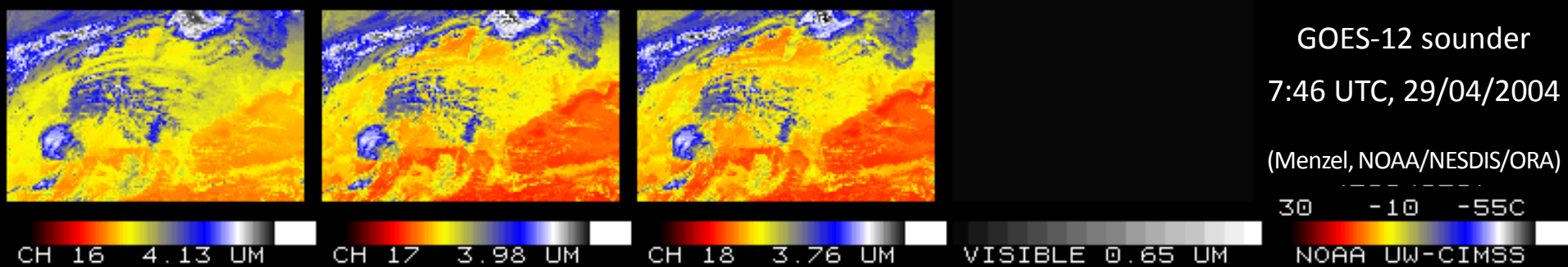


- Fire signal low at $1\mu\text{m}$ and large at $2.5\mu\text{m}$. Why?
- Earth surfaces: very low signal at $2.5\mu\text{m}$. Why?

Perception vs. spectral domain: GOES-12 Sounder \Rightarrow Brightness temperature at several altitudes



- Signal is null in the visible band (0.65 μm). Why?
- In thermal infrared (TIR) bands:
 - The low (-50C) and large (20C) signals (brightness temperature T_B) correspond to?
 - The atmosphere thermal emission changes with spectral band (*i.e.*, lower/higher T_B). Why?



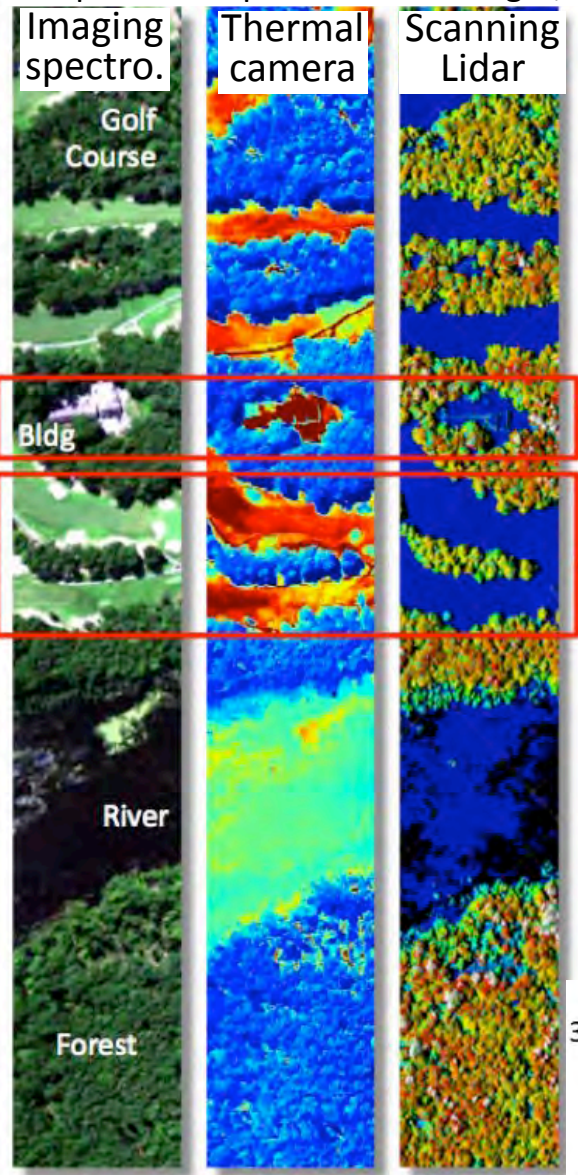
GOES-12 sounder
7:46 UTC, 29/04/2004
(Menzel, NOAA/NESDIS/OR)

Perception vs. spectral domain and passive vs. active sensor: G-LIHT images (NASA)

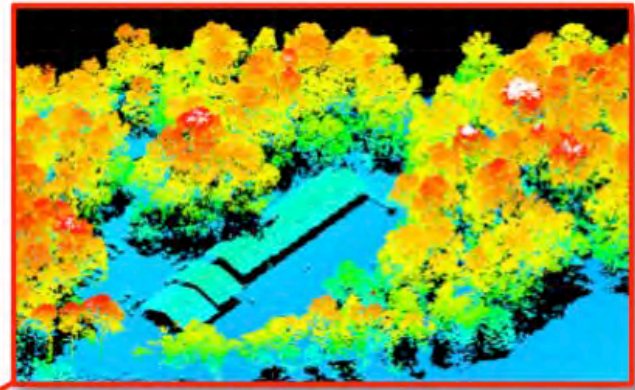
Airborne G-LIHT sensor:

Scanning lidar	
Swath width/FOV	387 m (60°)
Footprint diameter	10 cm (0.3 mrad)
Range precision	5 cm (2 σ)
Sampling density at surface	6 pulses m ⁻²
Max. returns per pulse	8
Irradiance spectrometer	
Swath width/FOV	hemispheric (180°)
Spectral range	350 to 1,100 nm
Sample/Band width	1.5 and 1.5 nm
Acquisition rate	1 Hz
Imaging spectrometer	
Swath width/FOV	310 m (50°)
Cross track pixels	1,004
Spectral range	420 to 950 nm
Sample/Band width	1.5 and 5.0 nm
Acquisition rate	50 Hz
Thermal camera	
Swath width/FOV	173 m (30°)
Imaging array size	384 x 288
Spectral range	8 to 14 μ m
Sensitivity (NETD)	>50 mK at 30°C
Acquisition rate	25 Hz

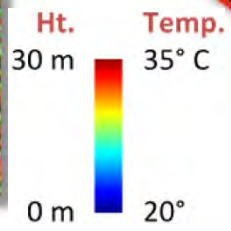
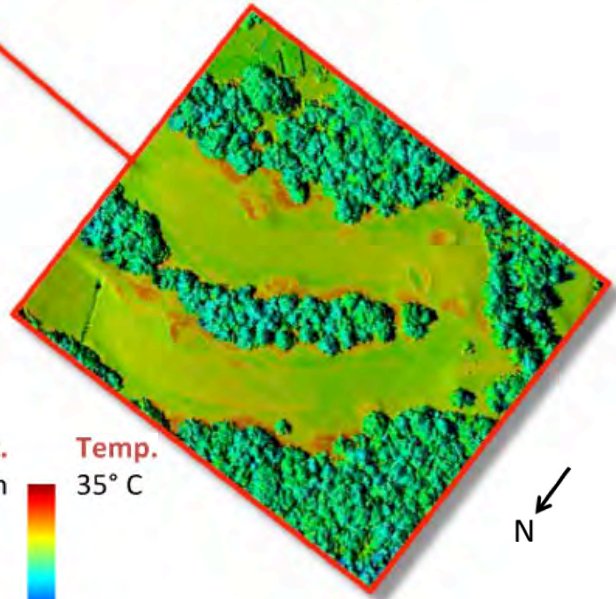
RGB color Brightness DSM \Rightarrow DEM,
 composite temperature tree height,...



3D vegetation structure



LiDAR apparent reflectance

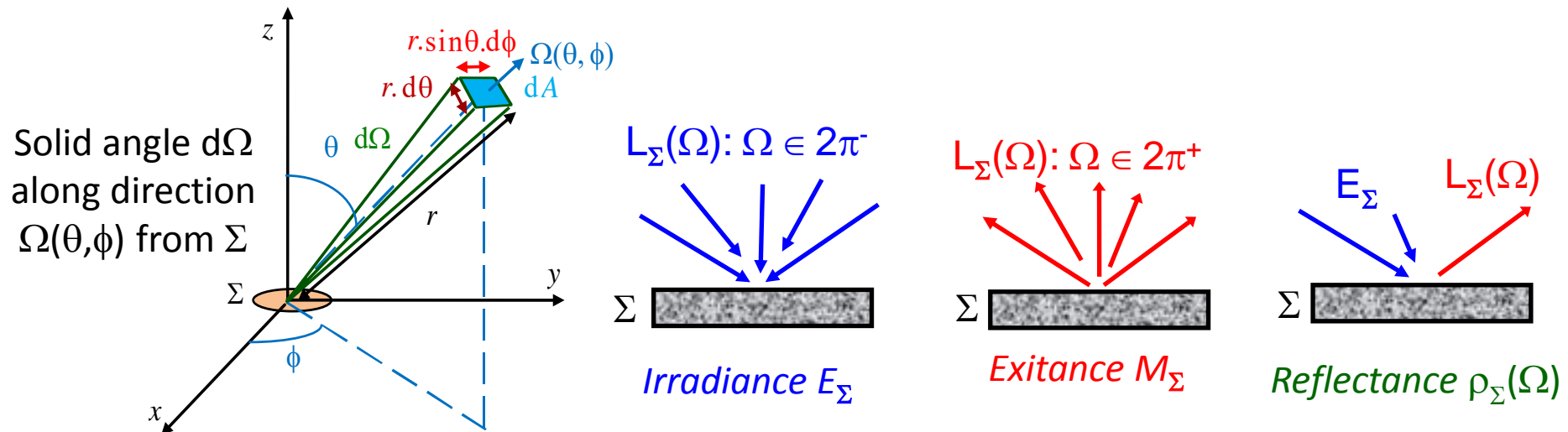


- Why brightness temperature is larger for grass than for trees?
- How 3D vegetation is obtained?
- What is LiDAR apparent ρ ?
- What is the usefulness of the irradiance spectrometer?

← 170 m →

Radiometry: definitions

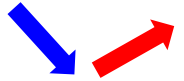
- **Solid angle $d\Omega$ of direction $\Omega(\theta, \phi)$:** $d\Omega = \sin\theta \cdot \cos\phi \cdot d\theta \cdot d\phi$ with θ = zenith and ϕ = azimuth
- **Radiance $L_{\Sigma}(\Omega)$ of Σ along (Ω) :** $L_{\Sigma, \lambda}(\Omega)$ W/m²/sr/ μm (/ effective m² !), $L_{\Sigma, \Delta\lambda}(\Omega)$: W/m²/sr
- **Irradiance E_{Σ} of Σ (in flux):** $E_{\Sigma, \lambda} = \int_{2\pi^-} L_{\Sigma, \lambda}(\Omega) \cdot |\cos\theta| \cdot d\Omega$ W/m²/ μm $E_{\Sigma, \Delta\lambda} = \int_{2\pi^-} L_{\Sigma, \Delta\lambda}(\Omega) \cdot |\cos\theta| \cdot d\Omega$: W/m²
- **Exitance M_{Σ} of Σ (out flux):** $M_{\Sigma, \lambda} = \int_{2\pi^+} L_{\Sigma, \lambda}(\Omega) \cdot \cos\theta \cdot d\Omega$ W/m²/ μm $M_{\Sigma, \Delta\lambda} = \int_{2\pi^+} L_{\Sigma, \Delta\lambda}(\Omega) \cdot \cos\theta \cdot d\Omega$ W/m²
- **Reflectance factor $\rho_{\Sigma}(\Omega)$ of Σ along (Ω) :** $\rho_{\Sigma, \lambda}(\Omega) = \frac{\pi \cdot L_{\Sigma, \lambda}(\Omega)}{E_{\Sigma, \lambda}}$ if Σ is lambertian: $\rho_{\Sigma, \lambda}(\Omega) = \text{cst}$



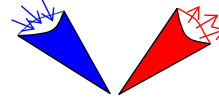
👉 What is the physical quantity that is measured by a satellite radiometer?

Different reflectance factors (*direct d, hemispherical h, conical c*)

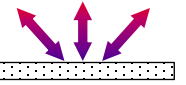
- **In or Out 'direct'** flux (index d): flux along a unique direction (*i.e.*, $d\Omega=0$).



- **In or Out 'conical'** flux (index c): flux within a cone (Ω , $d\Omega \neq 0$).

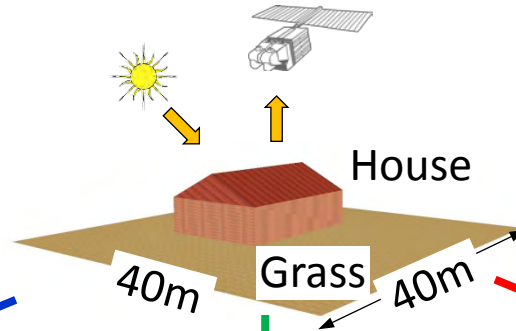
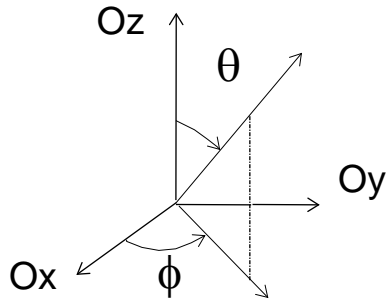


- **In or Out 'hemispherical'** flux (index h): flux within an hemisphere (*i.e.*, $d\Omega=2\pi$).

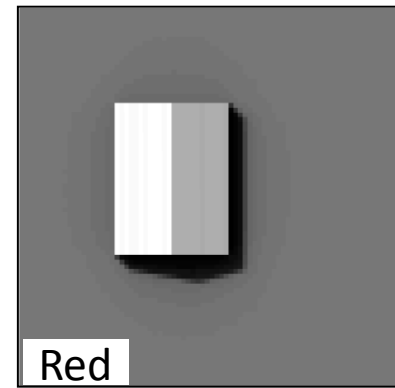
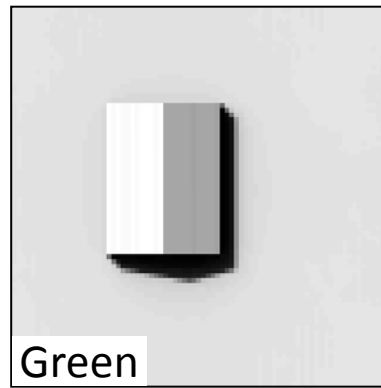
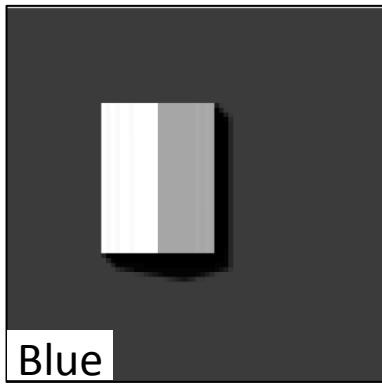


- ☞ Which reflectance is derived from the measurement of a satellite radiometer?
- ☞ Which reflectance is used for computing the albedo of our planet?

Satellite image acquisition and display



Landscape: grass, house
Atmosphere
Sun (upward): $\theta_s=30^\circ$, $\phi_s=330^\circ$
Satellite: - nadir view direction
- 3 bands: B, G, R



DART simulations



☞ Sun at nadir: what are the zenith and azimuth angles?

Satellite image acquisition and display

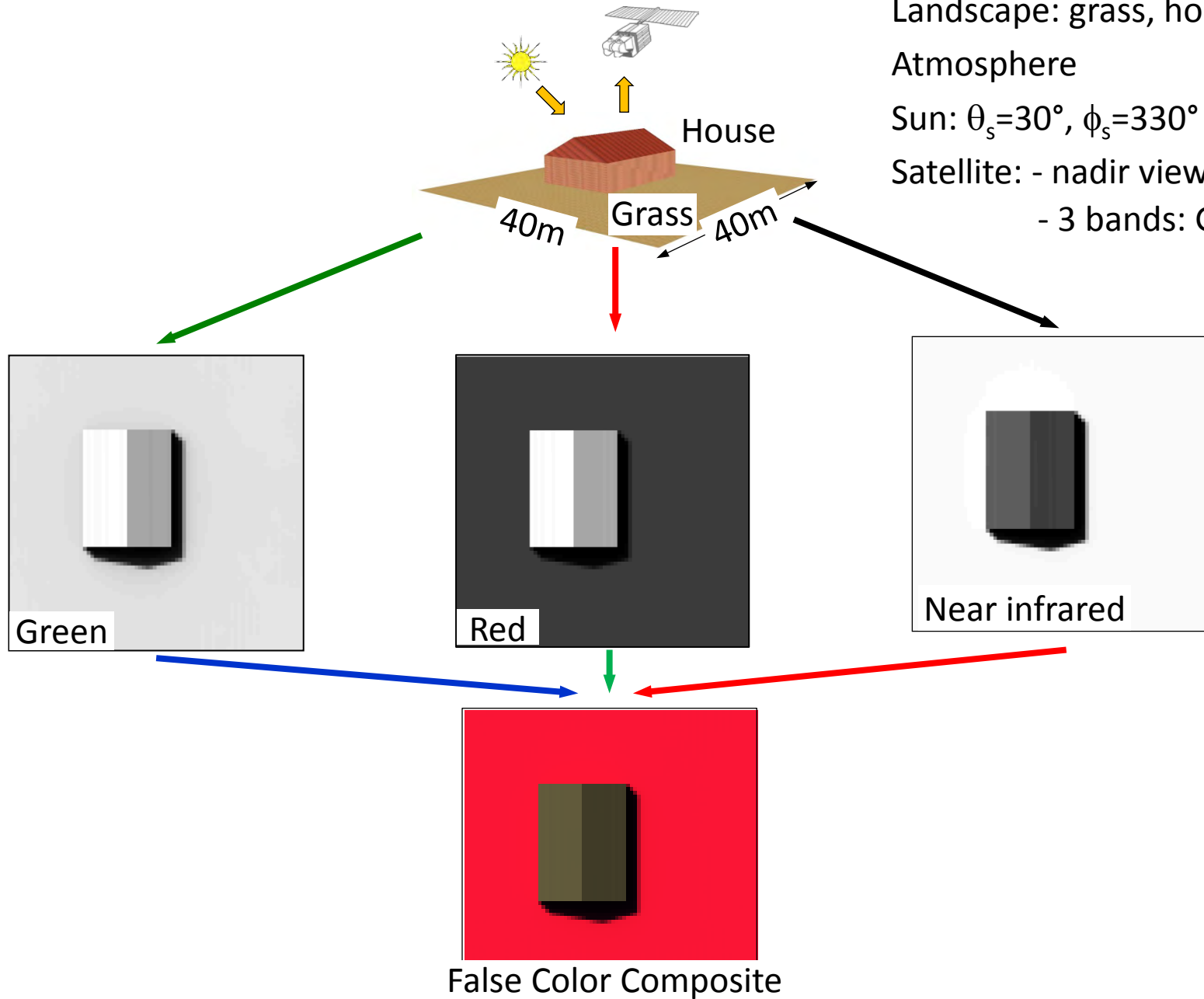
Landscape: grass, house

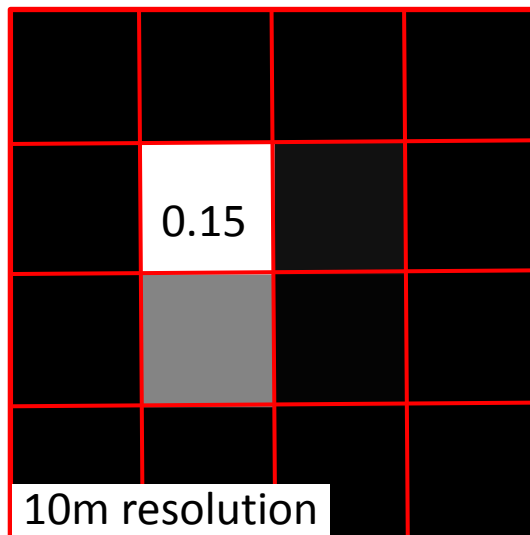
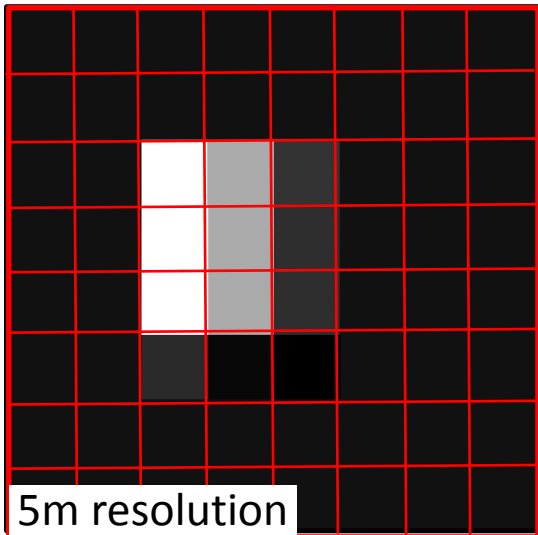
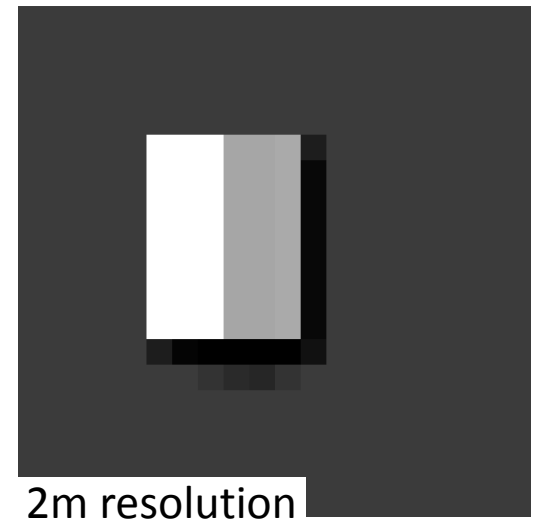
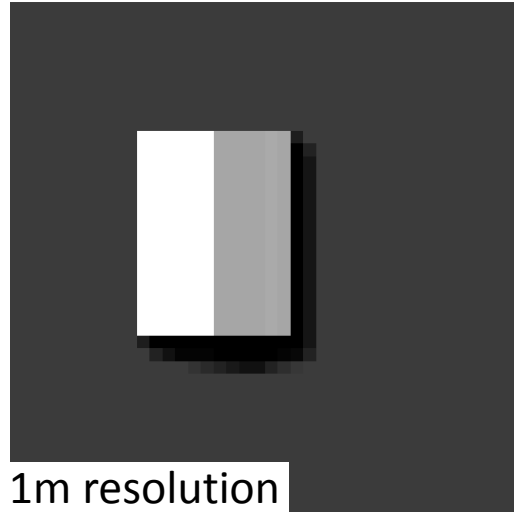
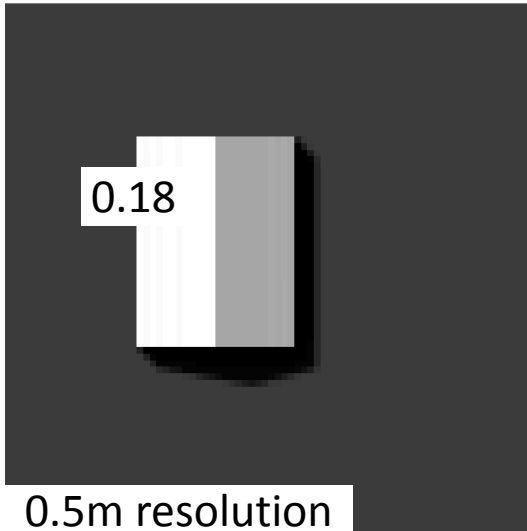
Atmosphere

Sun: $\theta_s=30^\circ$, $\phi_s=330^\circ$

Satellite: - nadir view direction

- 3 bands: G, R, NIR





Red spectral band

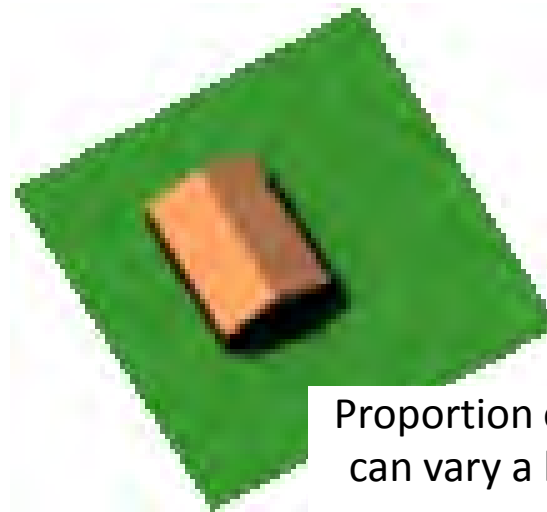
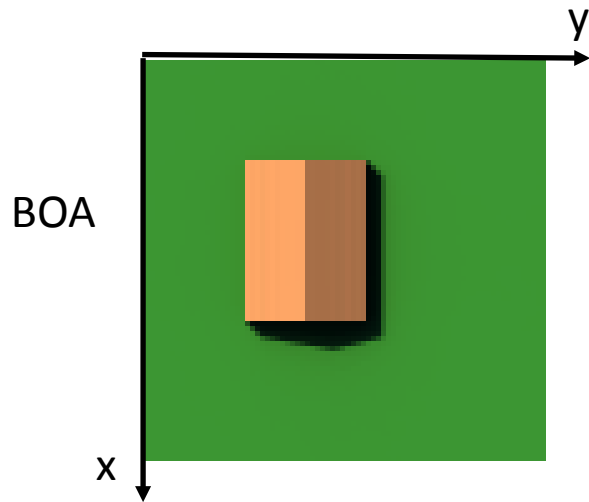
Spatial sampling
⇒ Change of DN's

TOA (Top of Atmosphere) and BOA (Bottom of Atmosphere) acquisitions

Nadir view direction

$(\theta_v=22^\circ, \phi_v=30^\circ)$ view direction

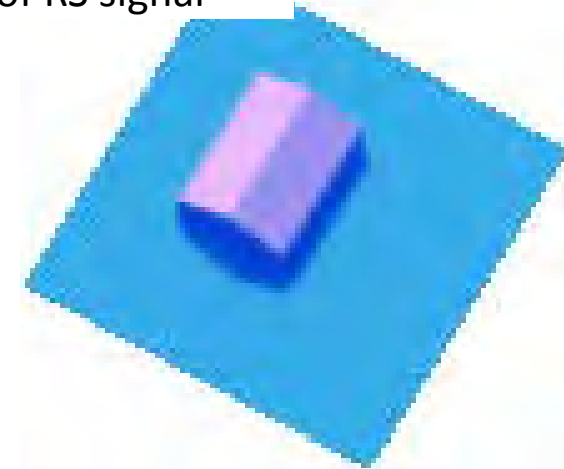
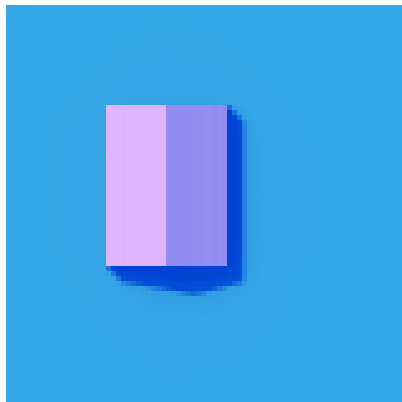
$(\theta_v=22^\circ, \phi_v=330^\circ)$ view direction



Proportion of observed shadows
can vary a lot with view direction

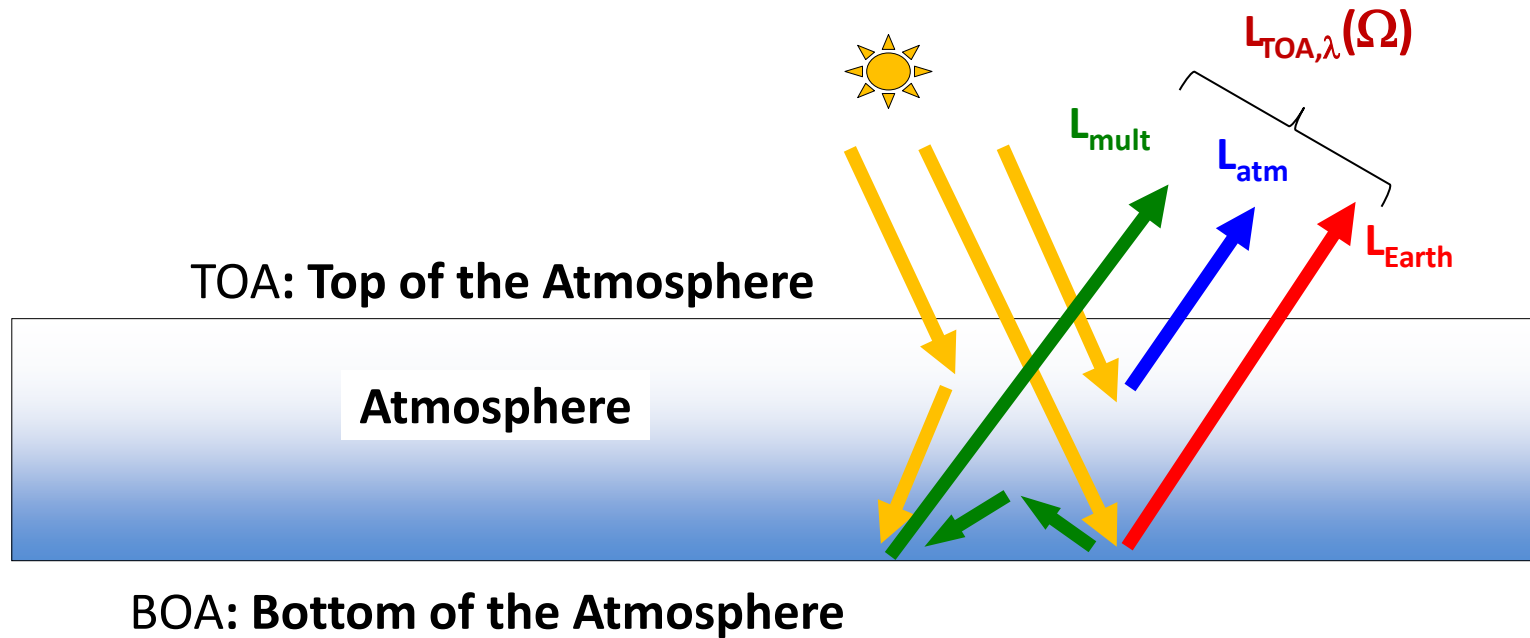
⇒ Anisotropy of RS signal

TOA



☞ Why TOA images are bluish?

💣 Atmosphere characteristics (atmosphere model), sun direction, etc.



$L_{TOA,\lambda}(\Omega) =$ "Radiance $L_{Earth,TOA,\lambda}(\Omega)$ due to scattering of sun flux by the Earth, only"

+

"Radiance $L_{atm,TOA,\lambda}(\Omega)$ due to scattering of sun flux by the Atmosphere, only"

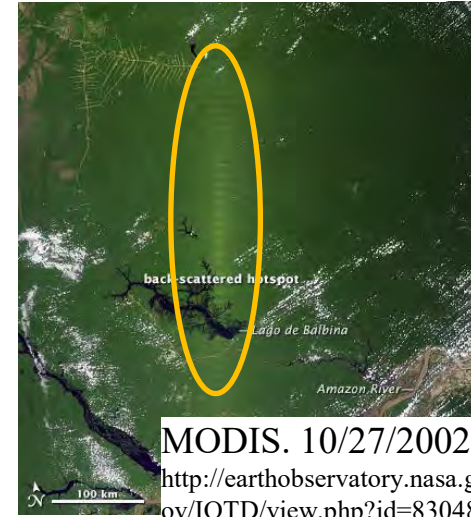
+

"Radiance $L_{mult,TOA,\lambda}(\Omega)$ due to scattering of sun flux by {Earth + Atmosphere}"

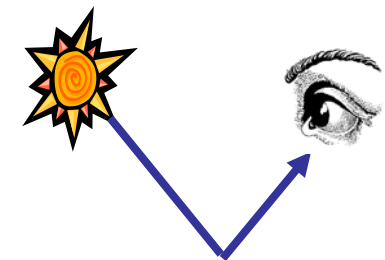
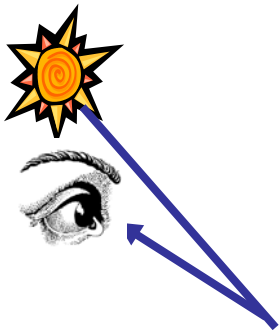
Hot spot: sensor view direction = sun direction \Rightarrow maximal reflectance



<http://academic.emporia.edu/abe/rjame/remote/lec10/hotspot.jpg>



MODIS. 10/27/2002
<http://earthobservatory.nasa.gov/IOTD/view.php?id=83048>



From Donald Deering

Reflectance of lambertian and natural surfaces

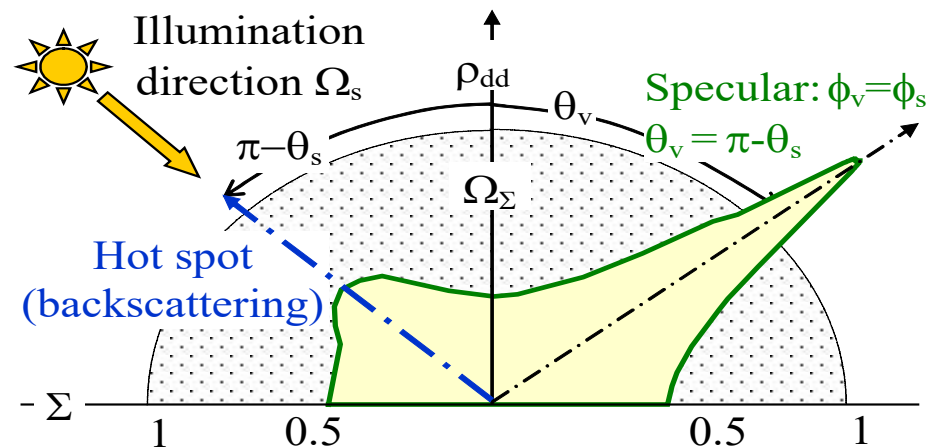
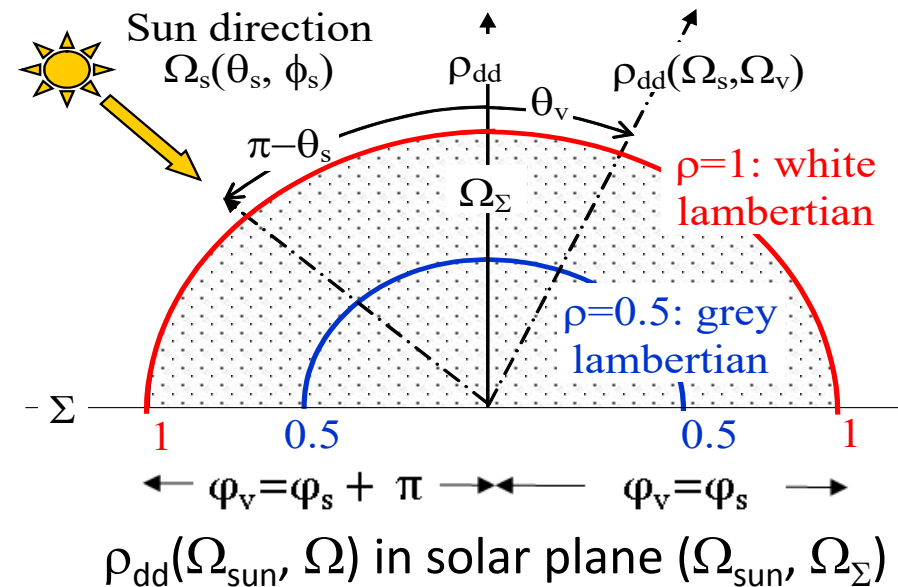
☞ How can there be hot spot? Indeed, a sensor with the sun behind it should see its own shadow...

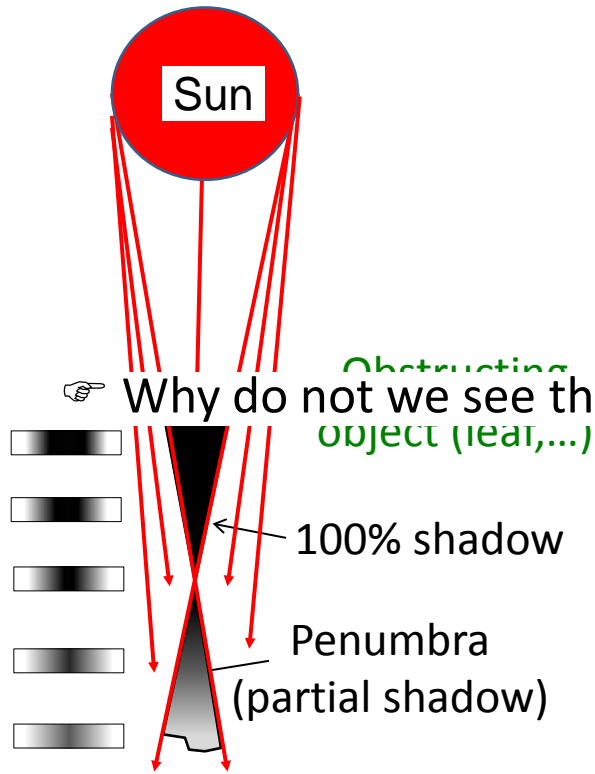
Lambertian surface: $\rho_{dd} = \rho_{dh} = \rho_{hd} = \rho_{hh} = \text{cst.}$

- White lambertian surface: $\rho = 1$
- Grey lambertian surface: $\rho = \text{cst} < 1$.

Natural surface: $\rho_{dd}(\Omega)$ varies with (Ω) .

Here, ρ_{dd} is maximal for specular direction (water?) with local maximum (vegetation?) for sun direction (hot spot: the sensor does not see shadow)

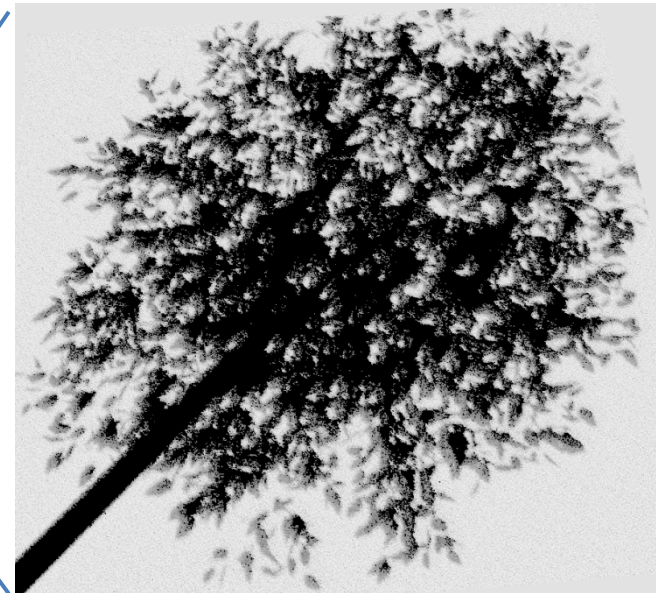
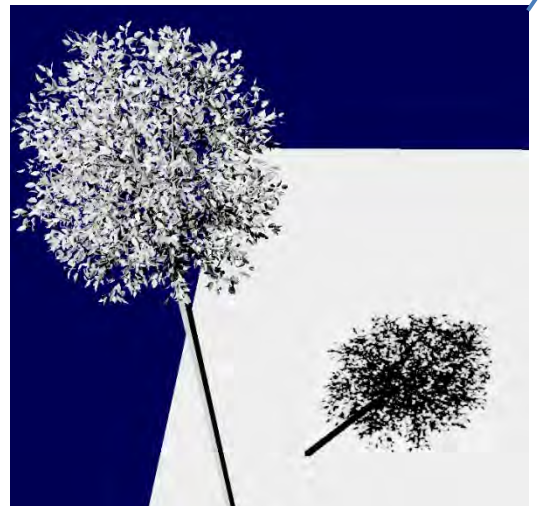




Why do not we see the shadows of satellite and planes on the Earth surfaces?



Parallel sun rays

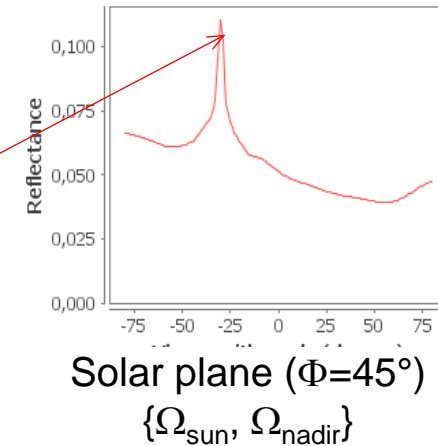
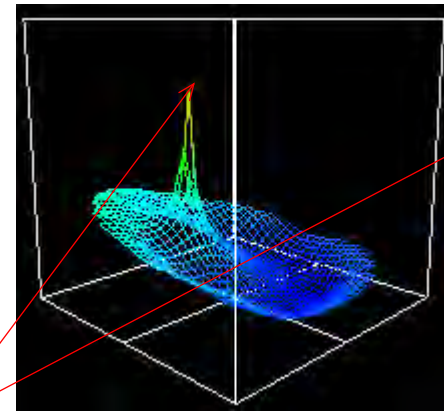
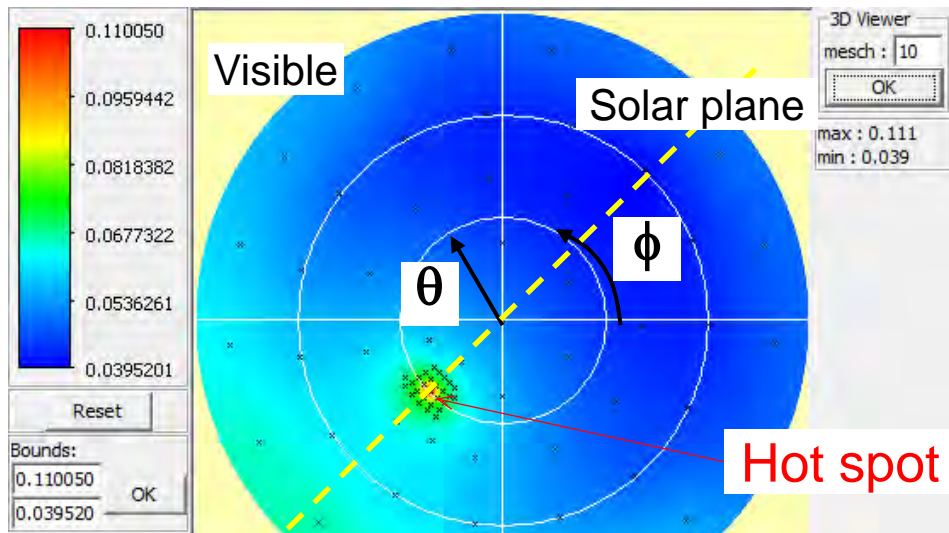
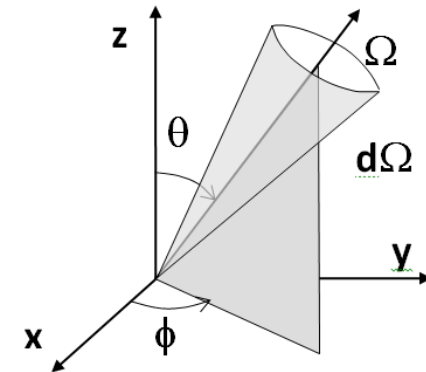
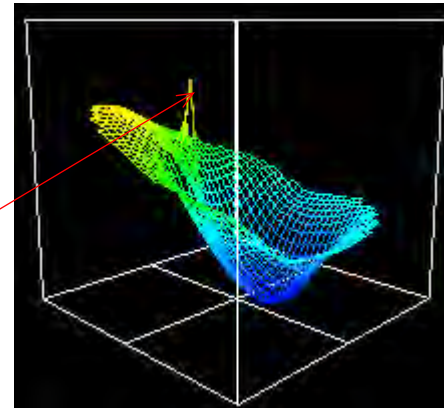
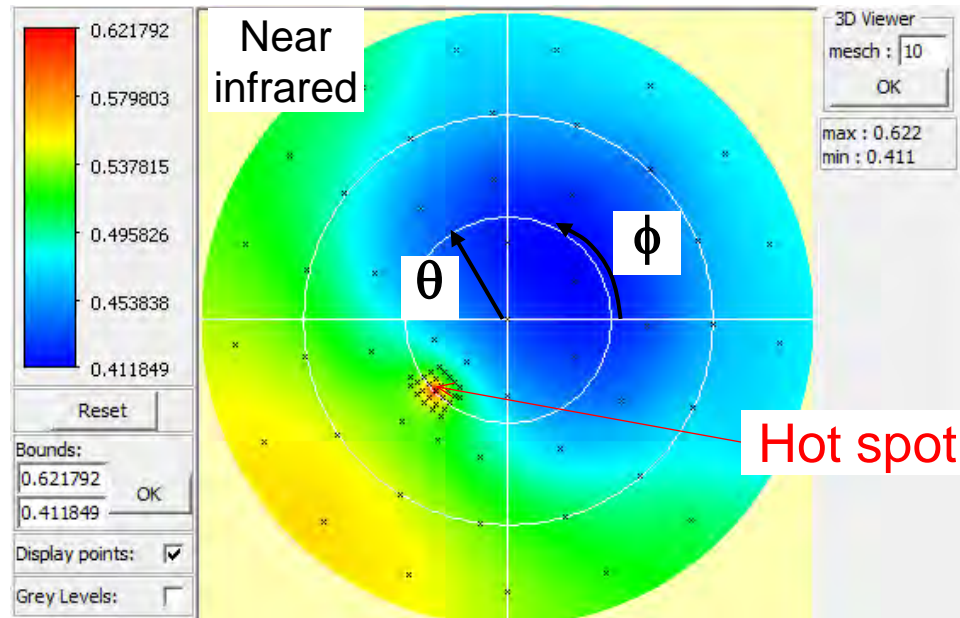


Actual sun rays: $\Delta\Omega_{\text{sun}} = 32'$

Sun rays are not parallel
⇒ shadow is total at short distance and more and more partial as distance increases

1D, 2D (polar) and 3D plots of vegetation reflectance

Displays of DART model



☞ For large view zenith angles θ_{view} vegetation reflectance increases in near infrared (top) and decreases in the visible (bottom). Which simple landscape (tree + bare ground) can explain it?

Albedo and spectral reflectance of Earth surface elements

Albedo (A_{dh} or A_{hh}): integral of reflectance $\rho_\lambda(\Omega_s, \Omega_v)$ weighted by incident flux $L_\lambda(\Omega_s)$ over scattering directions ($2\pi^+$) and all / part of the spectrum.

$$A_{dh}(\Delta\Omega_s=0, \Delta\lambda) = \frac{\text{Exitance: reflexion over } 2\pi^+}{\text{Irradiance (d) along } \Omega_s} = \frac{1}{\pi} \frac{\int_{\Delta\lambda} \int_{2\pi} \rho_{dd}(\Omega_s, \Omega_v, \lambda) \cdot \mu_v \cdot E_\lambda(\Omega_s) \cdot \mu_s \cdot d\Omega_v \cdot d\lambda}{\int_{\Delta\lambda} E_\lambda(\Omega_s) \cdot \mu_s \cdot d\lambda} \quad \text{with } \Delta\lambda \approx [0.2 \text{ } 4 \text{ } \mu\text{m}]$$

At the Earth surface, one uses often: $A_{hh}(2\pi^-, \Delta\lambda) = \frac{\text{Exitance: reflexion over } 2\pi^+}{\text{Irradiance (h) along } 2\pi^-}$

Material	Albedo (%)
<i>Planet Earth</i>	≈ 33 (≈ 36 for Visible domain)
<i>Cloud (stratus)</i> : - depth < 200 m	5-65
- depth [200 1000 m]	30-85
<i>Snow</i> : fresh and dry / old	75 - 90 / 45 - 70
<i>Ground</i> : - white sand	35 - 40; increases from blue to red
- dark moist / dry	5 - 6 / 5 - 15; increases from blue to red
<i>Vegetation</i> : green crop / forest	5 - 15 / 10 ; maximum in the green
<i>Water</i> : sun zenith $0^\circ/30^\circ/60^\circ/70^\circ/80^\circ/85^\circ/>87^\circ$	2/ 2,2 / 6 / 13,4 / 35,8 / ≈ 60 / >90

Very variable albedo
/reflectance values

Thermal emission (Planck's law) and brightness temperature

Planck's law: $L_{B,\lambda}(\Omega) = \frac{2 \cdot h \cdot c^2}{\lambda^5 \cdot (e^{\lambda k T} - 1)}$ (W/m²/sr/m) with $h = 6.63 \cdot 10^{-34}$ J.s, $k = 1.3807 \cdot 10^{-23}$ J/K

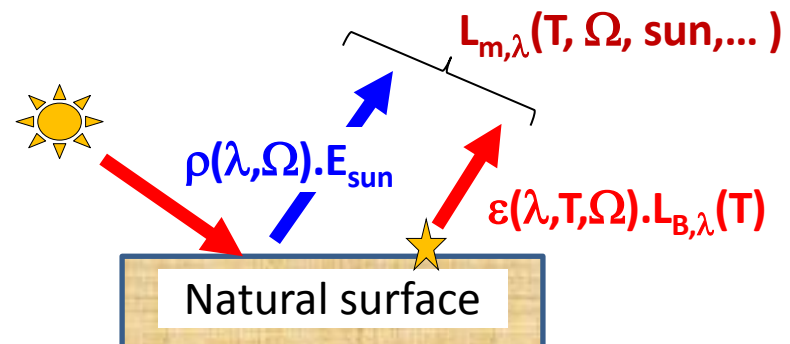
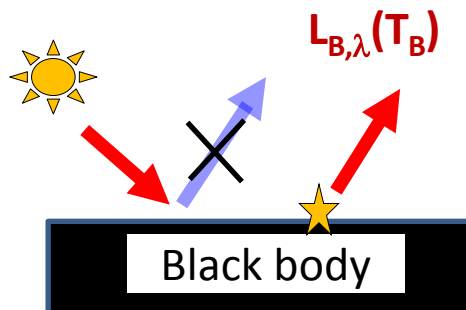
Wien law: $M(\lambda)$ is maximal for $\lambda_m = \frac{a}{T}$ ($a = 2899 \mu\text{m} \cdot \text{K}$)

Stephan-Boltzmann law: $M = \int_{\infty} L_{B,\lambda} \cdot d\lambda = \sigma \cdot T^4$, with $\sigma = 5.6704 \cdot 10^{-8}$ W/m²/K⁴

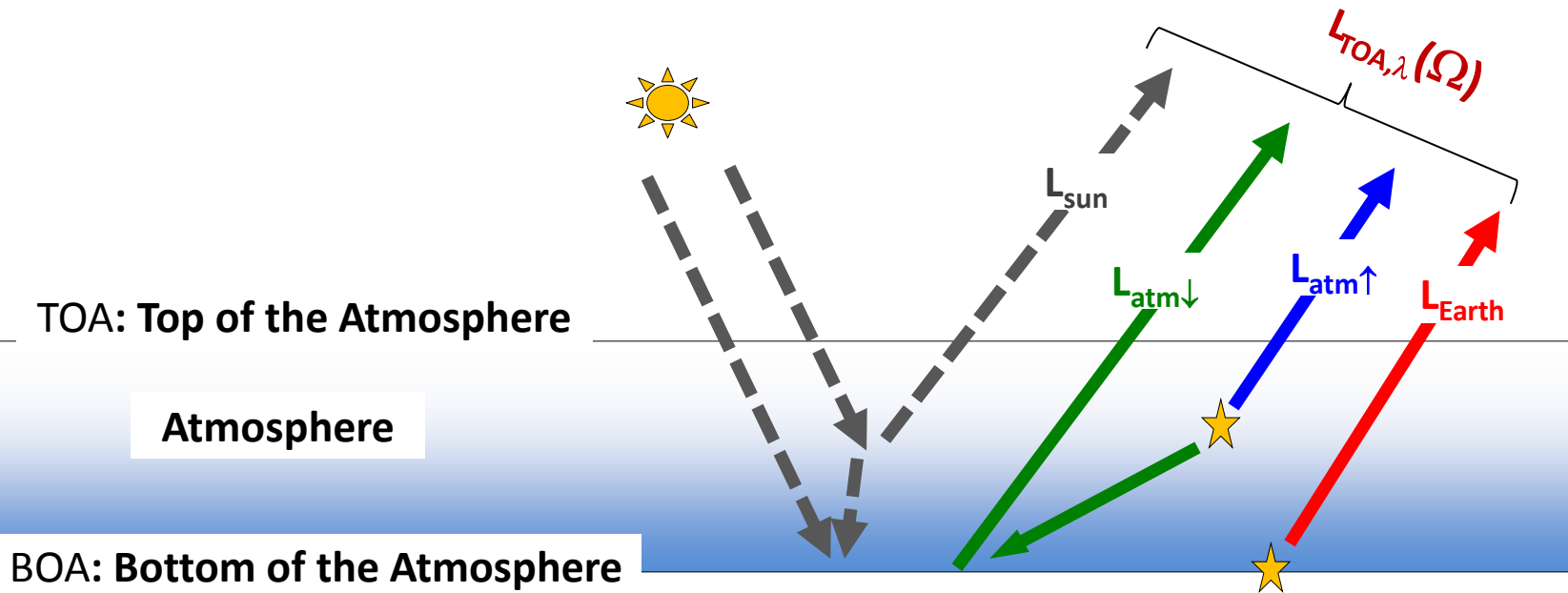
Emissivity $\varepsilon(\lambda, T, \Omega)$: natural body $\Rightarrow L_{\lambda}(T, \Omega) = \varepsilon(\lambda, T, \Omega) \cdot L_{B,\lambda}(T)$, with $\varepsilon(\lambda, T, \Omega) = 1 - \rho_{\text{nd}}(\lambda, T, \Omega)$

Brightness temperature T_B : temperature of the blackbody that emits the measured radiance L_m

$$L_{m,\lambda}(\Omega) = L_{B,\lambda}(T_B) \Rightarrow T_B = L_{B,\lambda}^{-1}(L_{m,\lambda}(\Omega)) = f(\lambda, T, \Omega)$$



Satellite signal (TOA radiance) $L_{TOA,\lambda}(\Omega)$ - long wavelengths



$L_{TOA,\lambda}(\Omega) =$ "Radiance $L_{Earth,TOA,\lambda}(\Omega)$ due to thermal emission by the Earth, only"

+

"Radiance $L_{atm\uparrow,TOA,\lambda}(\Omega)$ due to thermal emission by the Atmosphere, only"

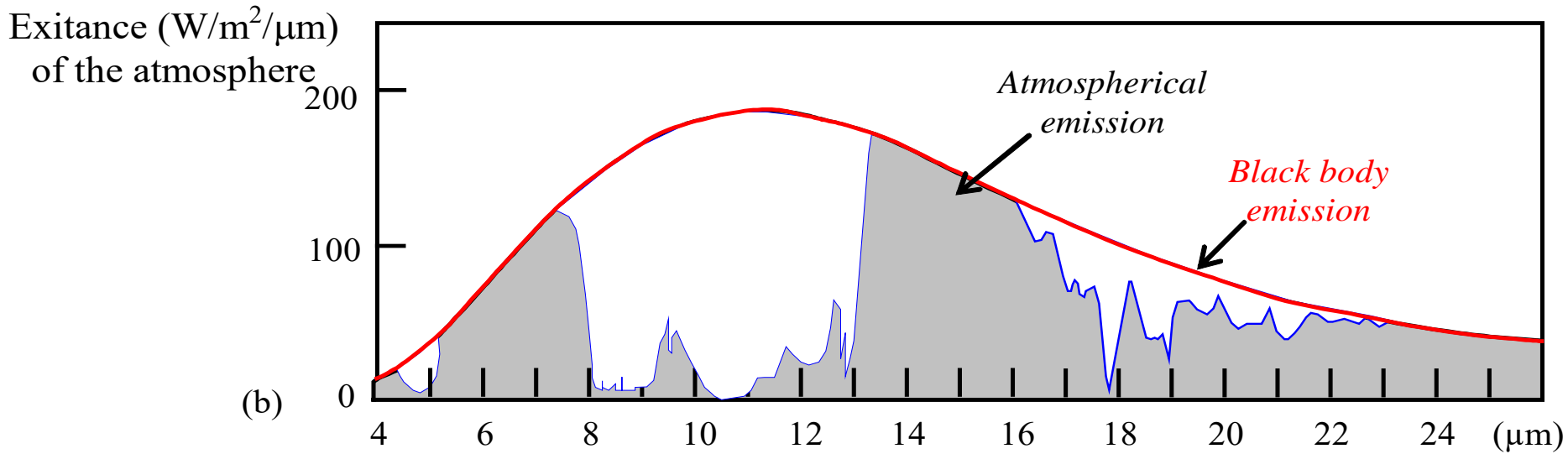
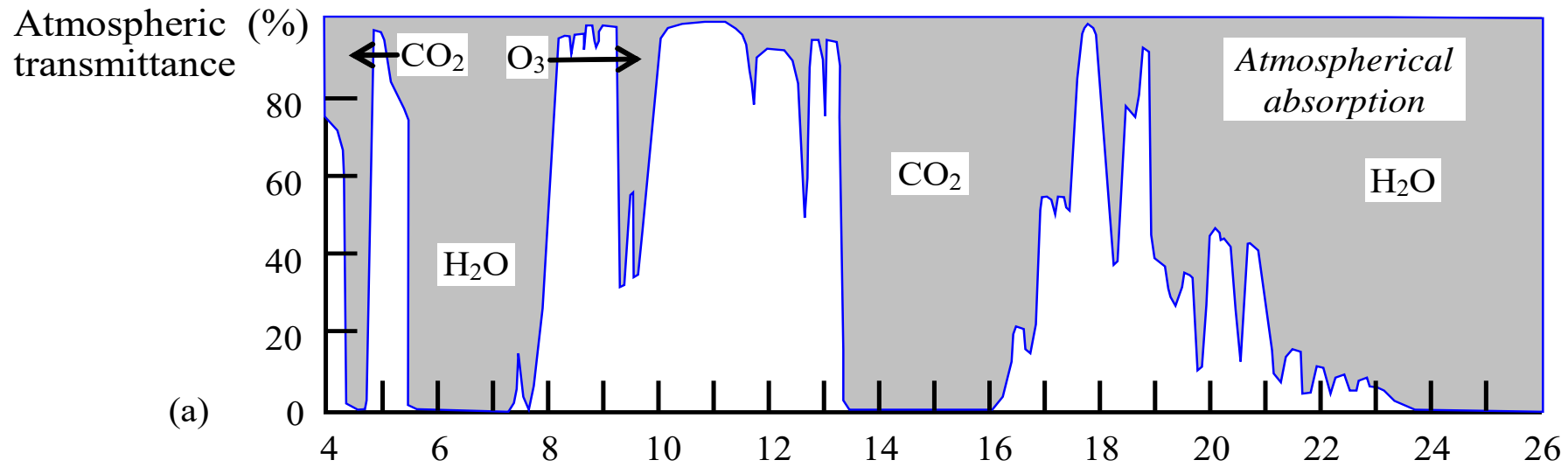
+

"Radiance $L_{atm\downarrow,TOA,\lambda}(\Omega)$ due to Earth scattering of Atmosphere thermal emission"

+

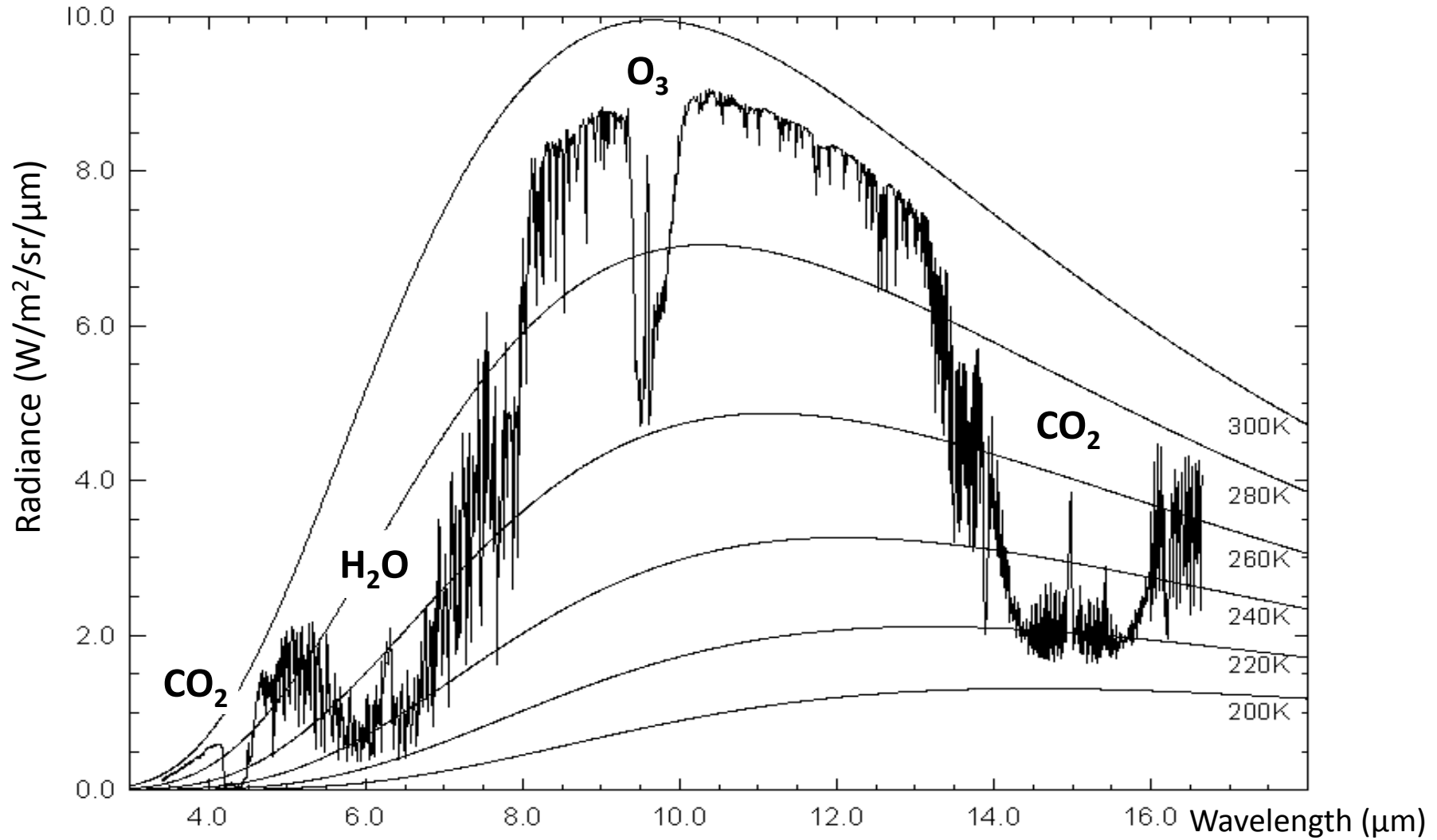
"Radiance $L_{sun,TOA,\lambda}(\Omega)$ due to {Earth, Atmosphere} scattering of sun radiation"

($L_{sun,TOA,\lambda}(\Omega) = 0$ at night, and usually neglected for $\lambda > 4\mu\text{m}$)

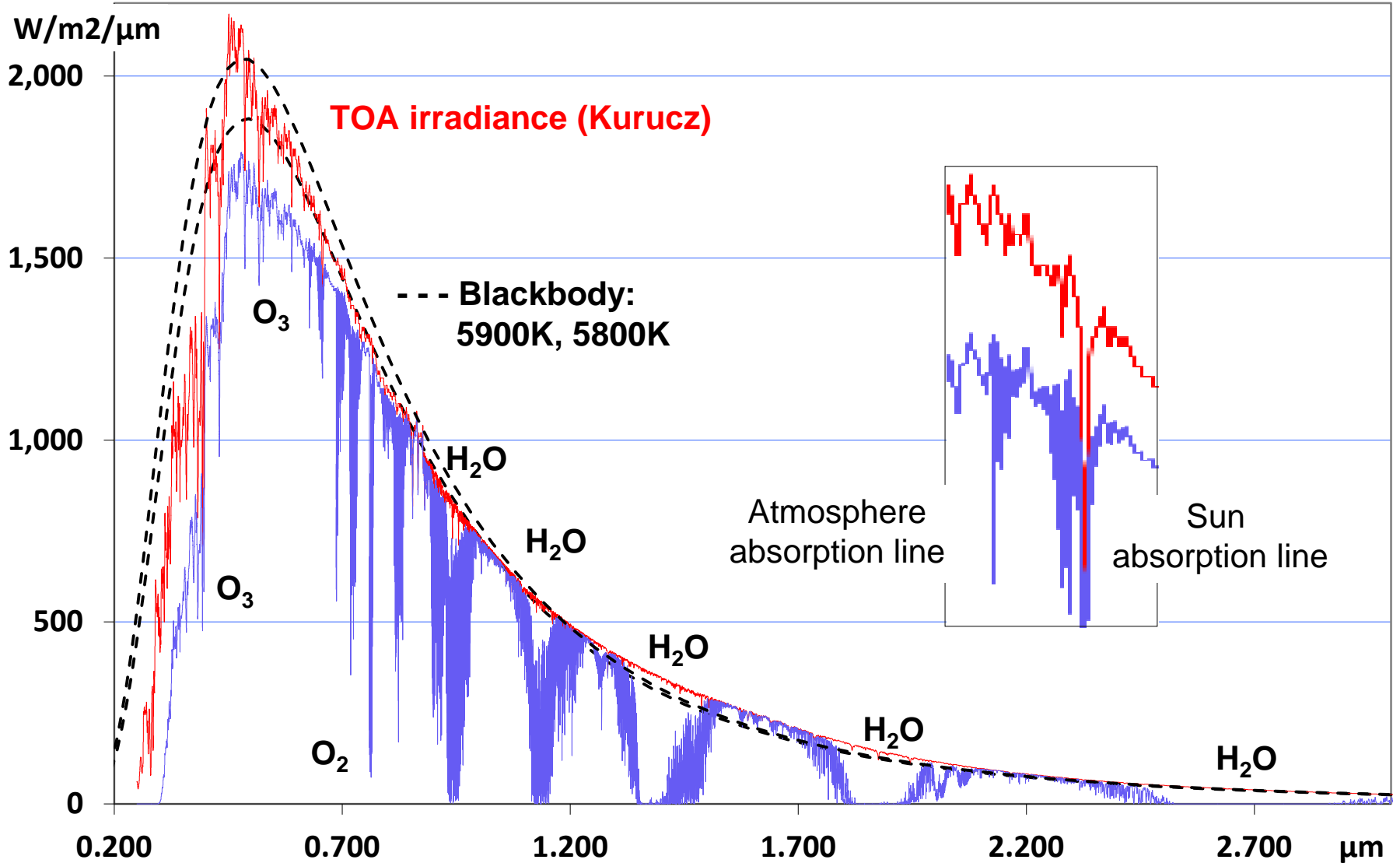


☞ Why does the atmosphere emits radiation in spectral regions where its transmittance is small?

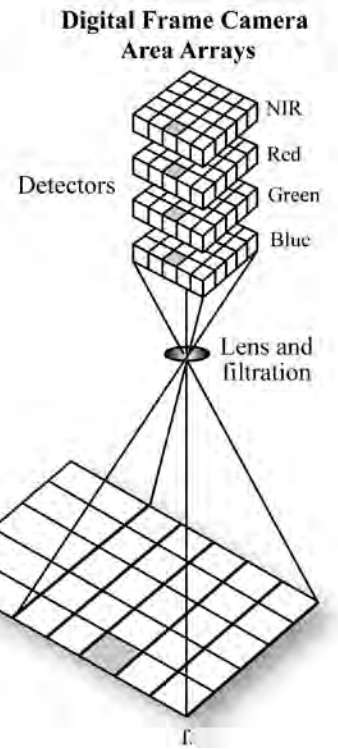
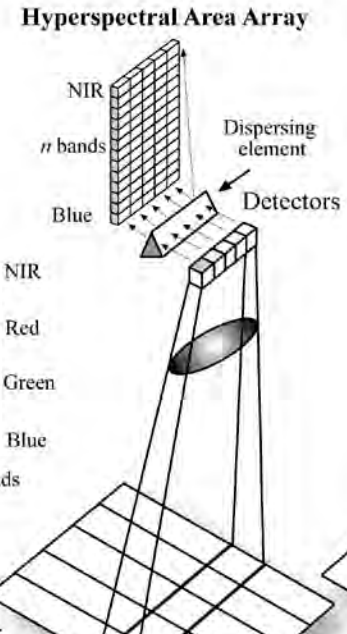
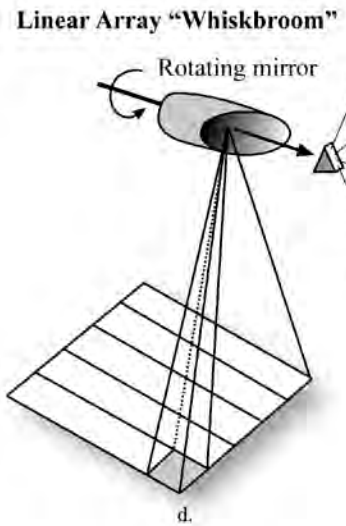
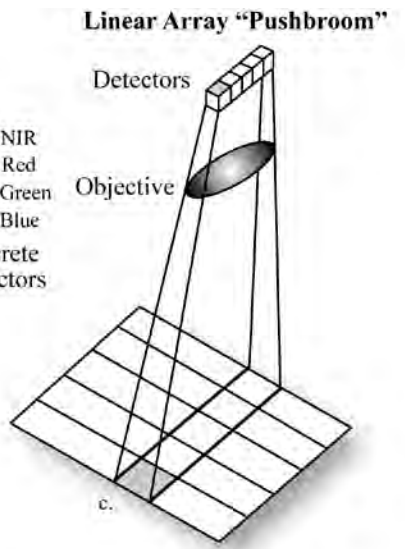
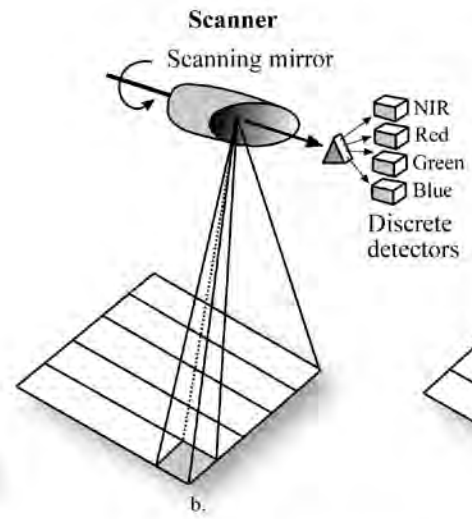
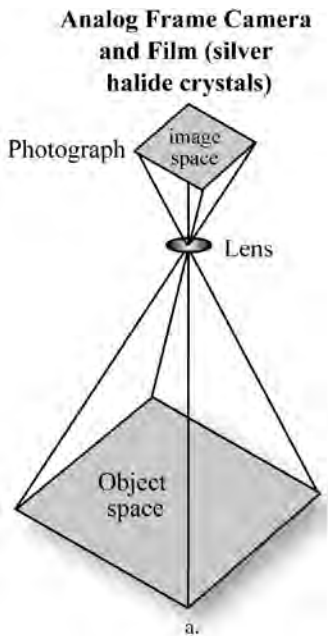
TOA radiance vs. Blackbody radiance (Planck's law)



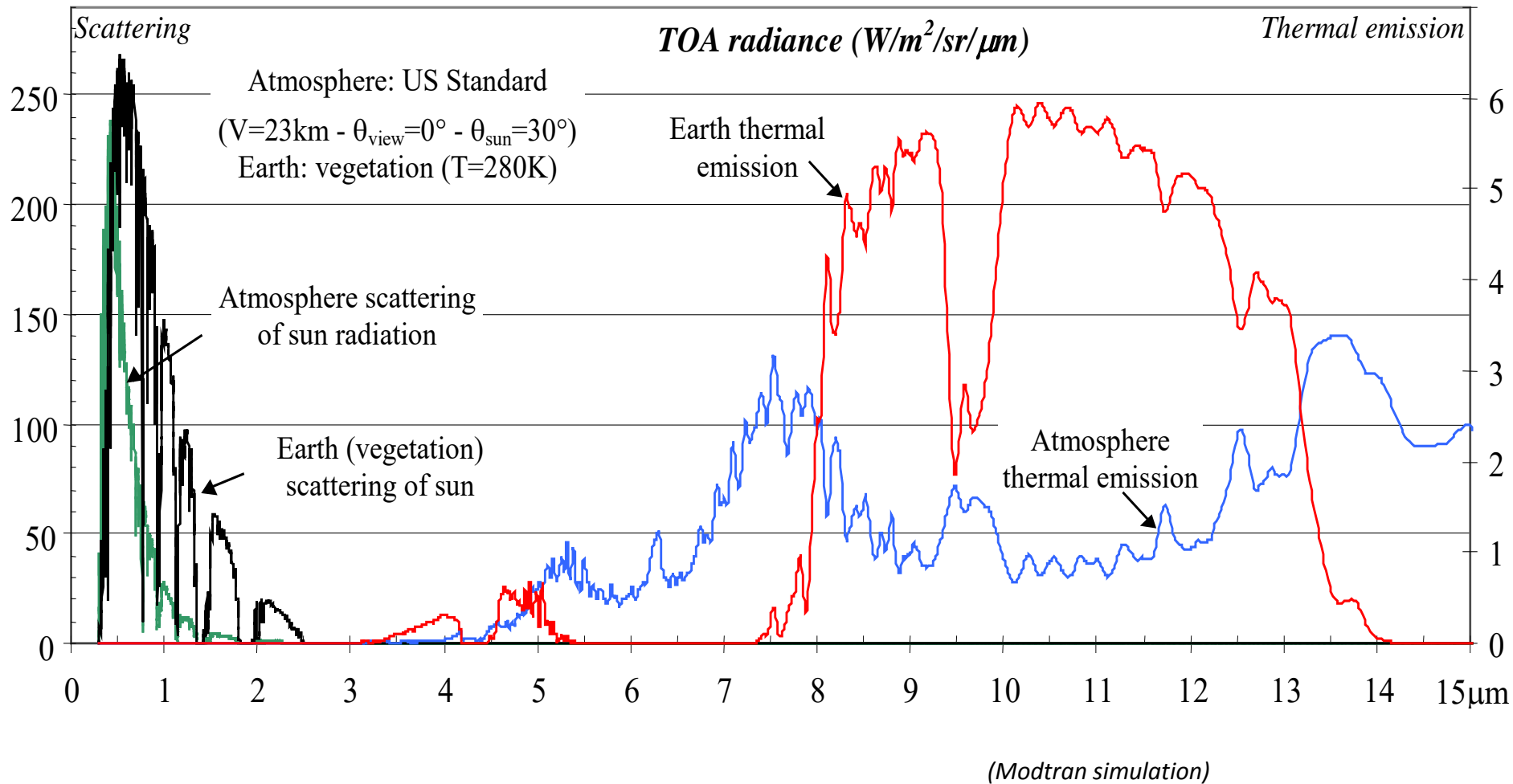
☞ Why does the "apparent" (brightness temperature) of the Earth change with wavelength?

TOA and BOA sun spectral irradiance

- Discrete detectors and scanning mirrors**
 MSS, TM, ETM+, GOES, AMS, AVHRR, SeaWiFS, ATLAS
- Linear Arrays**
 SPOT, IRS, IKONOS, ASTER, ORBIMAGE, Quickbird, MISR
- Liner and area arrays**
 AVIRIS, CASI, MODIS, ALI, Hyperion, LAC

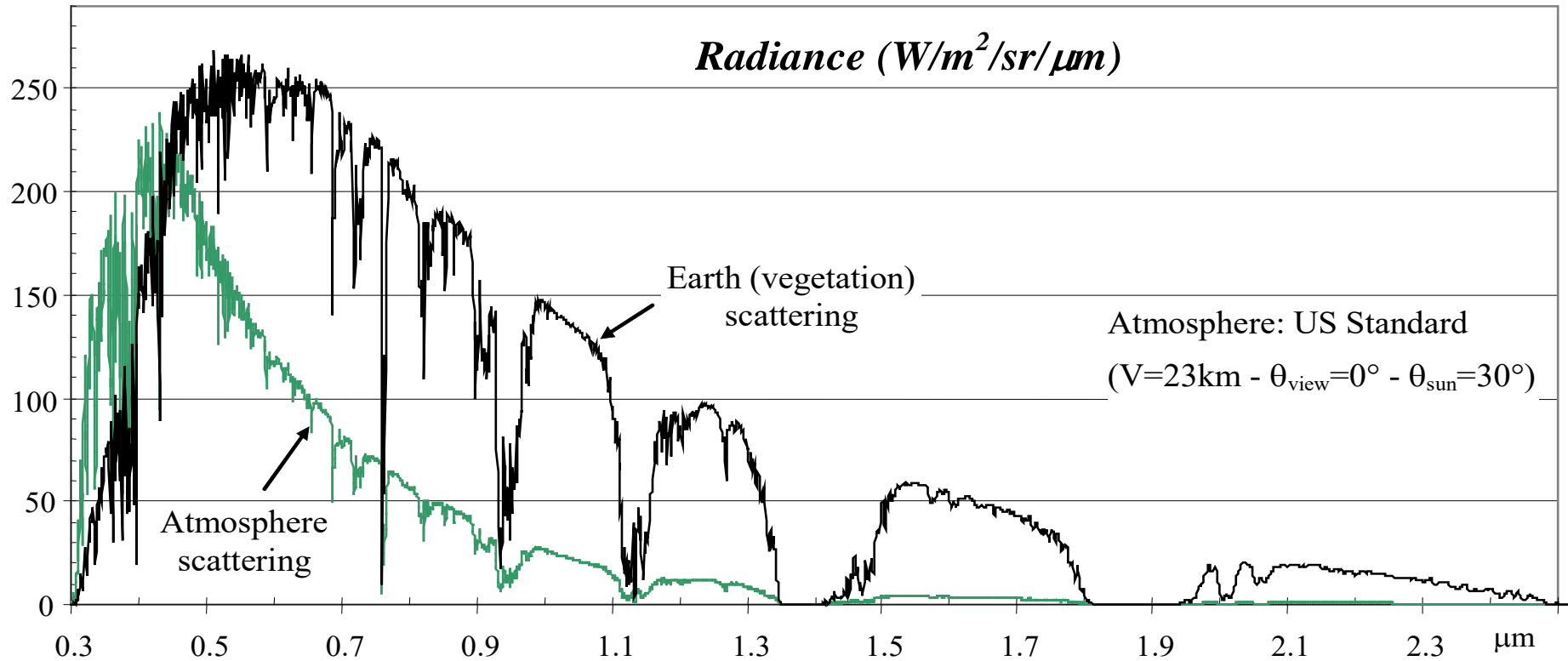


TOA radiance components: Earth and atmosphere scattering / thermal emission

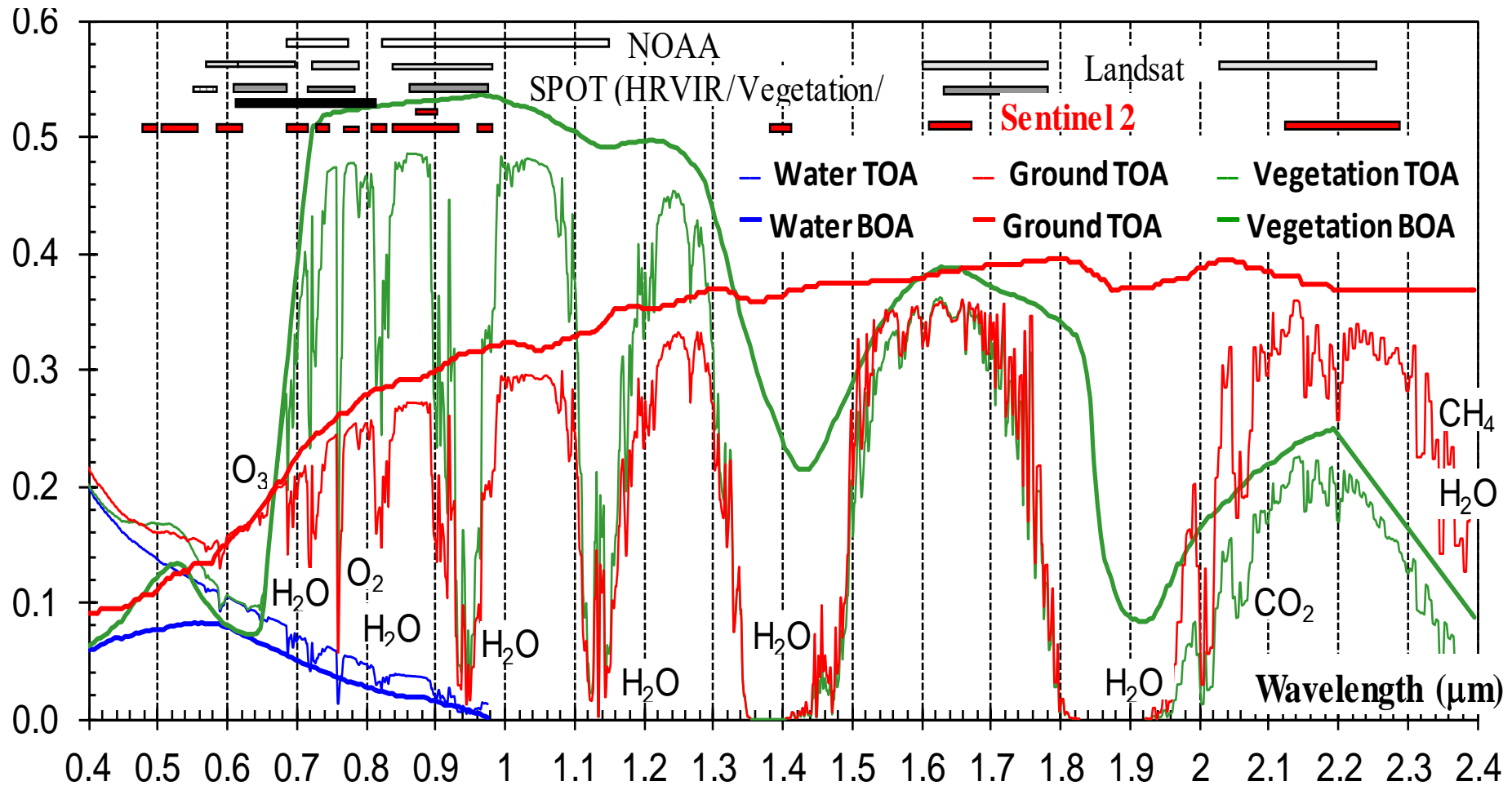


☞ For which wavelengths can we consider that TOA radiance is mostly due to either Earth surface scattering or thermal emission?

TOA radiance components: Earth and atmosphere scattering



👉 How the influence of atmosphere does change with (θ_v , θ_s , V , etc.)?

BOA and TOA spectra of **water**, **ground** and **vegetation**

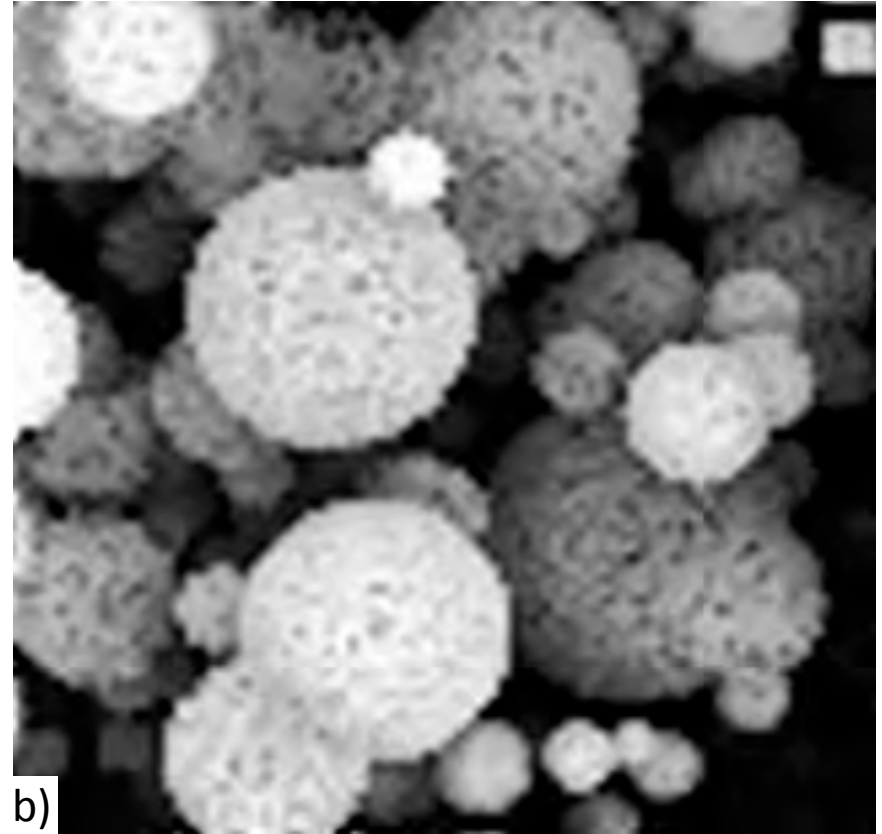
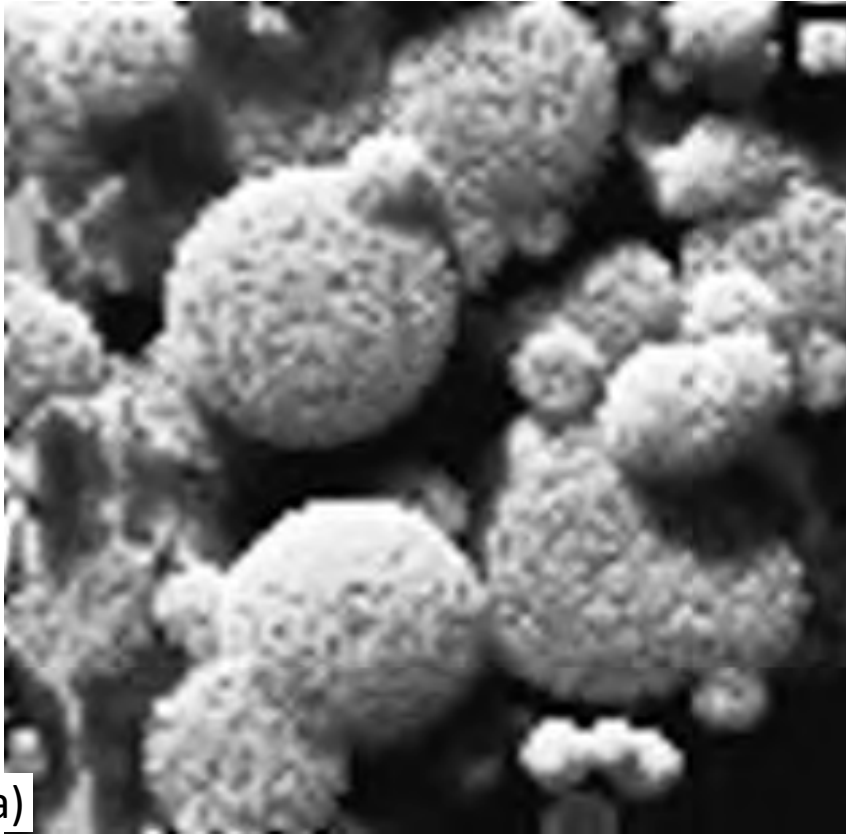
☞ For all surfaces, with $\lambda < 0.55\mu\text{m}$, $\rho_{\text{TOA}} > \rho_{\text{BOA}}$. Why?

☞ Why: - Ground: $\rho_{\text{TOA},g} > \rho_{\text{BOA},g}$ for $\lambda < 0.55\mu\text{m}$, and $\rho_{\text{TOA},g} < \rho_{\text{BOA},g}$ for $\lambda > 0.65\mu\text{m}$,

- Water: $\rho_{\text{TOA},w} > \rho_{\text{BOA},w}$ at all wavelengths.

Sky illumination: nadir image of a tropical forest (Sumatra, Indonesia) with 2 sky illuminations

DART simulations



a) SKYL = 0, $\theta_s = 35^\circ$. b) SKYL = 1. $SKYL = \frac{\text{Atmosphere irradiance}}{\text{Total irradiance}}$. Simulations with DART model.

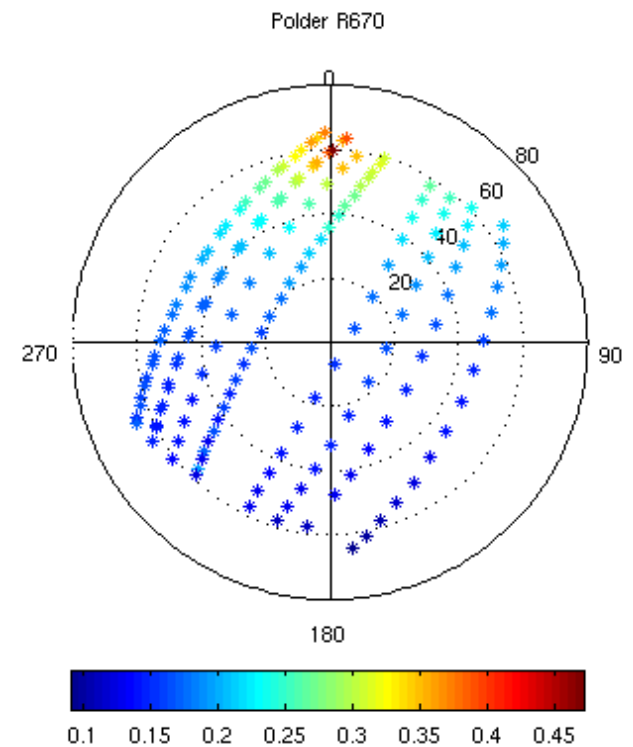
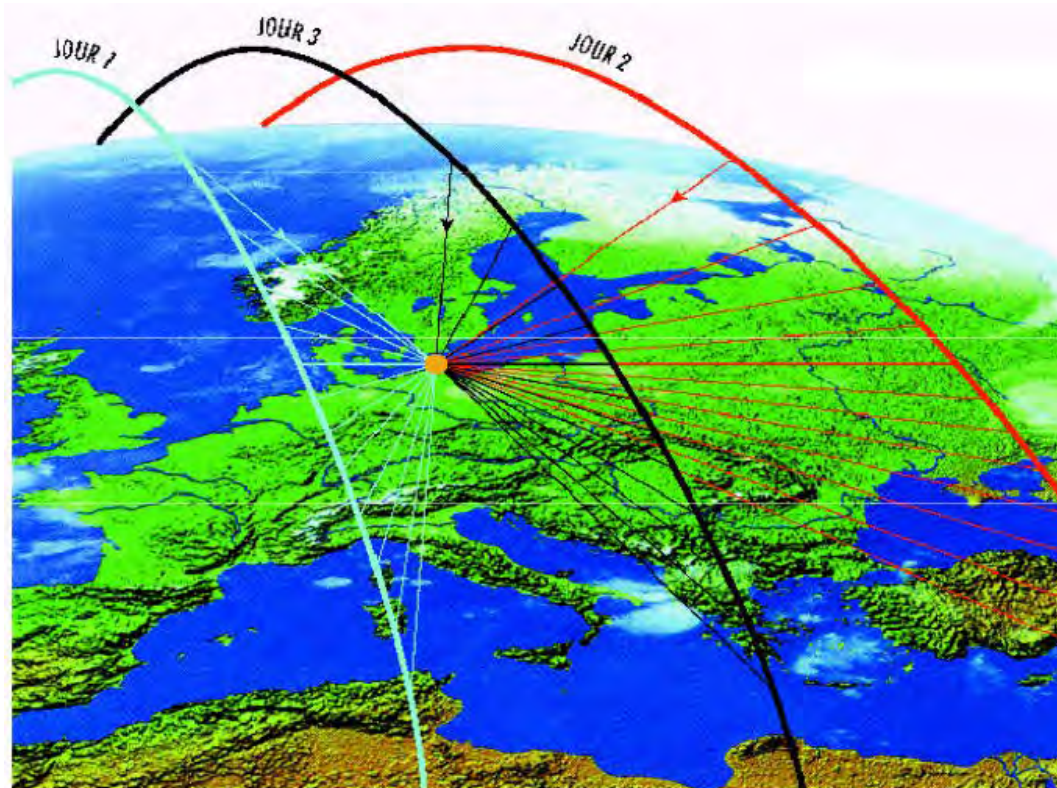
☞ Does a SKYL increase, makes the reflectance of Earth surfaces larger, more anisotropic?

View direction: **POLDER** (Polarization and Directionality of Earth Reflectances) - **114° FOV, 6km**

The anisotropy of the Earth surfaces reflectance ρ strongly affects TOA radiance.

ρ : described by BRDF or Bidirectional Reflectance Distribution Function (BRDF)

BRDF = function of sun direction (θ_s, ϕ_s) & view direction (θ_v, ϕ_v) . In practice: $\rho(\theta_s, \theta_v, \phi_s - \phi_v)$

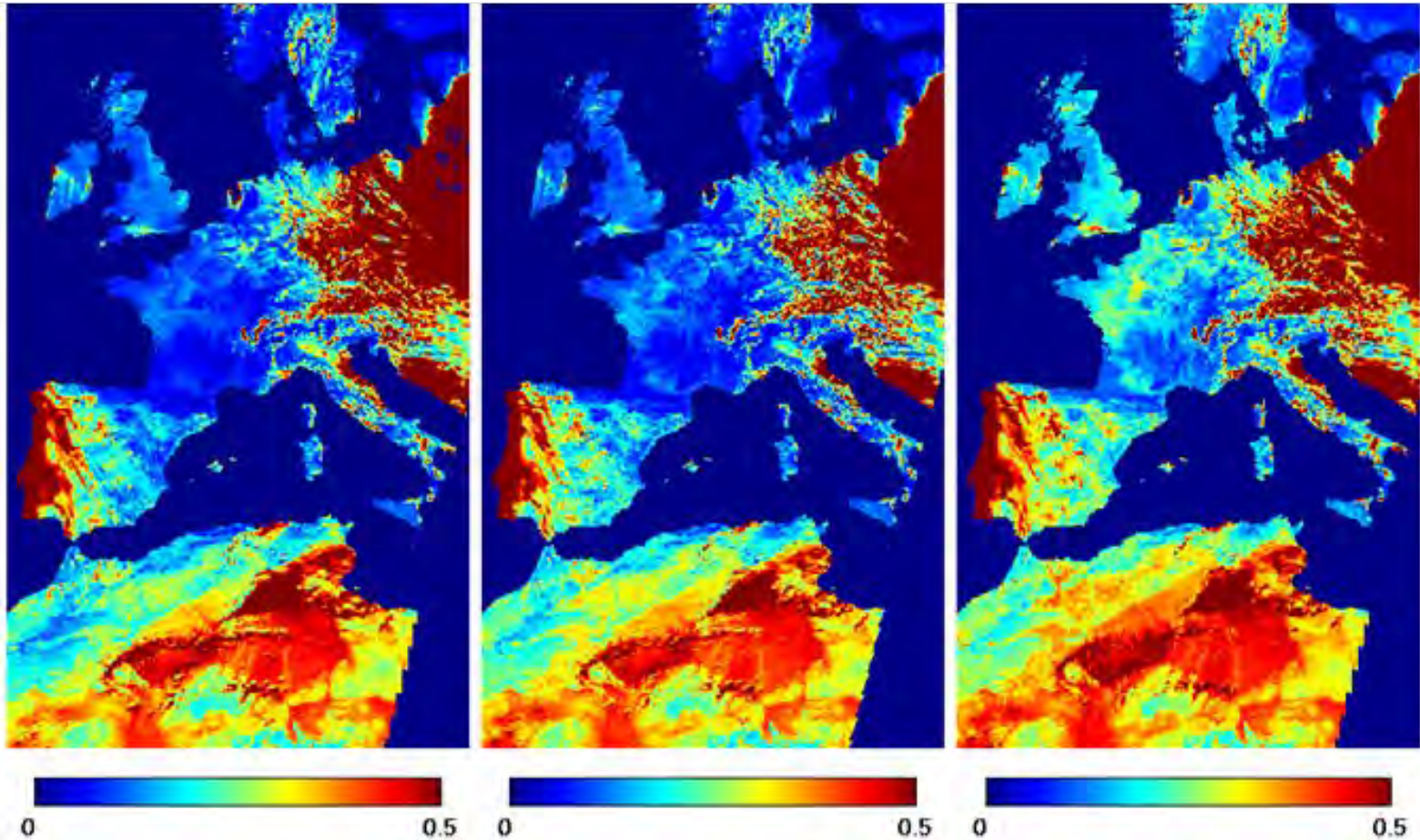


(E. Vermote, C. Justice and Breon,
NASA supported Land LTDR Project)

Back

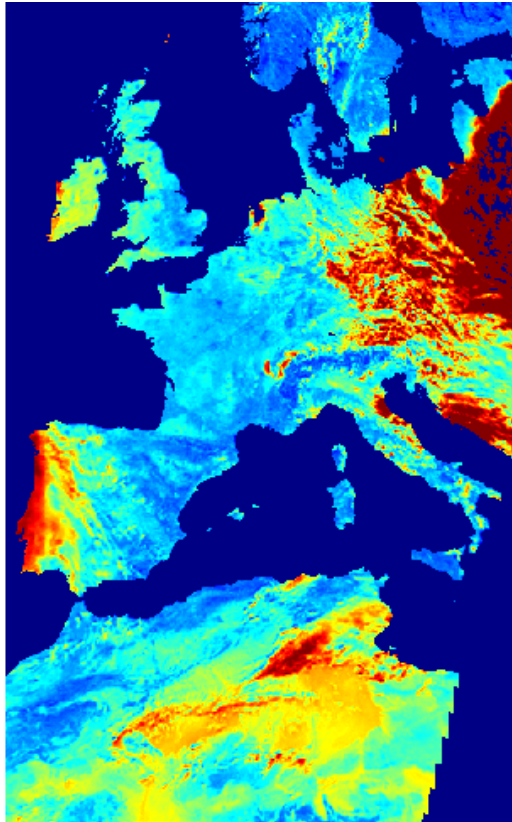
Nadir

Forward

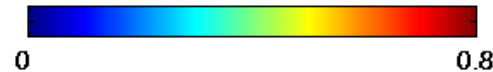
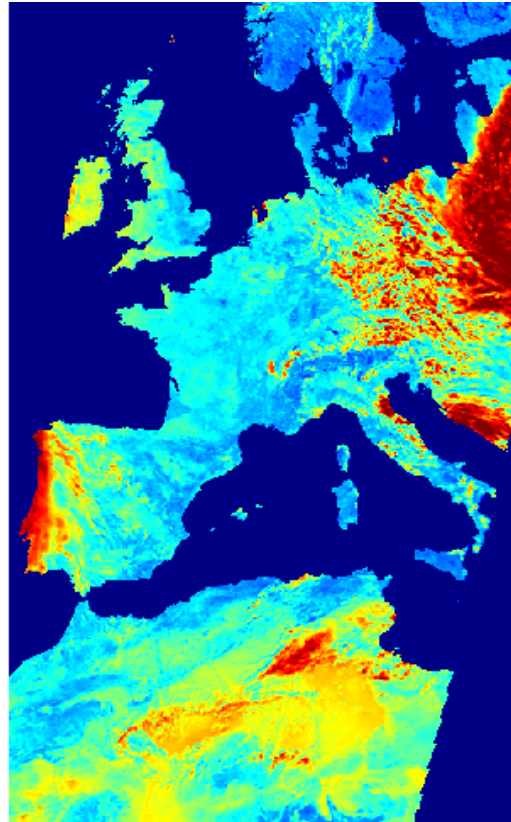


- ☞ Which elements do have the larger reflectance value (reddish tones)?
- ☞ Why does reflectance change with view direction with a maximum in the forward direction?

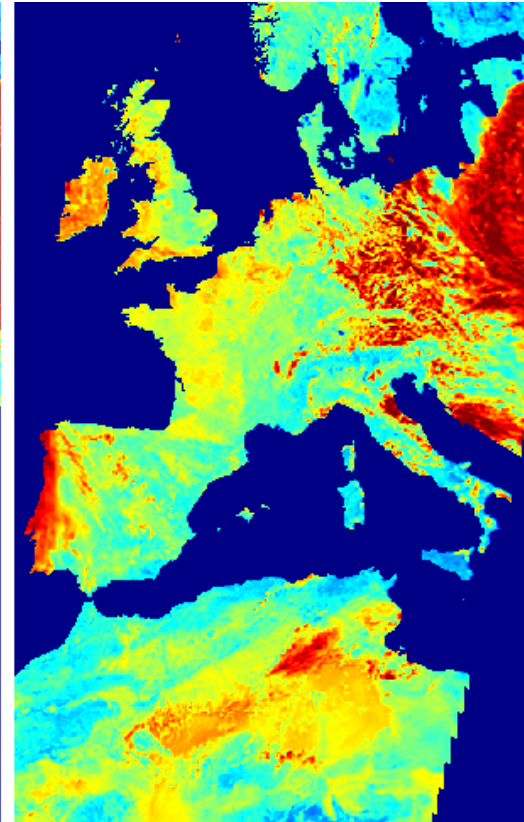
Back



Nadir



Forward



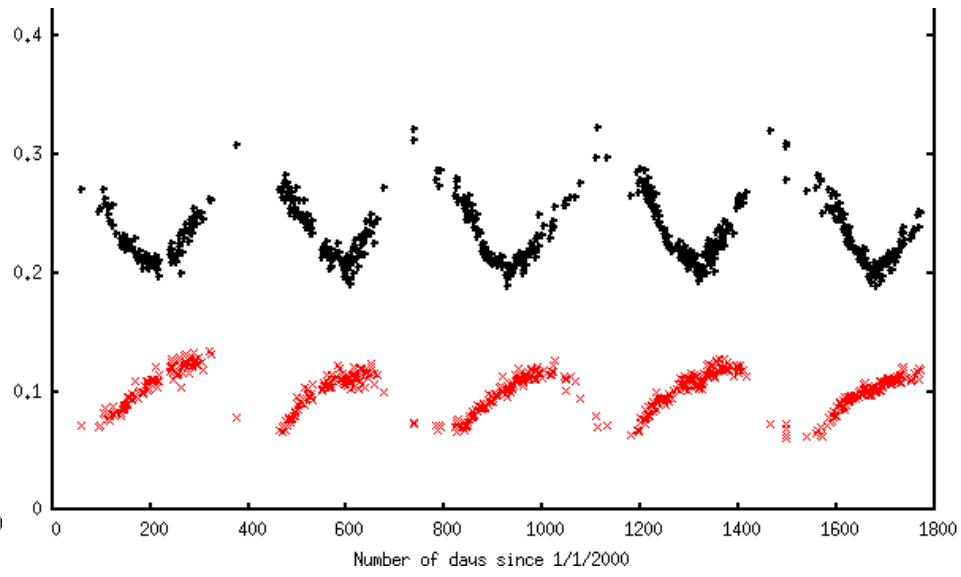
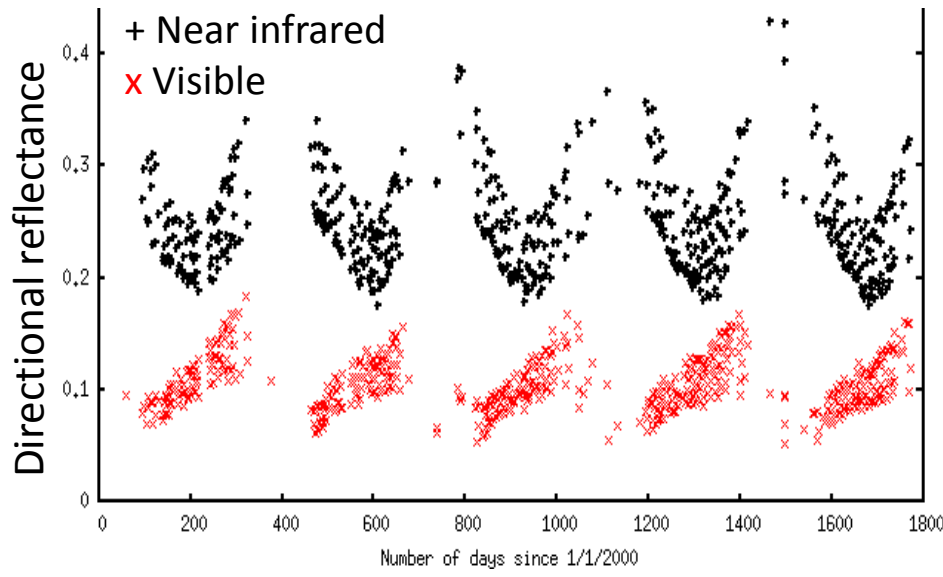
☞ For which configuration, a schematic landscape {bare ground + trees} has a strongly anisotropic reflectance with a maximum at nadir. Same, with minimum at nadir.

MODIS daily VIS / NIR surface reflectance: south Africa tropical savanna, 2000-2004

Not normalized reflectance

Normalized reflectance (using BRDF model calibrated with POLDER data)

⇒ Reflectance accuracy is much improved



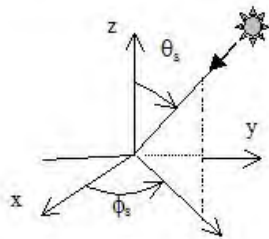
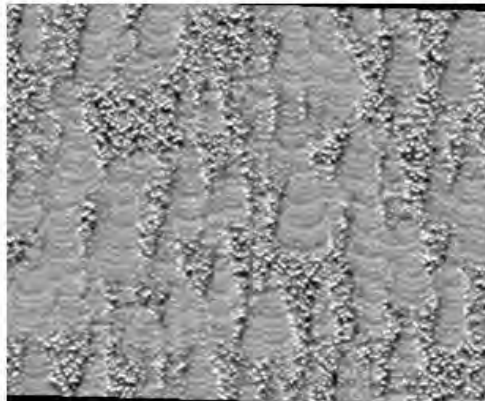
(E. Vermote, C. Justice and Breon, NASA supported Land LTDR Project)

☞ Does the variability of Earth surface reflectance increase or decrease if satellite spatial resolution coarsens?

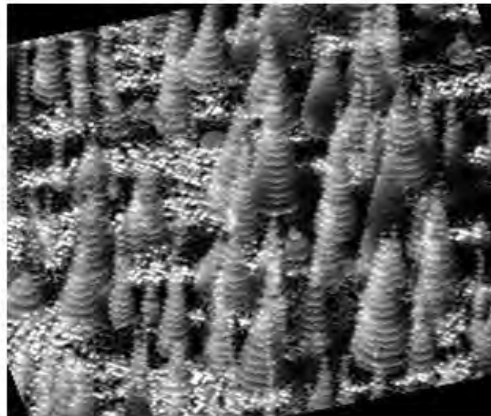
OLD BLACK SPRUCE

- DART SIMULATIONS: NIR -

Hot spot ($\rho_{PIR} \approx 0.287, \theta_v = 35^\circ, \phi_v = 0^\circ$)

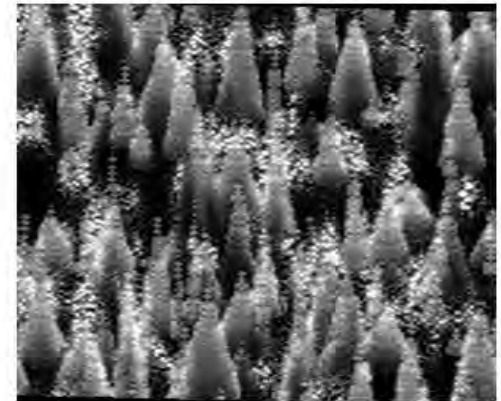
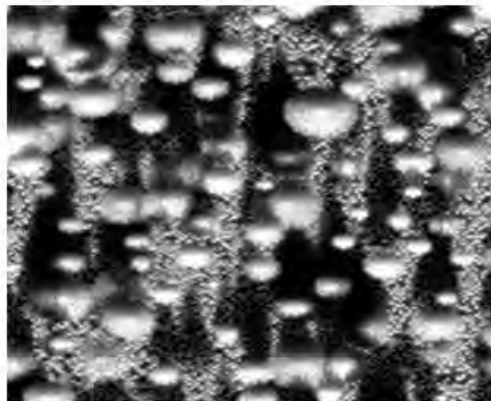


Sun direction: $\theta_s = 35^\circ, \phi_s = 0^\circ$



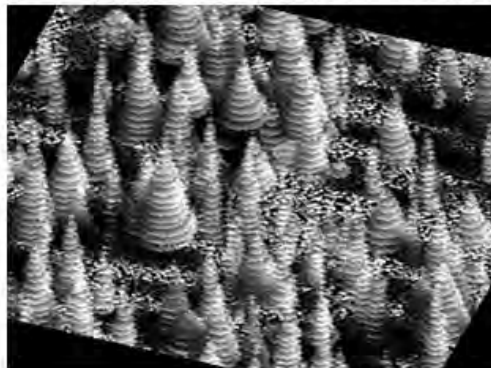
($\rho_{PIR} \approx 0.168, \theta_v = 35^\circ, \phi_v = 72^\circ$)

($\rho_{PIR} \approx 0.156, \theta_v = 35^\circ, \phi_v = 180^\circ$)

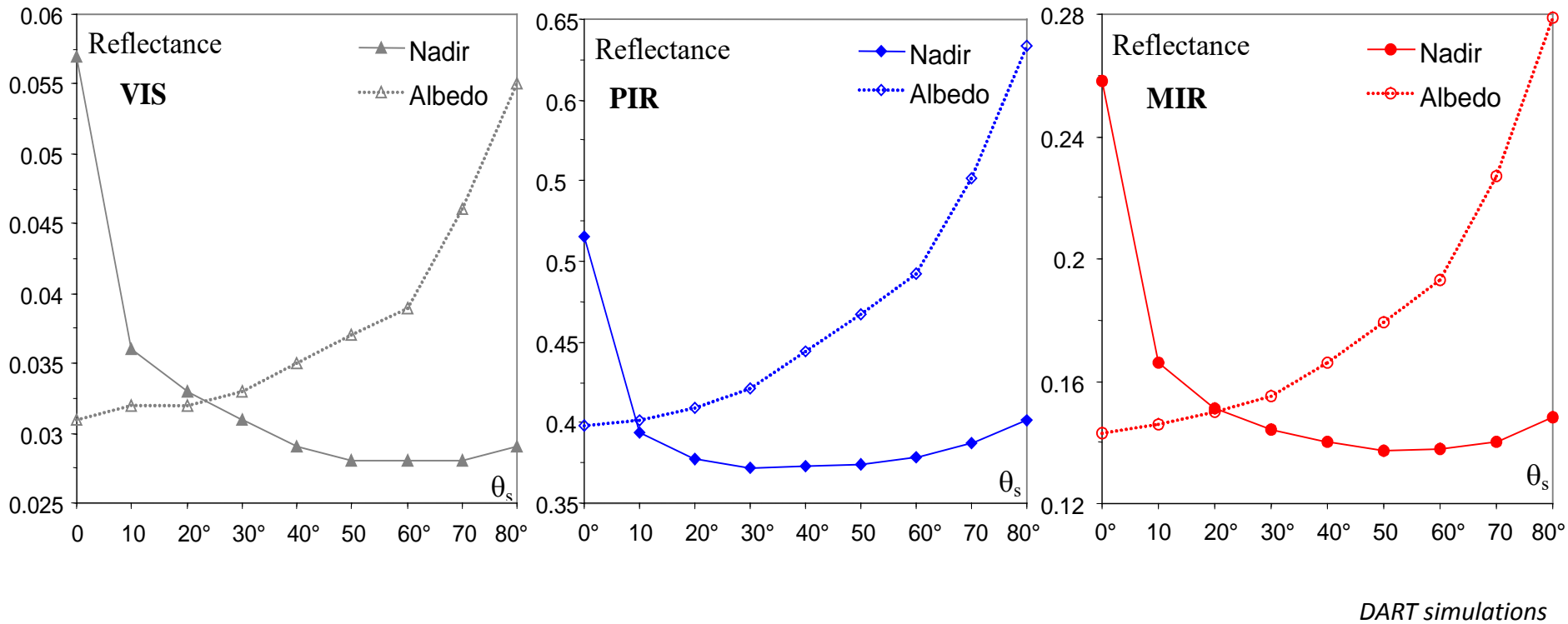


Nadir ($\rho_{PIR} \approx 0.147, \theta_v = 0^\circ$)

($\rho_{PIR} \approx 0.173, \theta_v = 35^\circ, \phi_v = 288^\circ$)

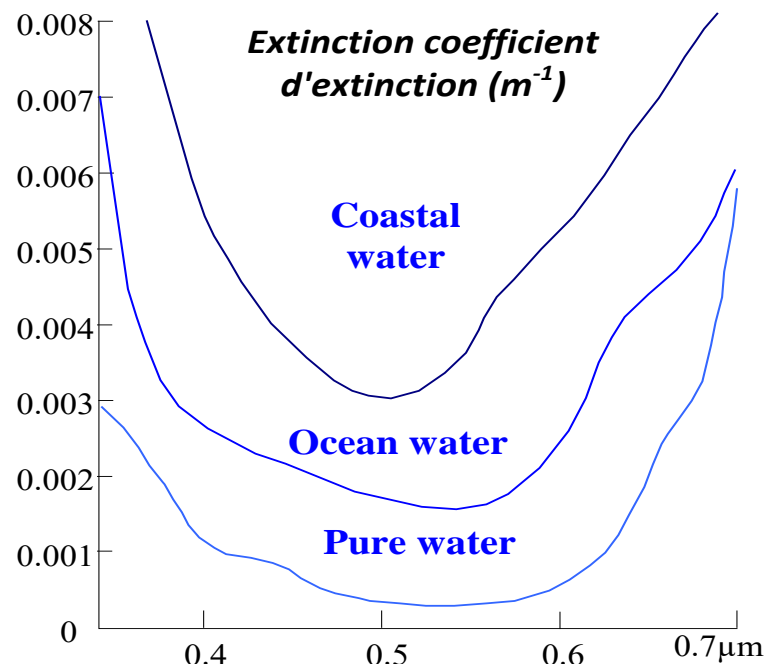
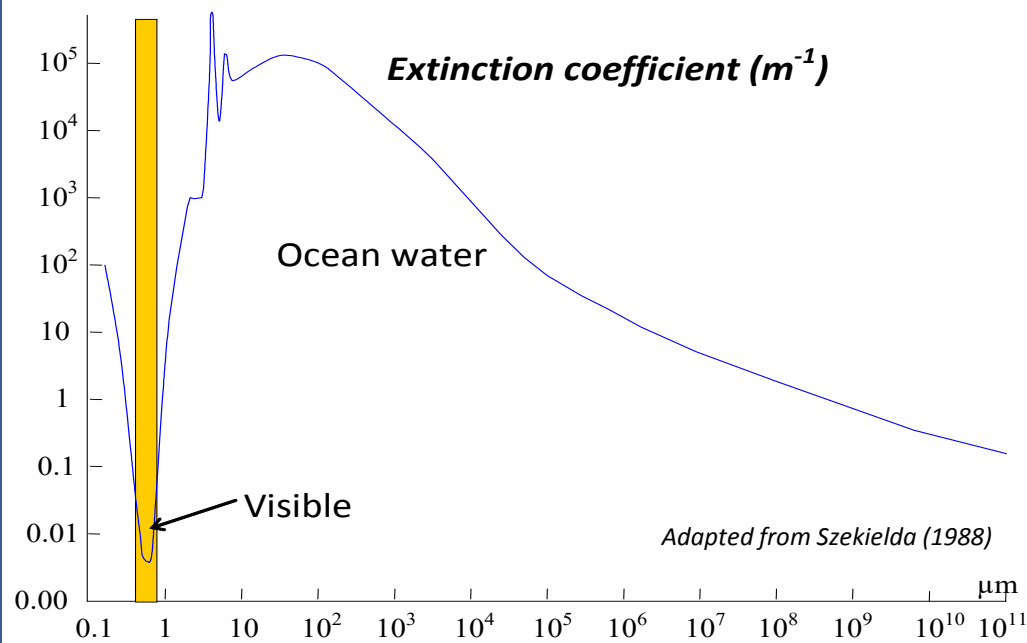
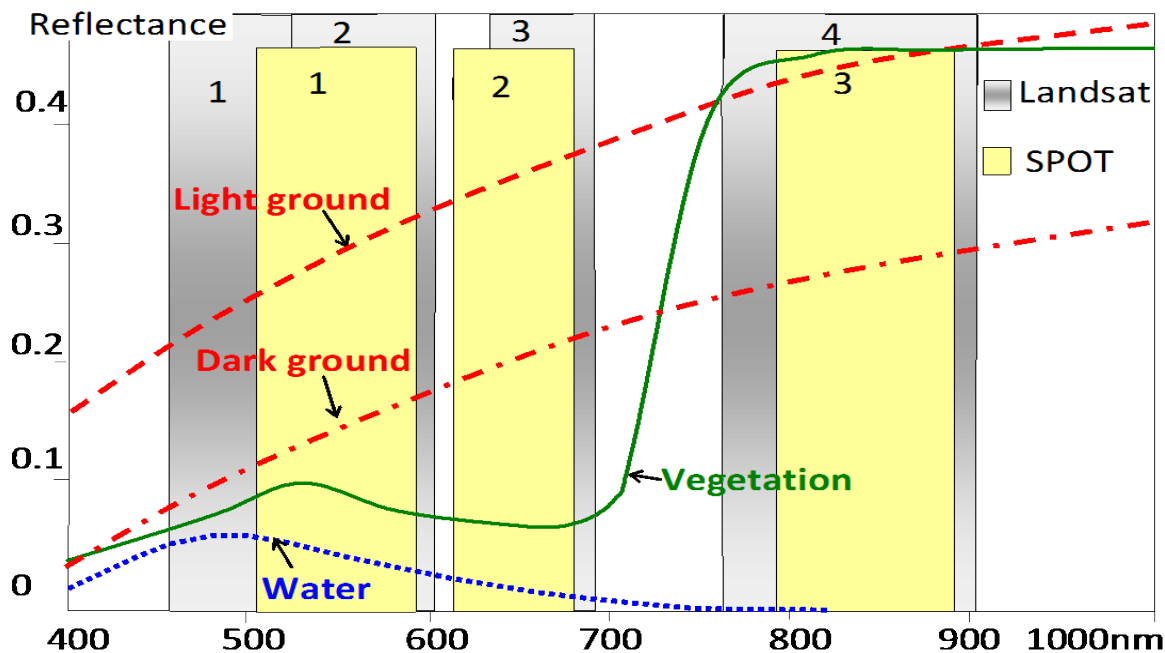


Reflectance varies from
0.147 to 0.287!!!

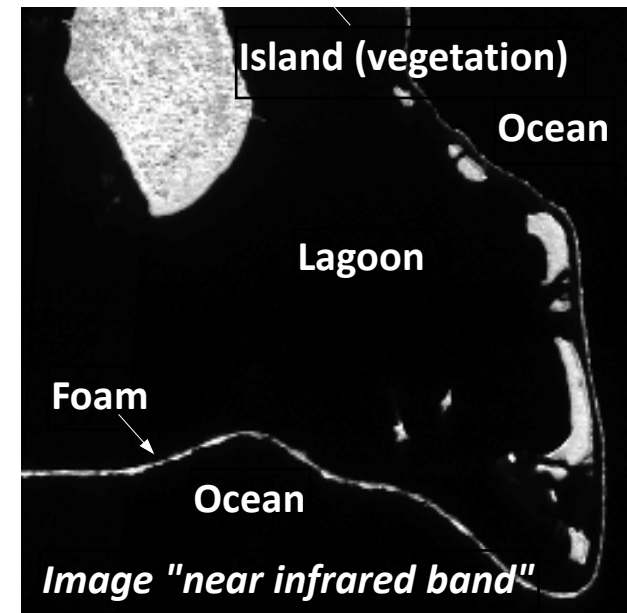
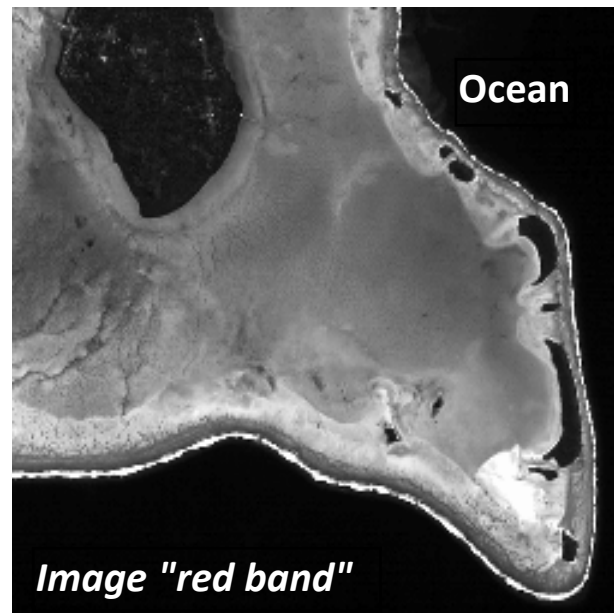
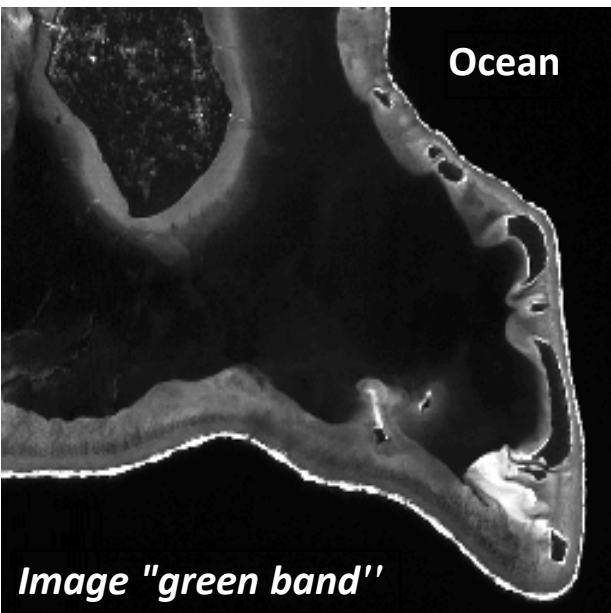


👉 Nadir reflectance and albedo values can differ a lot. Hence, to approximate the Earth surface albedo as a directional reflectance value can be very erroneous.

Spectral analysis: reflectance (ground, water, vegetation) and extinction coefficient (water)



Spectral analysis: Aitutaki (Cook island) BOA radiance images (grey tone proportional to radiance)

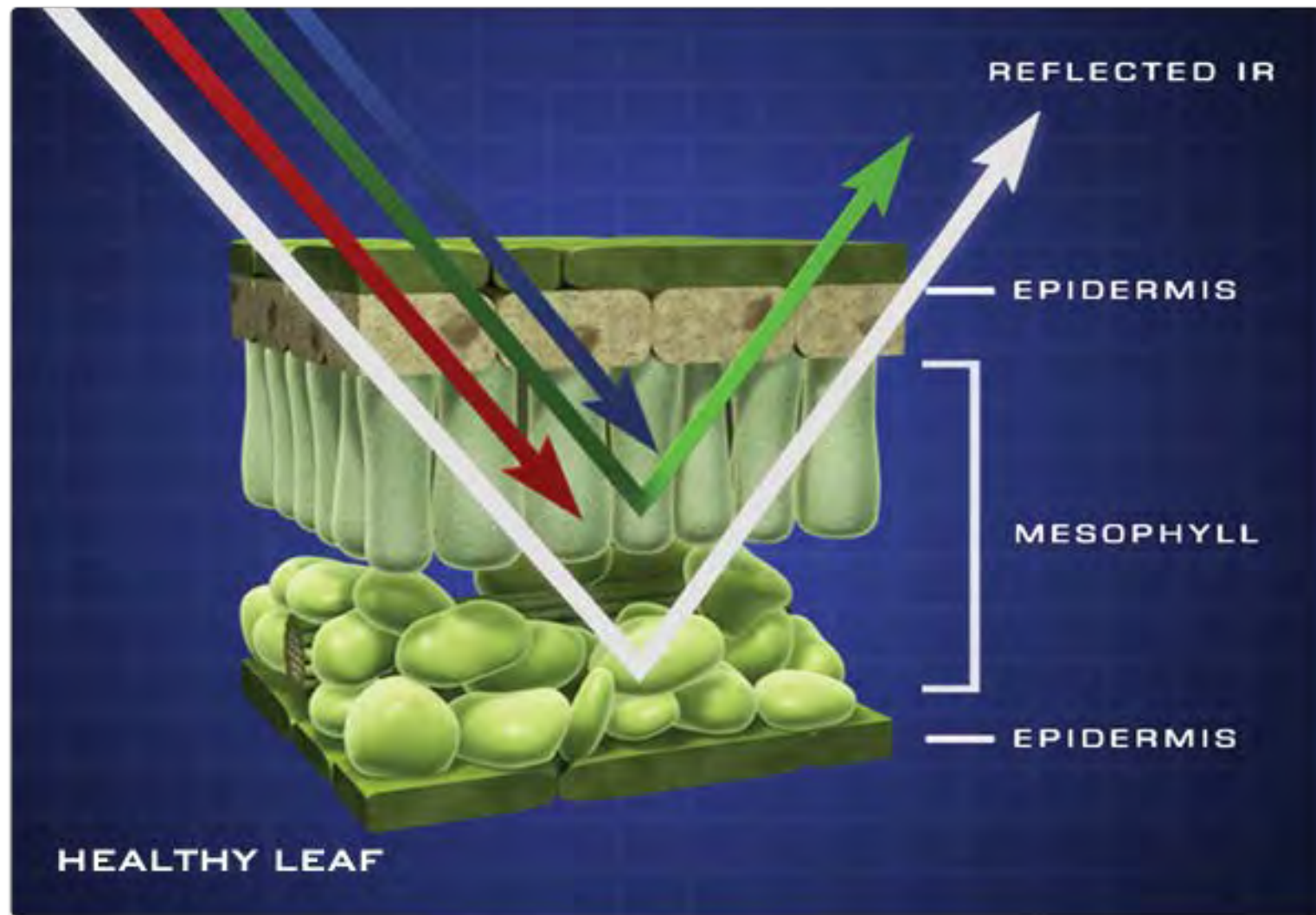


Hypotheses: same water in ocean & lagoon, vegetated islands.

Why :

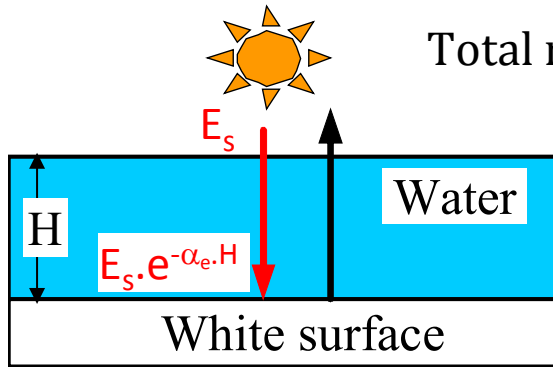
- Ocean: dark tone in 3 images (darker in NIR image)?
- Island: dark tone in "green" & "red", and light tone in "NIR"?
- Foam: light tone in 3 images, conversely to water surfaces?
- Lagoon: light tone in "red" band, conversely to the ocean?

Foam scattering: large reflectance due to multiple scattering



Reflectance of a fluid (water) volume

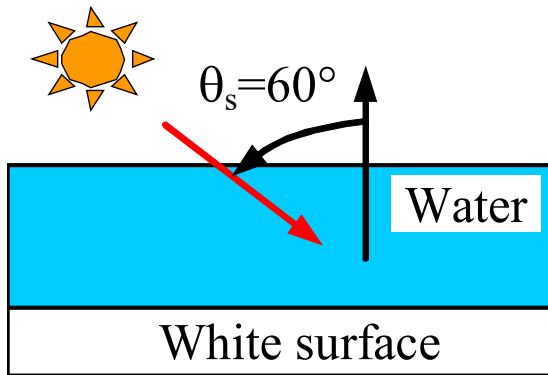
Objective: to manipulate extinction coefficient α_e and Beer law $e^{-\alpha_e \Delta l}$ along path Δl



Total reflectance: $\rho = \rho_{white\ surface} \cdot e^{-\alpha_e \Delta l} = \rho_{white\ surface} \cdot e^{-\alpha_e \cdot 2 \cdot H}$

Depth H	0.5 - 0.6 μm	0.6 - 0.7 μm	0.7 - 0.8 μm	0.8 - 1.1 μm
1 m	$\rho = 92\%$	$\rho = 55\%$	$\rho = 9\%$	$\rho = 0.2\%$
5 m	$\rho = 67\%$	$\rho = 5\%$	$\rho = 0\%$	$\rho = 0\%$
α_e (m^{-1})	0.04	0.30	1.2	3.1

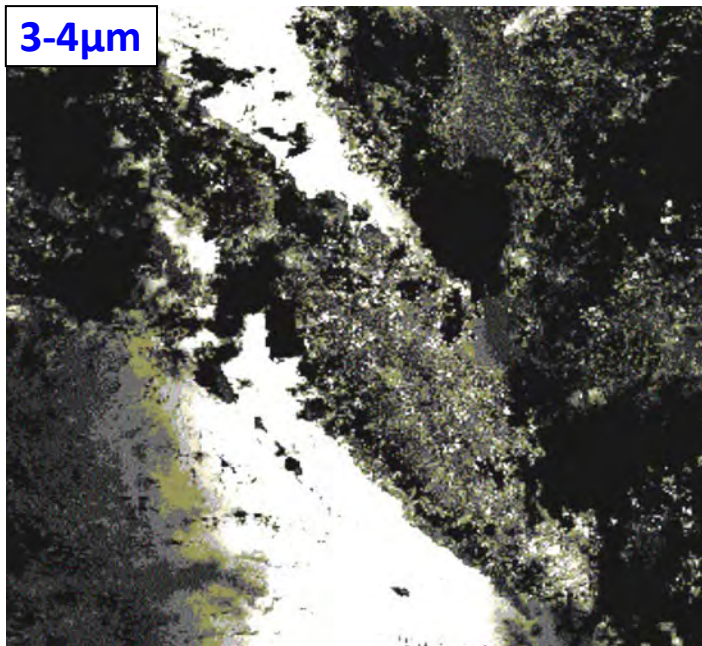
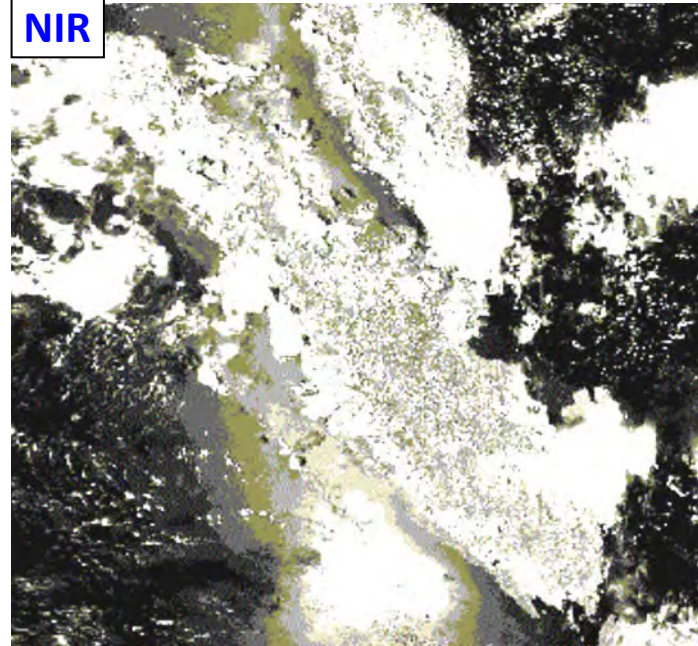
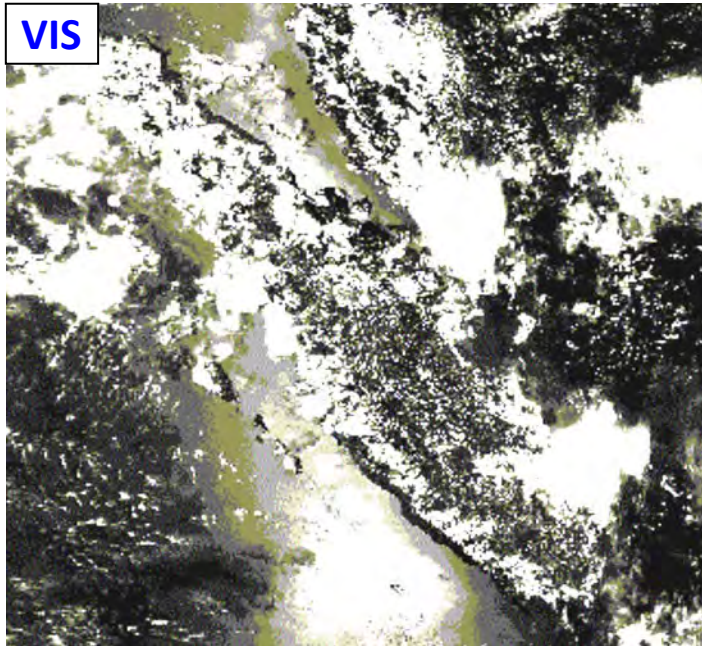
☞ Compute reflectance ρ for a sun direction with a zenith angle equal to 60°



Depth H	0.5 - 0.6 μm	0.6 - 0.7 μm	0.7 - 0.8 μm	0.8 - 1.1 μm
1m	$\rho = 89\%$	$\rho = 68\%$	$\rho = 28\%$	$\rho = 4\%$
5m	$\rho = 55\%$	$\rho = 15\%$	$\rho = 0.17\%$	$\rho = 1\text{E-}07\%$

$$\rho = \rho_{white\ surface} \cdot e^{-\alpha_e H} \cdot e^{-\alpha_e \frac{H}{\cos(60^\circ)}}$$

Spectral analysis: NOAA images (grey tone proportional to radiance) – Sumatra island, 1993

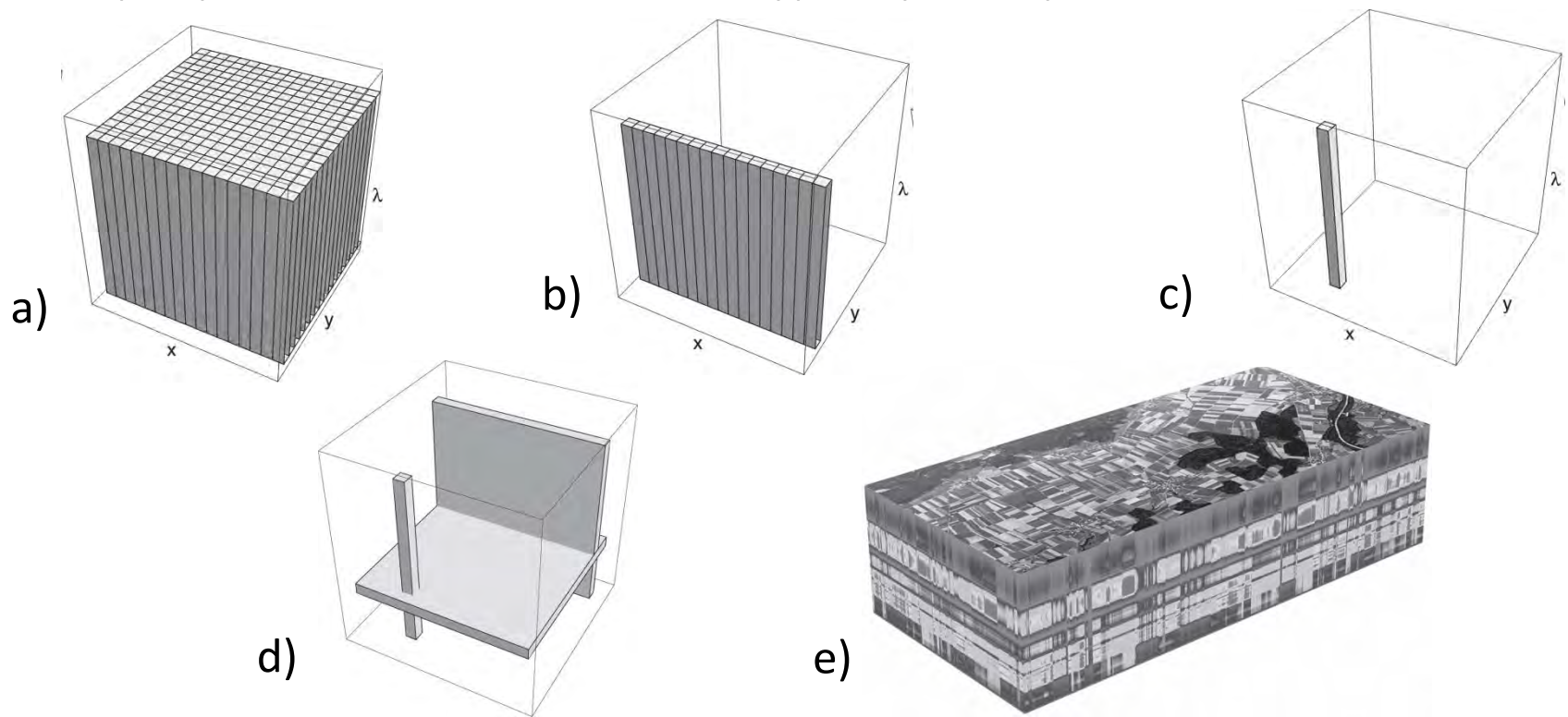


Why:

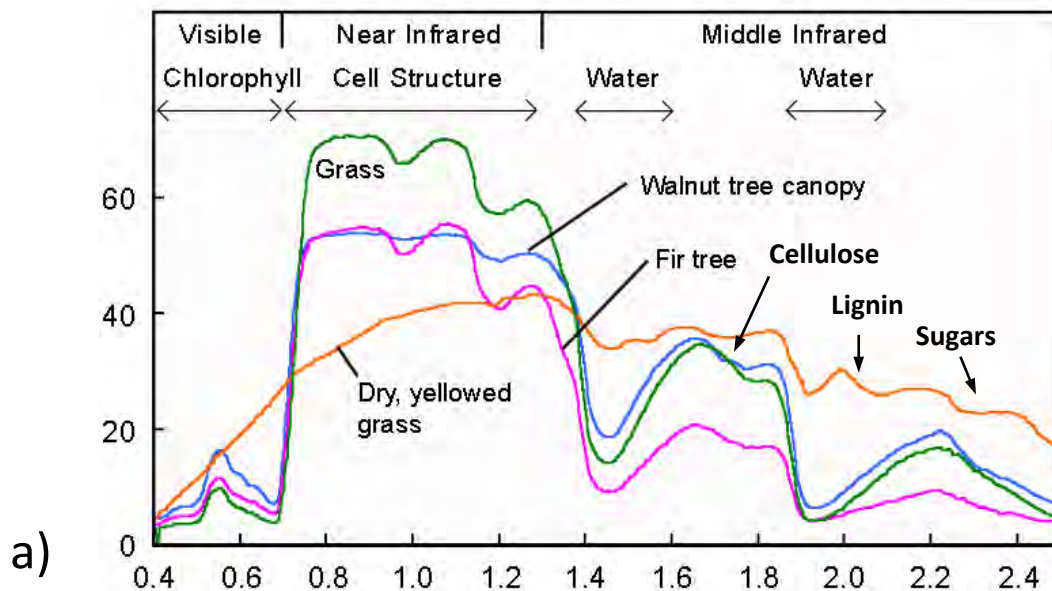
- Sumatra has dark tones in the VIS image and light tones in the NIR image?
- Clouds have light tones in the VIS image and dark tones in the "3-4 μ m" image
- In the VIS image, the bright spot below South Sumatra is not a cloud. What is it?

Hyperspectral sensor: simultaneous acquisition of spatially co-registered images, in many spectrally contiguous bands, measured in calibrated radiance units, from a remotely operated platform (Schaepman *et al.* 2006)

Many contiguous narrow spectral bands are necessary for sampling correctly landscape spectral features of interest, typically absorption bands.

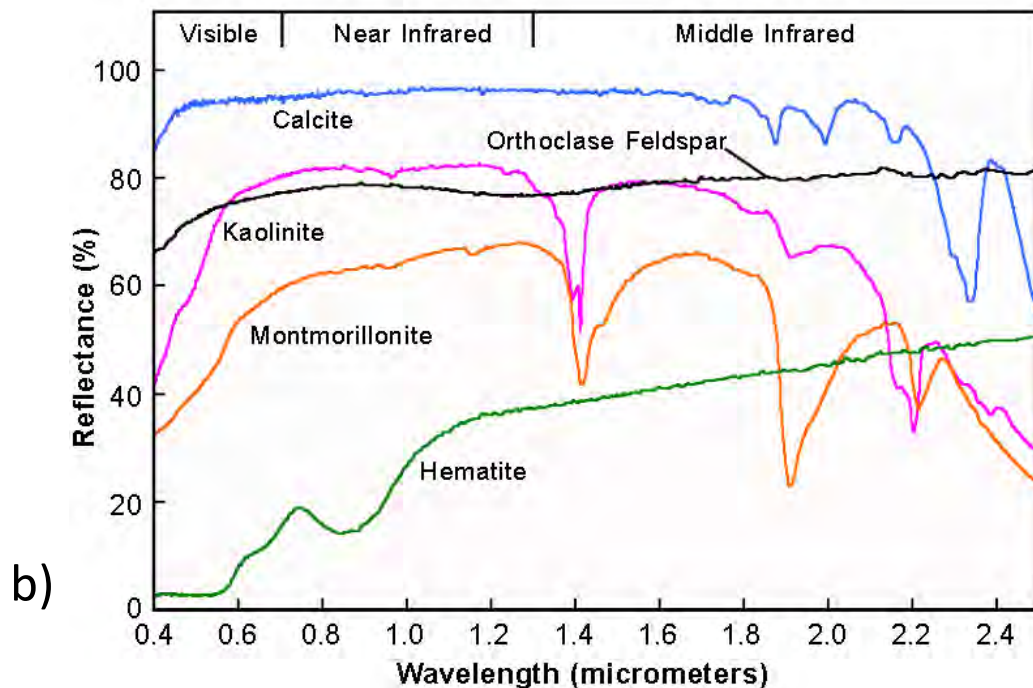


Conceptual imaging spectrometer data cube: 2 spatial (x, y) and 1 spectral (λ) domains. Typically acquired by a whiskbroom scanning system. a) The data cube. b) 1 scan line. c) 1 pixel. d) Pixel, spectral image and scan line. e) Actual data cube.



Typical spectra with absorption bands.

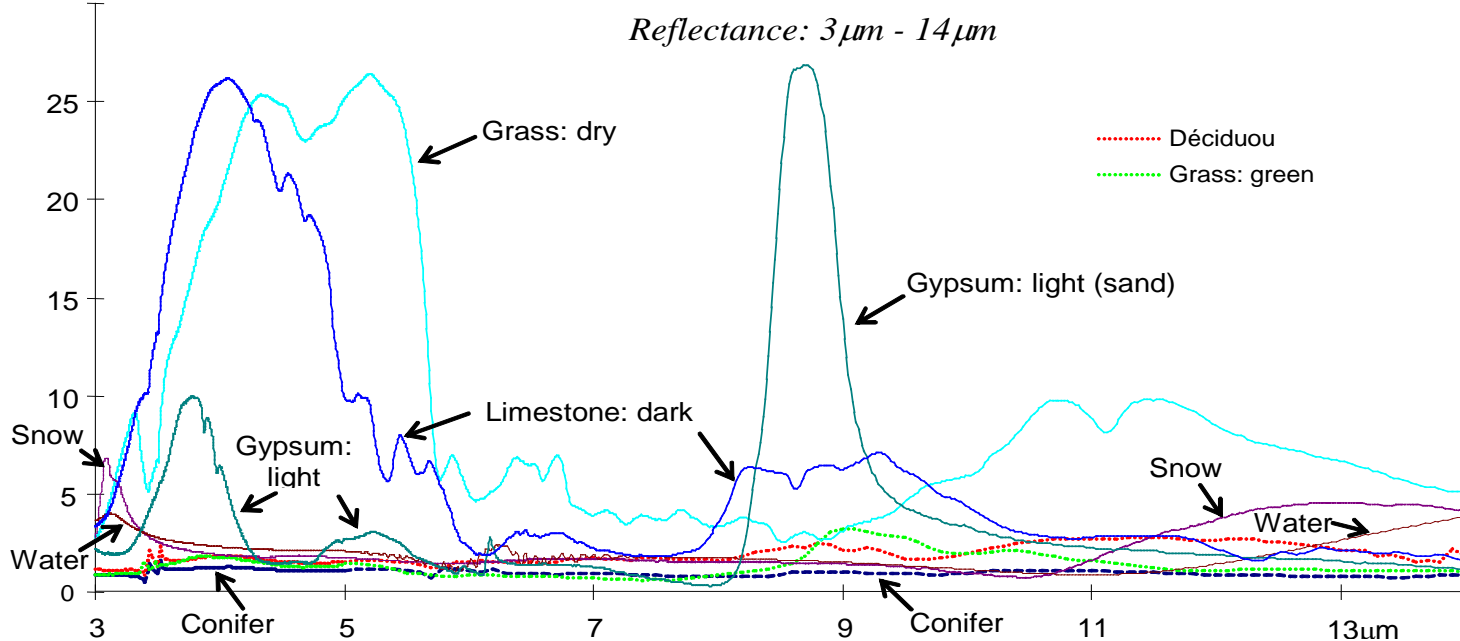
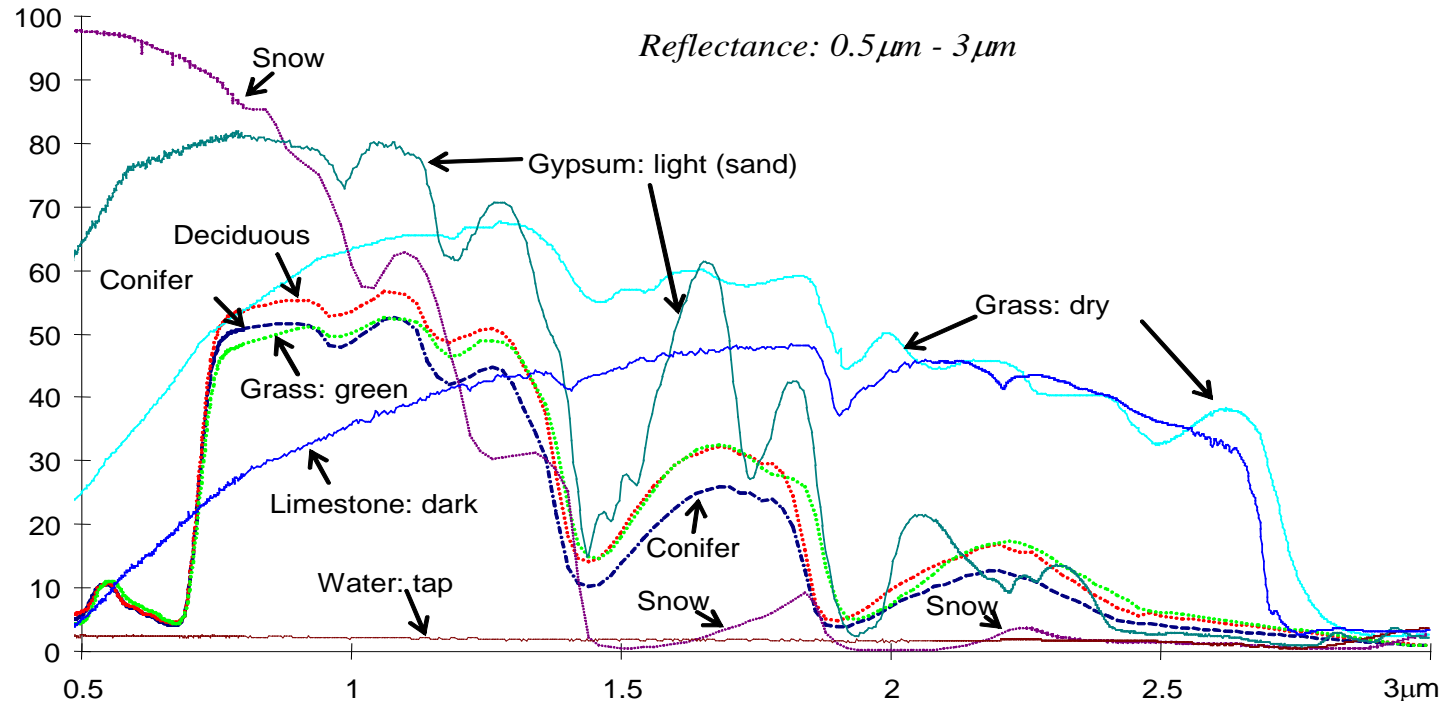
a) **Vegetation** at different growth stages.



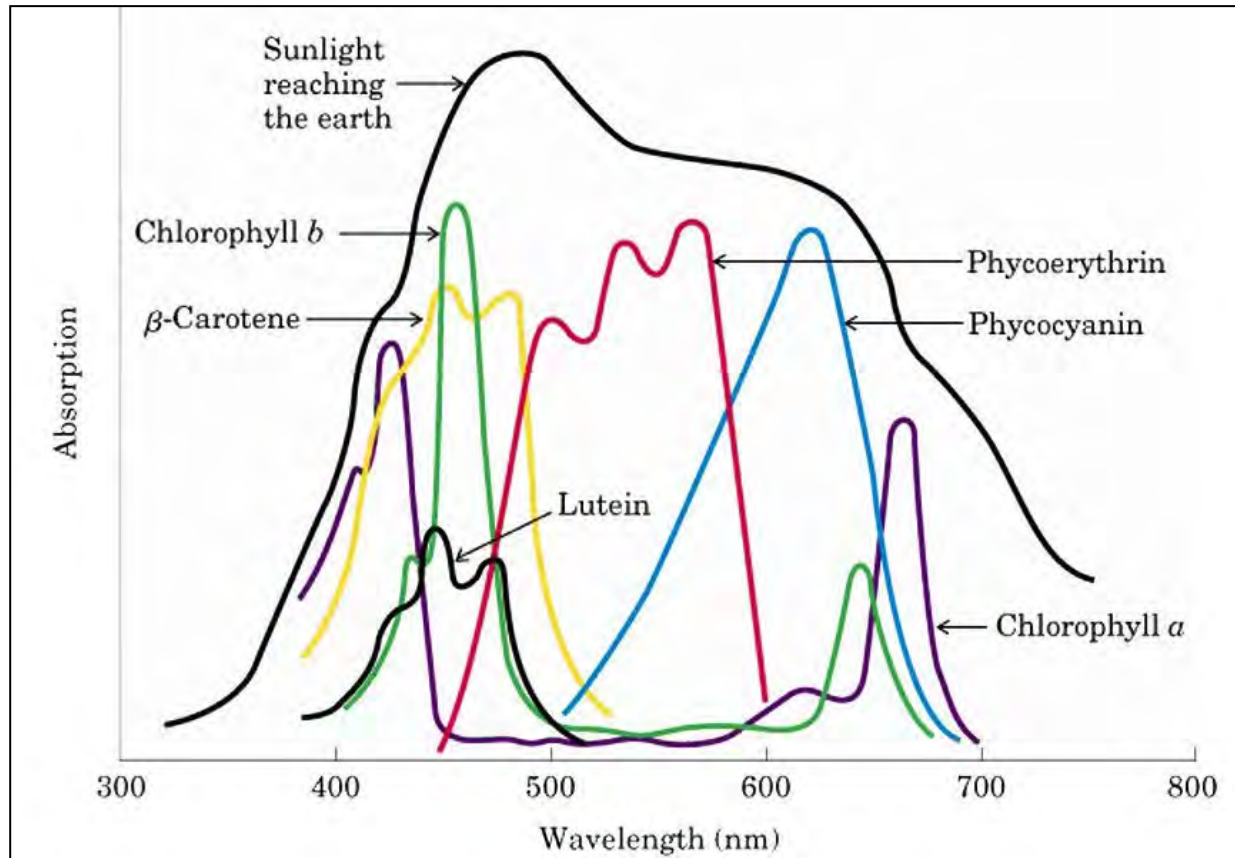
b) **Minerals.**

Spectral analysis: Optical properties of Earth surface elements

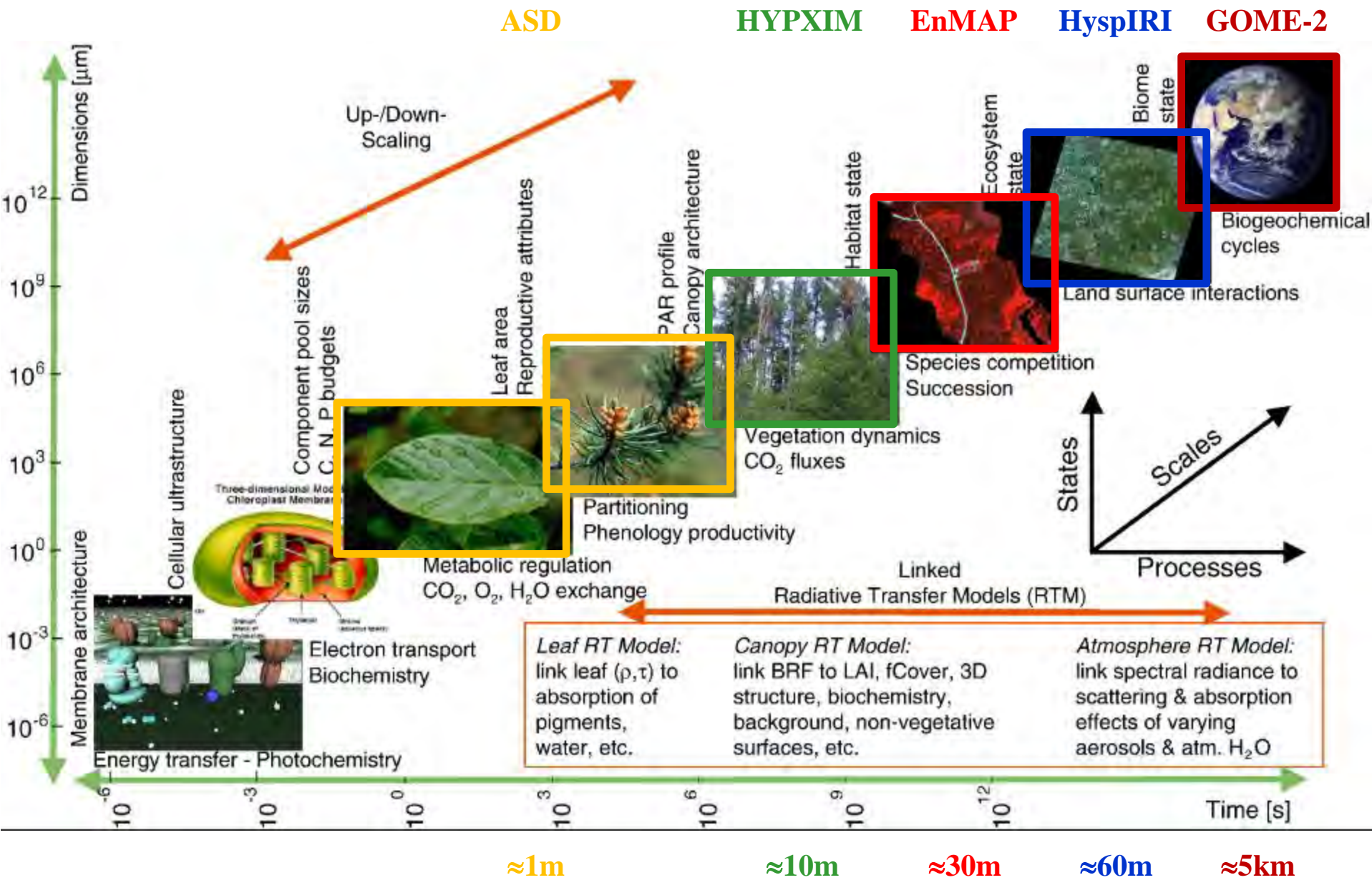
- ☒ Different acquisition configurations:
 - Illumination & view:
 $\rho_{dd}(\lambda), \rho_{hd}(\lambda), \dots$
 - State of material:
 grinded/dried ground, stack of leaves, etc.



Photosynthesis and Fluorescence



Absorption spectra of foliar pigments



Hyspiri (2019?)

- **Imaging Spectrometer (VSWIR)**
 - 380 to 2500nm in ≤ 10 nm bands
 - 60 m spatial sampling*
 - 19 days revisit*
 - Global land and shallow water
- **Thermal Infrared (TIR):**
 - 7 bands in 7.5-12 μ m + 1 band in 3-5 μ m
 - 60 m spatial sampling
 - 5 days revisit; day/night
 - 3-5 μ m band saturates at 1400K
 - 7.5-12 μ m bands saturate at 400K

EnMap (2018?)

Pointing range: 30° from nadir
 IFOV: 7.45" (30m x 30m au nadir);
 FOV: $\pm 1.06^\circ$ (30km)
 Waveband: - VNIR: 420 - 1030 nm (96 bands)
 - SWIR: 950 - 2450 nm (122 bands)
 Spectral sampling : - VNIR: 5 nm to 10 nm
 - SWIR: 10 nm
 Noise equivalent variance (mW/cm²/sr/ μ m):
 420 - 1030nm : 0.005
 900-1760nm: 0.003
 1950-2450nm: 0.001

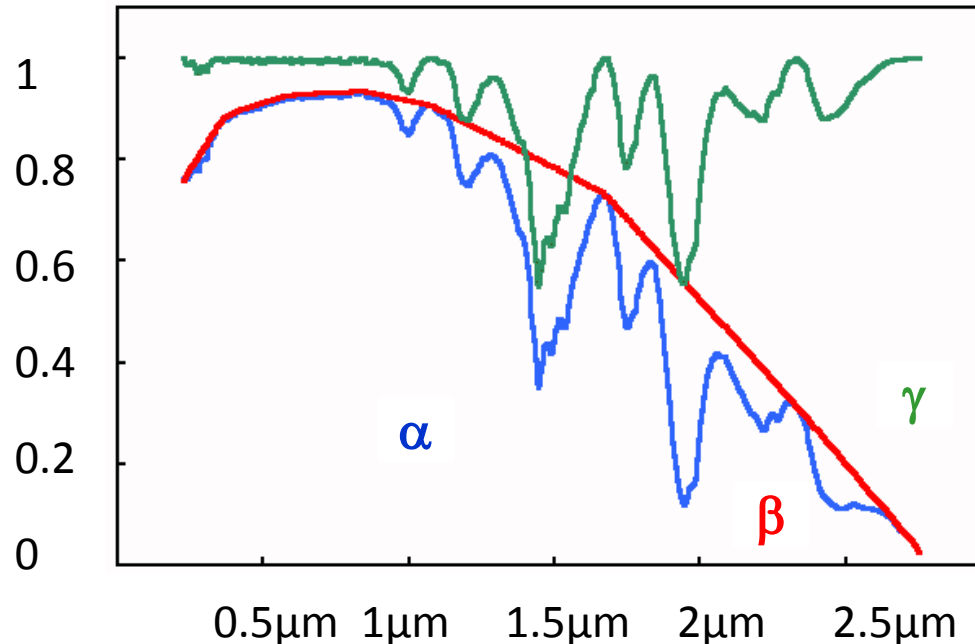
	Domain	Spectral range	Spectral resolution	Pixel size	SNR
HYPXIM (?)	VIS	400nm – 700nm	10nm	8m	≥ 250
	VNIR	700nm – 1100nm	10nm	8m	≥ 200
	SWIR	1100nm – 2500nm	10nm	8m	≥ 100
	PAN	400nm – 800nm	400nm	2m	≥ 90

Hyperspectral analysis: basic continuum removal technique

How to detect the absorption features in an hyperspectral pixel spectrum $\alpha(\lambda)$?

The continuum removal technique breaks down $\alpha(\lambda)$ into smooth spectrum β (continuum: lines joining local reflectance maxima) and narrow band features $\gamma = \alpha - \beta$

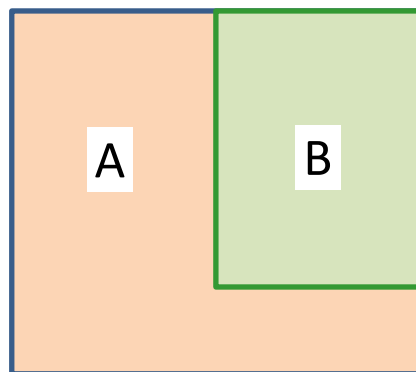
Then, a spectral matching technique can compare $\gamma(\lambda)$ to standard feature spectra.



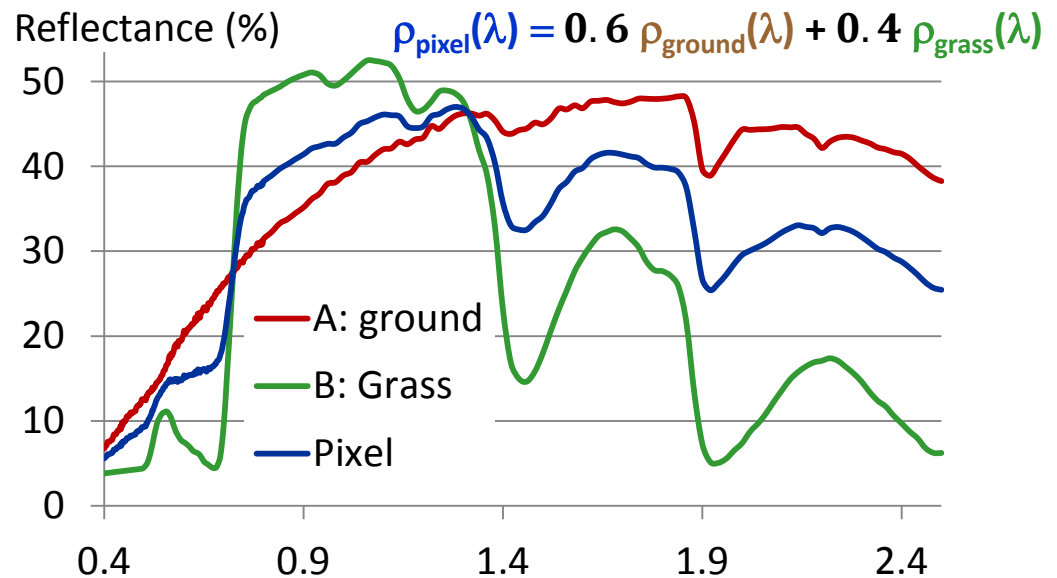
Hyperspectral analysis: basic unmixing approach

A pixel can include several materials (e.g., A, B). Then, it has a mixed spectrum $\rho_p(\lambda)$. An usual objective is to assess the material spectra ($\rho_A(\lambda), \rho_B(\lambda), \dots$) and fractions. Components that correspond to spectra $\rho_A(\lambda), \rho_B(\lambda), \dots$ are called "end members"

The approach is called: "unmixing", possibly linear ($\rho_p(\lambda) = \sum_{i=1}^I a_i \cdot \rho_i(\lambda)$) or not.



Pixel

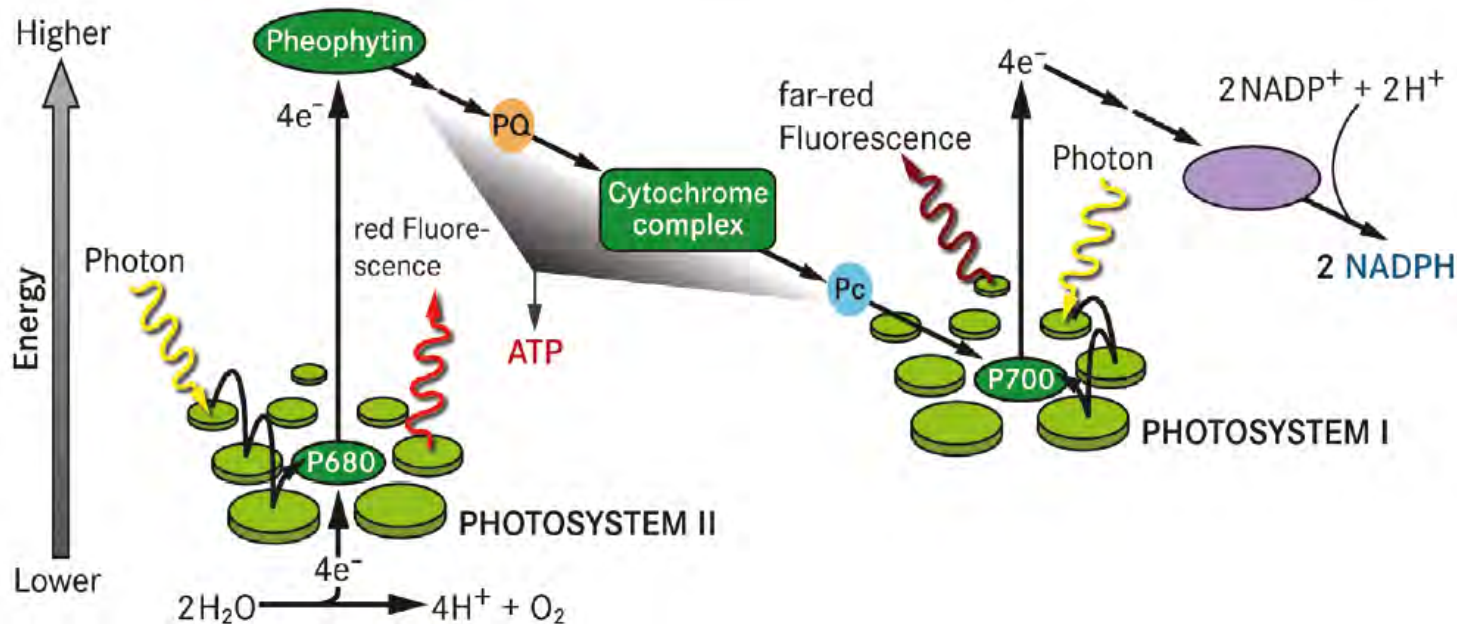


Photosynthesis and Fluorescence

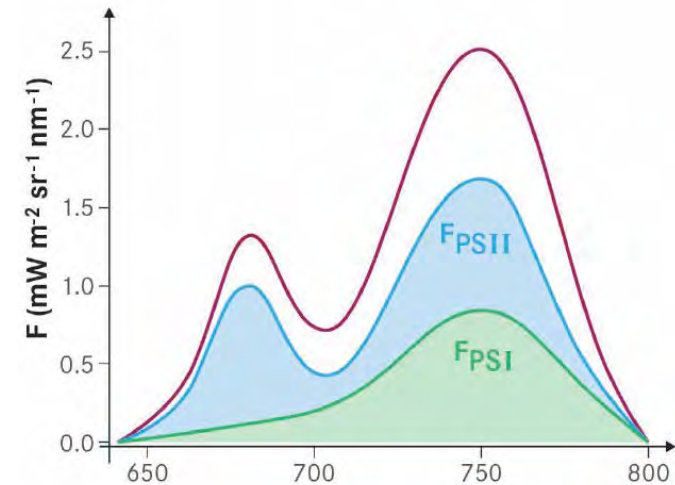
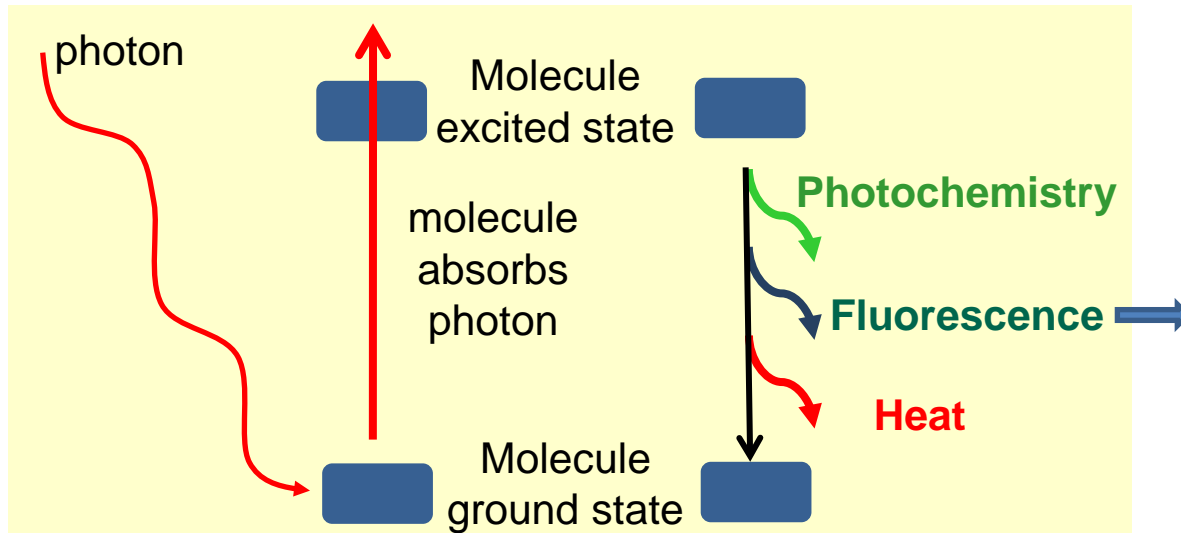
Photosynthesis:

- Plants use sunlight, water, nutrients and CO_2 to produce energy-rich biomolecules
- The mechanism for plant growth / productivity, and, thus, energy / mass exchange.
- Light is absorbed by plant photosynthetic pigments (Chl, Ca) in photosystems I & II
- The efficiency ($\approx 3\text{-}6\%$) with which absorbed light is converted into biochemical energy and energy-rich carbohydrates is an indicator of the plant functional status.
- Water deficit, temperature,... perturb the operation of the 2 photosystems.

CHEMICAL ENERGY + CARBON DIOXIDE = SUGAR

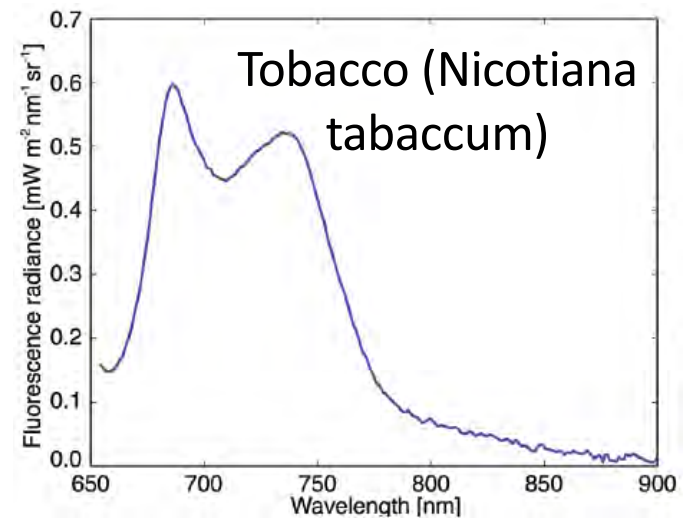
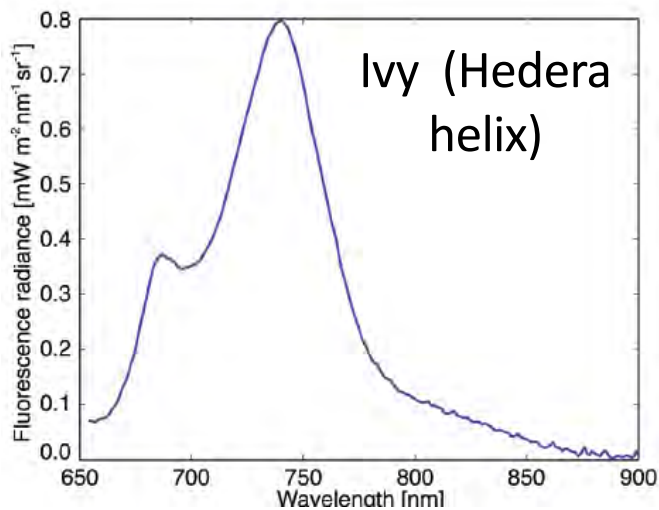


Photosynthesis and Fluorescence



Non photochemical energy is dissipated by heat transfer and fluorescence. It depends on plant stress.

Theoretical fluorescence of photosystems I and II.



Measured fluorescence of 2 vegetation covers. Valencia University.

Photosynthesis and Fluorescence

Under optimal conditions, $\approx 86\%$ of absorbed radiation is used for carbon assimilation (photochemistry). Remaining energy is lost as heat and dissipated as fluorescence.

Energy dissipation with fluorescence is directly related to plant stress

⇒ Fluorescence = indicator of plant health

⇒ Valuable tool for surveying / managing vegetation (crops, etc.).

⇒ Next FLEX satellite mission of ESA

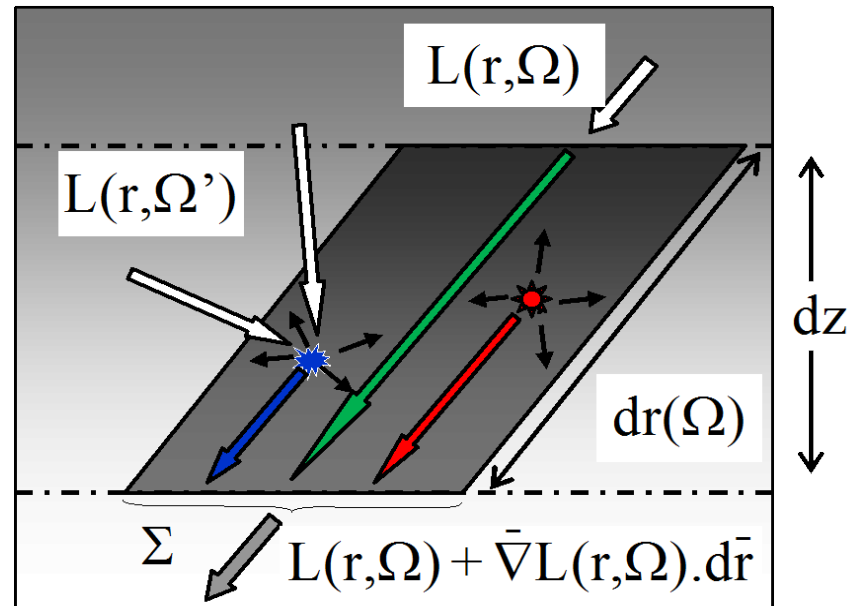
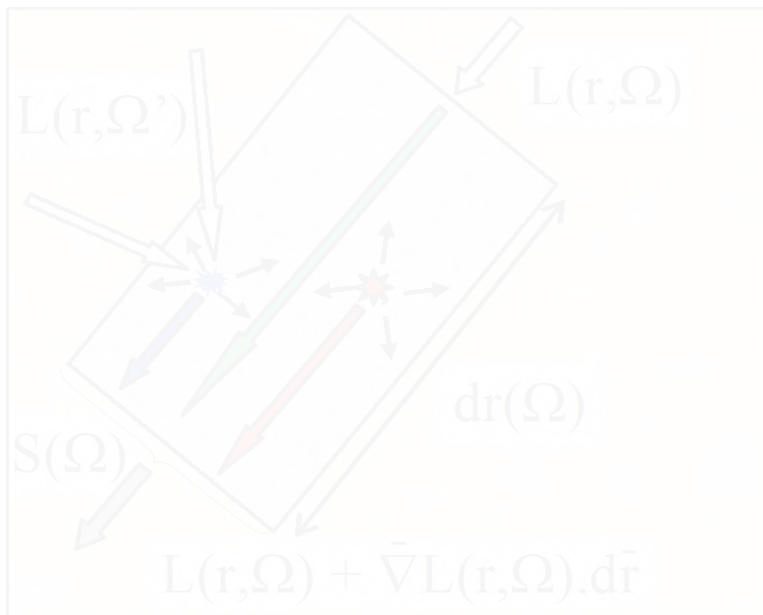
Canopy fluorescence differs from leaf fluorescence

⇒ Need of RS model to simulate "leaf fluorescence" + "vegetation 3D architecture"

RS signal = Fluorescence signal + Sun reflected radiation.

In order to assess fluorescence, one considers the ratio of narrow spectral bands inside and on the edge of very narrow absorption bands of the atmosphere (O_2 -A: 760nm, O_2 -B: 688.4nm,...) or of the sun corona (Fraunhofer lines).

⇒ Fluorescence detection requires hyperspectral sensors.

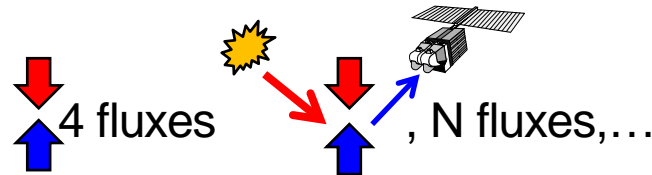


Classical equation to track radiation in 3D media: the Radiative Transfer Equation (RTE)

$$\bar{\Omega} \cdot \bar{\nabla} L(r, \Omega) = -\alpha(r, \Omega) \cdot L(r, \Omega) + \int_{4\pi} L(r, \Omega') \cdot \alpha_d(r, \Omega' \rightarrow \Omega) \cdot d\Omega' + \xi_{emis}(r, \Omega)$$

3D media: no analytic solution of RTE \Rightarrow **Numeric solution**

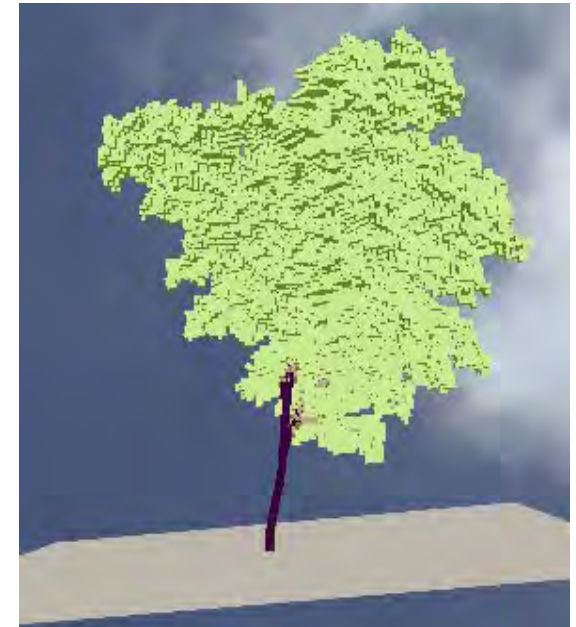
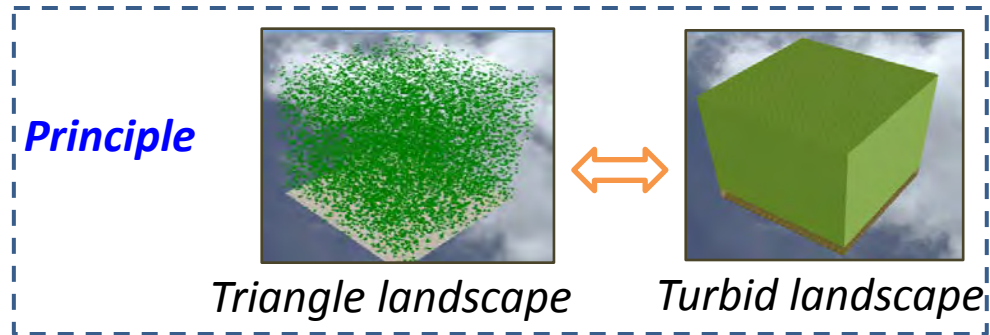
\Rightarrow **Simplified implementation of RTE: 2 fluxes**



\Rightarrow **Simplified landscape simulation: horizontal turbid layer**

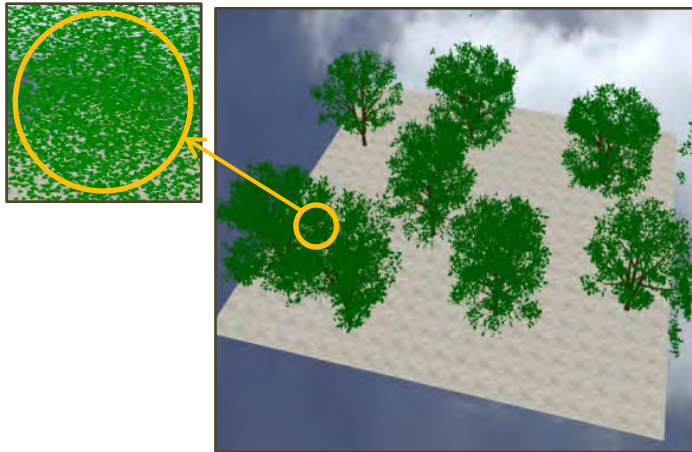


3D objects with many triangles are unmanageable \Rightarrow Transformation turbid 3D objects

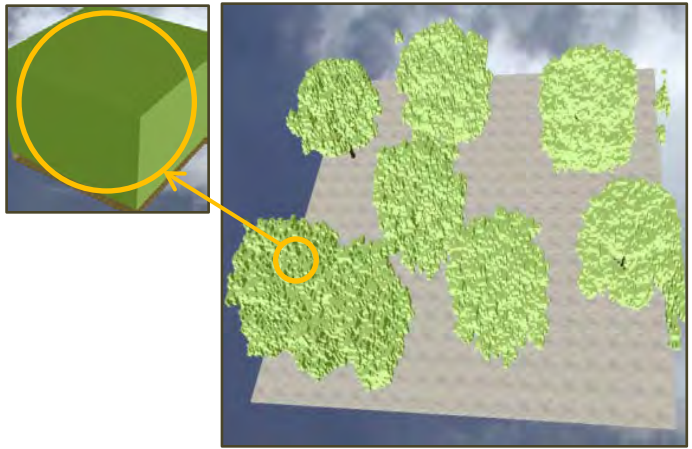


Example: Transformation of a "triangle" tree (left) into a "turbid" tree with 2 spatial resolutions: $\Delta x = \Delta y = \Delta z = 0.5\text{m}$ (center) and $\Delta x = \Delta y = \Delta z = 0.05\text{m}$ (right)

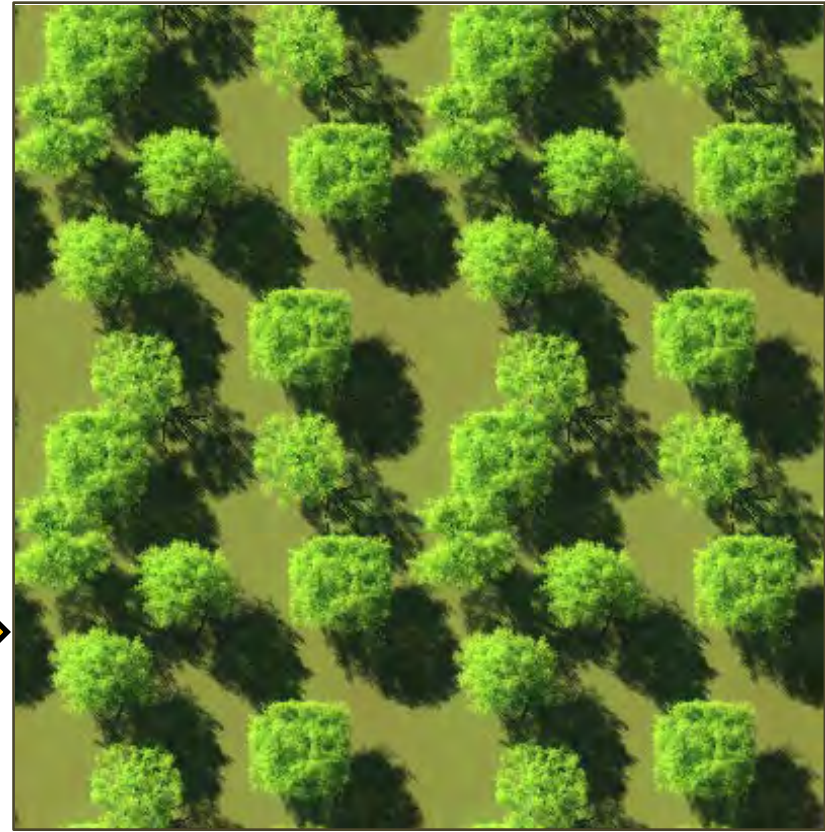
Dual approach (turbid + "triangle") for simulating Earth surface elements



Triangle trees

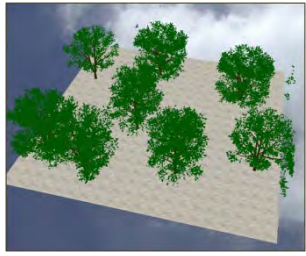


Turbid trees



DART RGB color composite (turbid trees)

Turbid trees derived from triangle trees can give realistic images



Triangles trees



Turbid trees from triangle trees ($\Delta r = 0.125m$)

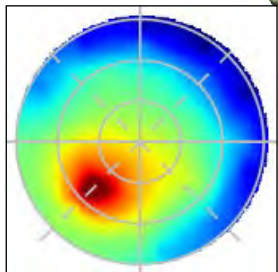
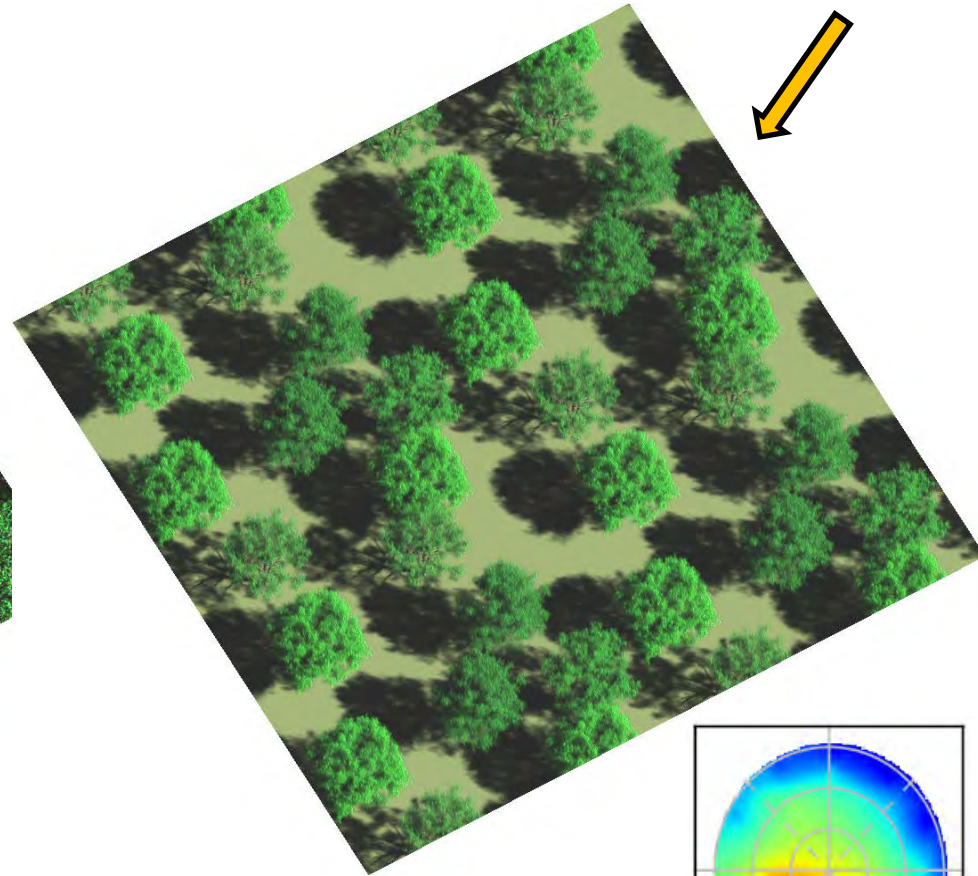
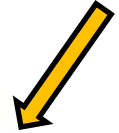
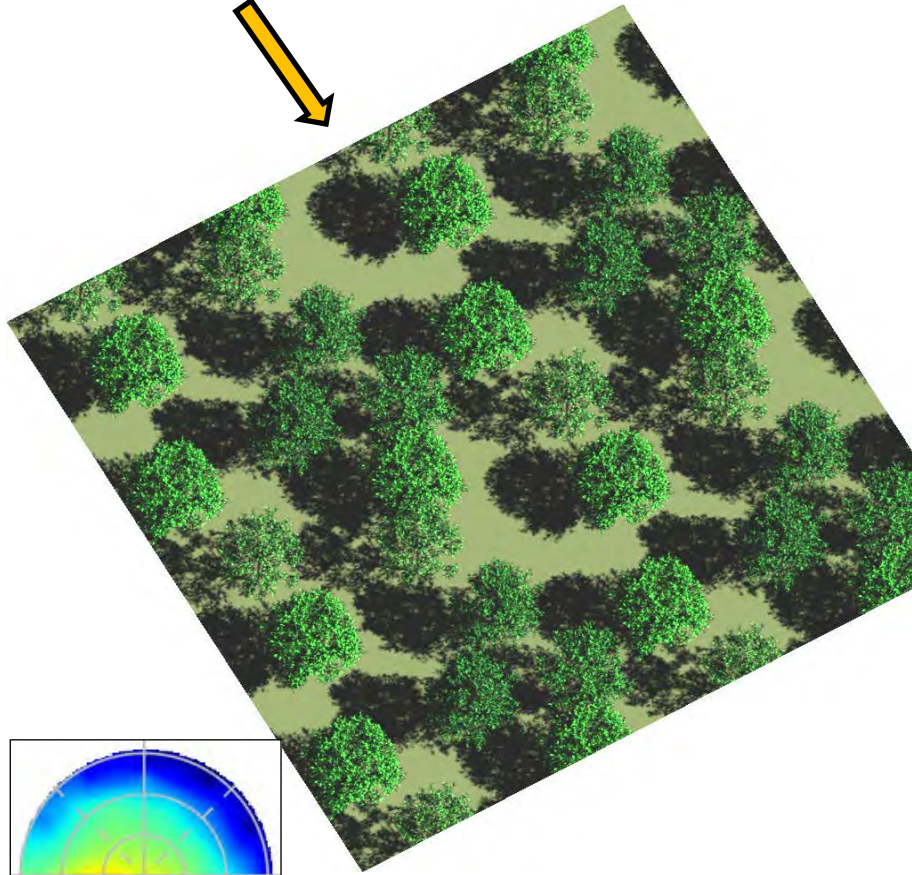
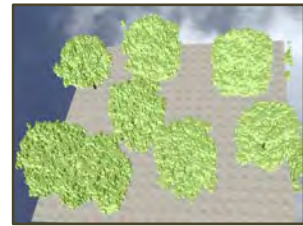
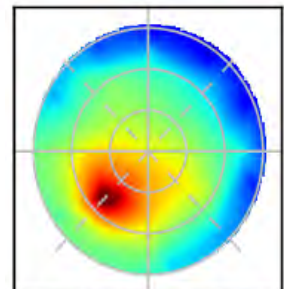
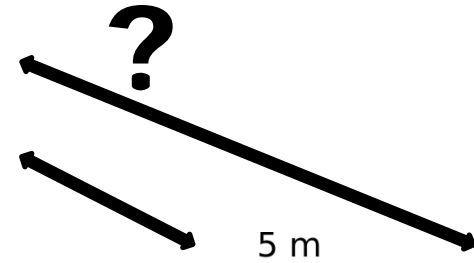
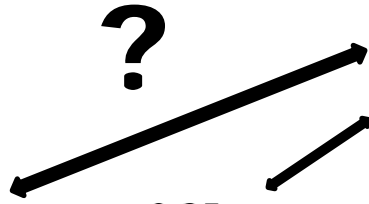
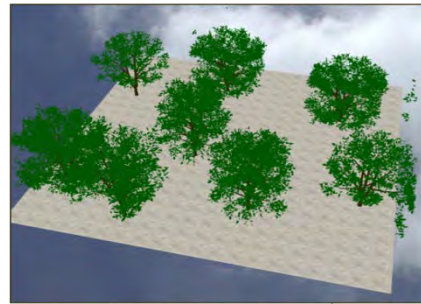


Image with turbid trees can be very similar to images with triangle trees



RMSE = 0.00225

DART presentation: *To simulate a landscape with which spatial resolution?*



0.125 m

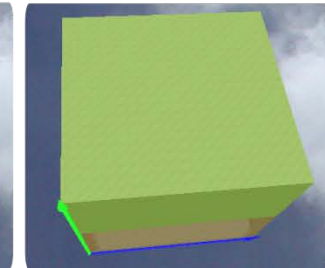
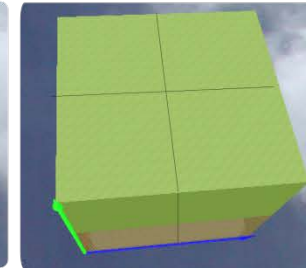
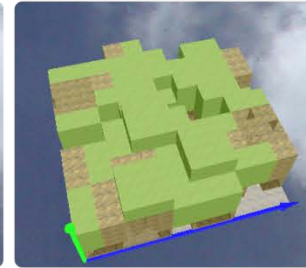
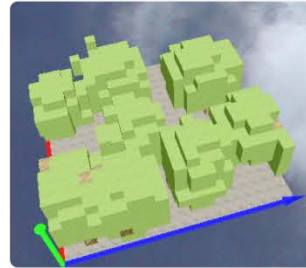
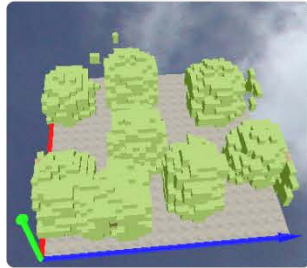
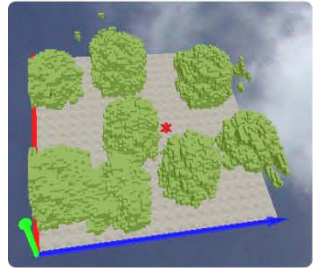
0.25 m

0.5 m

1 m

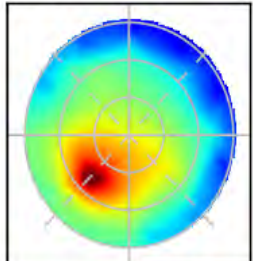
5 m

10 m



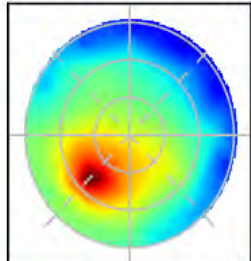
2D plots of directional reflectance

Turbide : $\Delta X = 0.125$



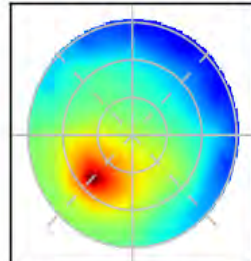
RMSE = 0.00225

Turbide : $\Delta X = 0.25$



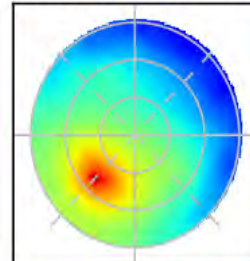
RMSE = 0.00207

Turbide : $\Delta X = 0.5$



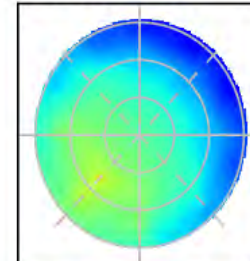
RMSE = 0.00304

Turbide : $\Delta X = 1$



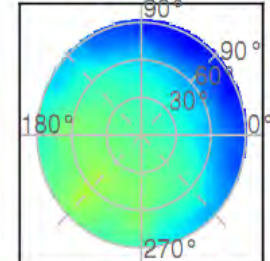
RMSE = 0.00519

Turbide : $\Delta X = 5$



RMSE = 0.01189

Turbide : $\Delta X = 10$



RMSE = 0.01267



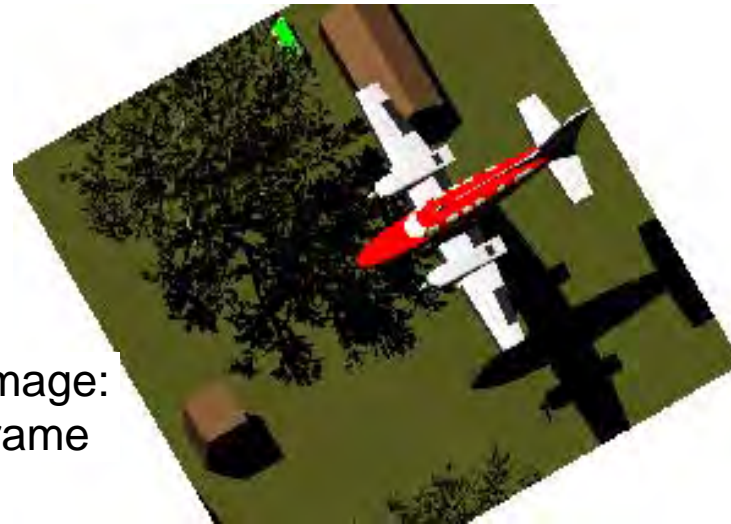
Simulation of scenes: **Example of DART images (scene = simulated + imported objects)**



DART Earth scene:
tree, car, plane, house



Oblique image:
sensor frame



Ortho-image

Nadir image ↓



$L_{x,y,ortho}=0$: unseen
for oblique direction

Simulating images of radiometers with finite FOV (perspective projection)

Diagram illustrating the geometry for a sensor at infinite distance. The tree is shown with its crown and trunk. The solar direction (red arrows) and view direction (blue arrows) are indicated. The projection image plane is shown as a horizontal plane. The resulting image shows the crown and shadow as parallel projections, where the crown projection and shadow projection are equal in size.

Sensor at infinite distance:
parallel projection $\Rightarrow \Phi_{\text{crown}} = \Phi_{\text{shadow}}$

Diagram illustrating the geometry for a sensor at a finite distance. The tree is shown with its crown and trunk. The solar direction (red arrows) and sensor orientation (magenta arrow) are indicated. The projection image plane is shown as a horizontal plane. The resulting image shows the crown and shadow as perspective projections, where the crown projection is larger than the shadow projection.

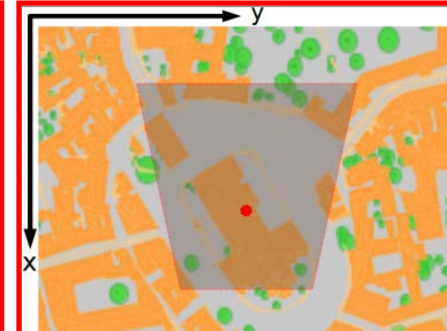
Camera: perspective proj $\Rightarrow \Phi_{\text{crown}} > \Phi_{\text{shadow}}$

Pushbroom/scanner: parallel + perspective projection

Flight track

Example of geometric distortion: Basilica St-Sernin (Toulouse, France)

Identical objects in a simulated landscape appear differently, depending on view configuration (distance, view angle)



Toulouse urban data base - DART scene

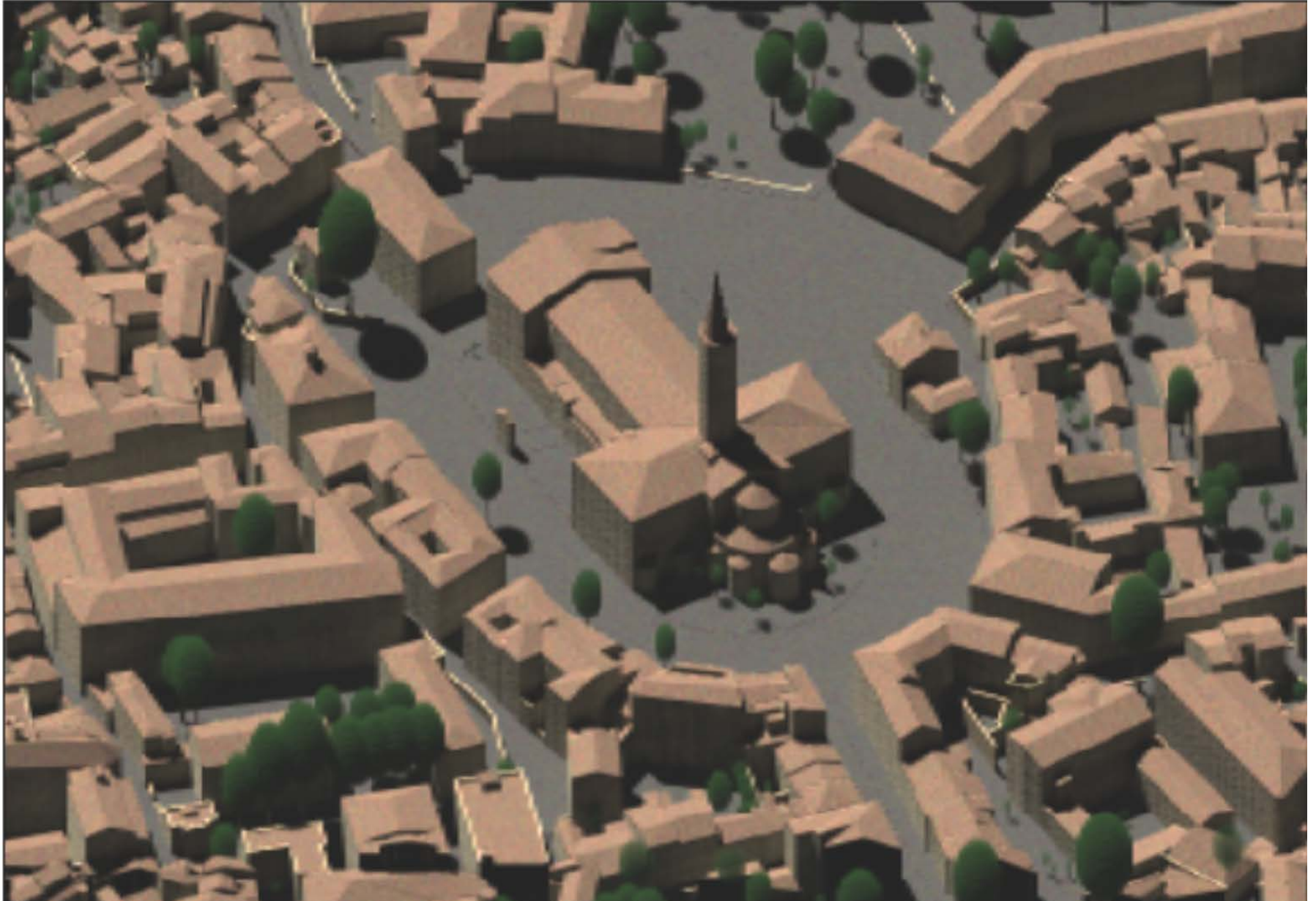


DART simulated images

Parallel projection (satellite, $\theta_v=50^\circ$, $\phi_v=0^\circ$)

Perspective projection (UAV camera, $z_s=140\text{m}$)

*The DART model: **dual approach (turbid + "triangle")** for simulating Earth surface elements*



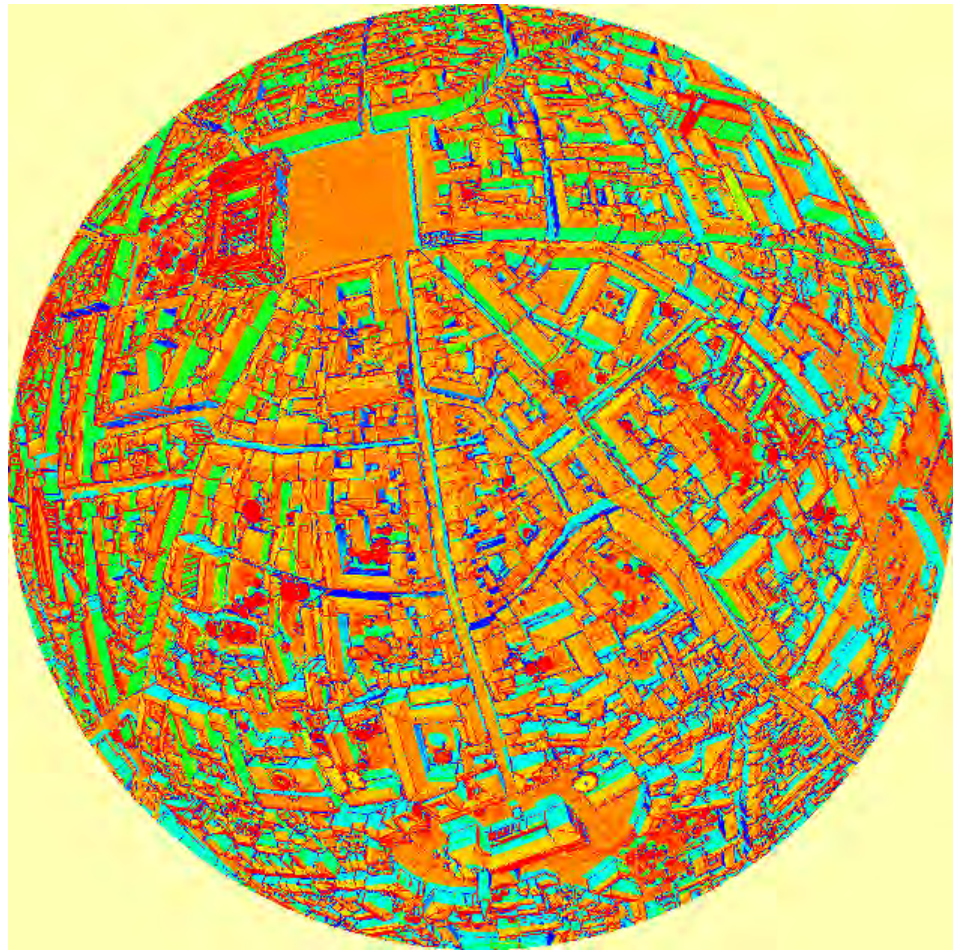
Oblique image of St Sernin district, Toulouse, France (RGB color

Radiance variability due to geometry: fish eye camera VIS/TIR images (Toulouse)

Why does radiance change with view direction in the VIS/NIR? In the TIR?



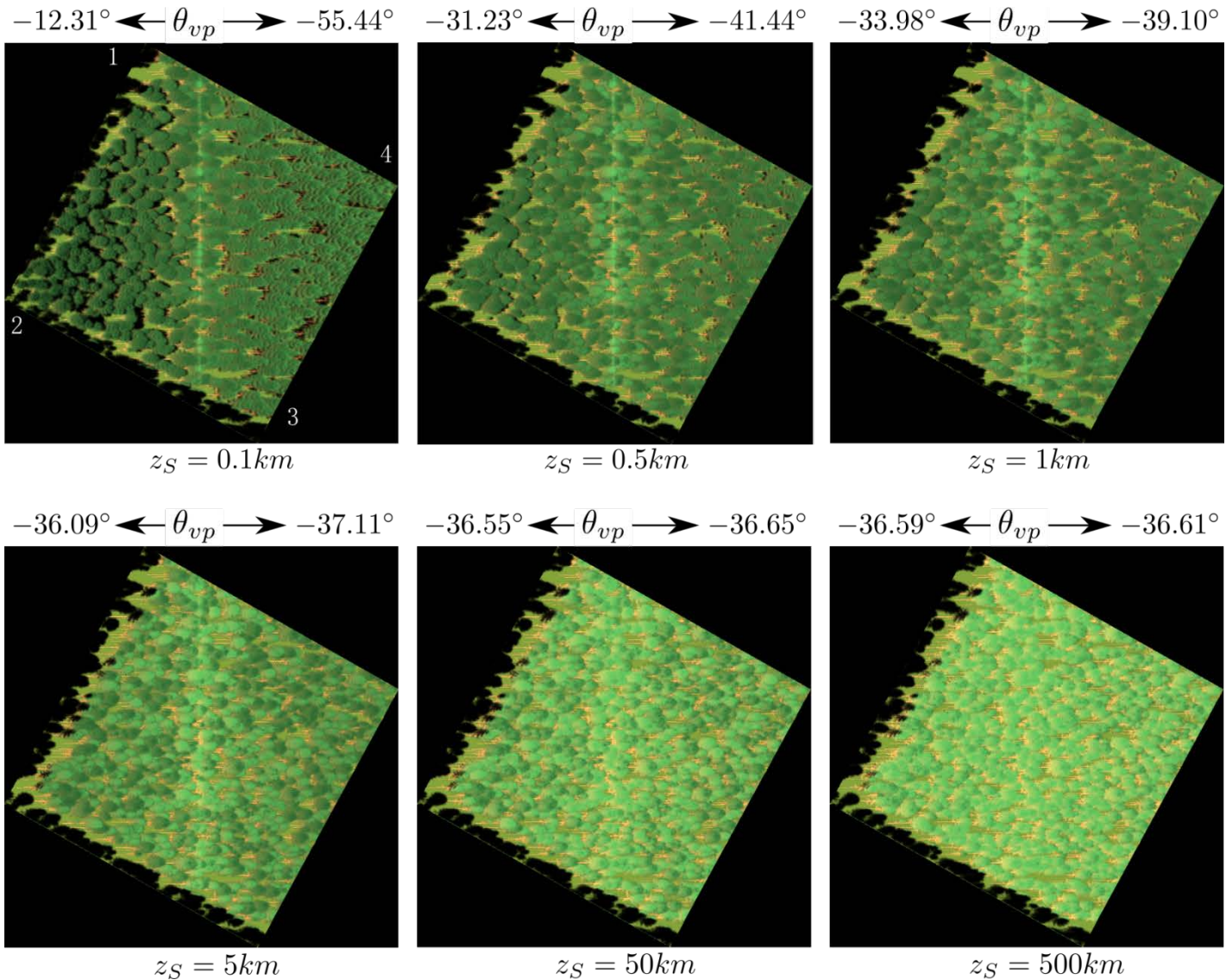
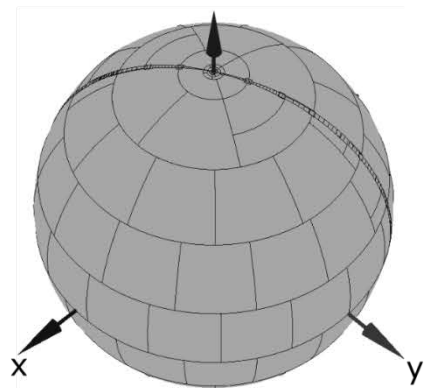
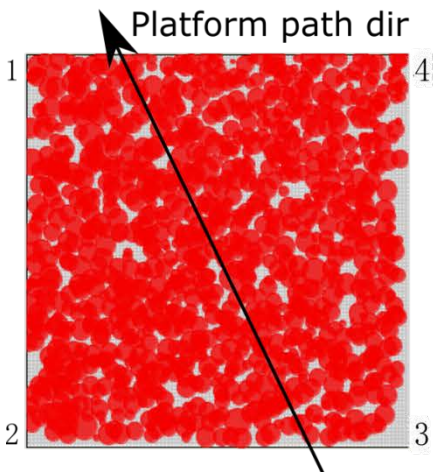
RGB color composite



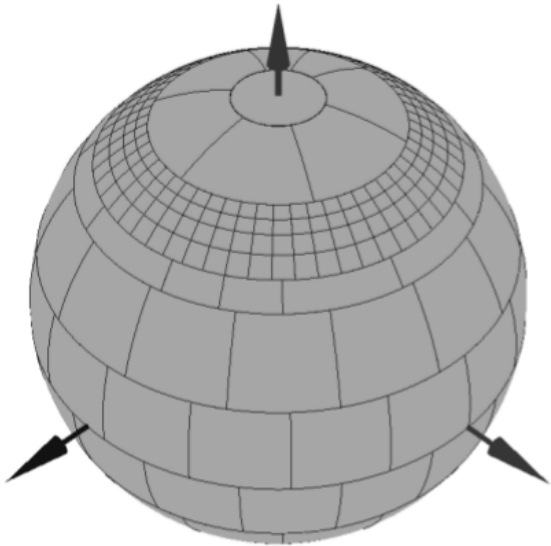
- Thermal infrared camera image
(DART simulated images)

Pushbroom hot spot effect at different altitudes

Sun direction:
 $\theta_s = 36.6^\circ$, $\phi_s = 299.06^\circ$



Direction oversampling
within camera FOV



Identical objects (trees,...)
appear with different
radiance values due to
sensor FOV (angular effects)

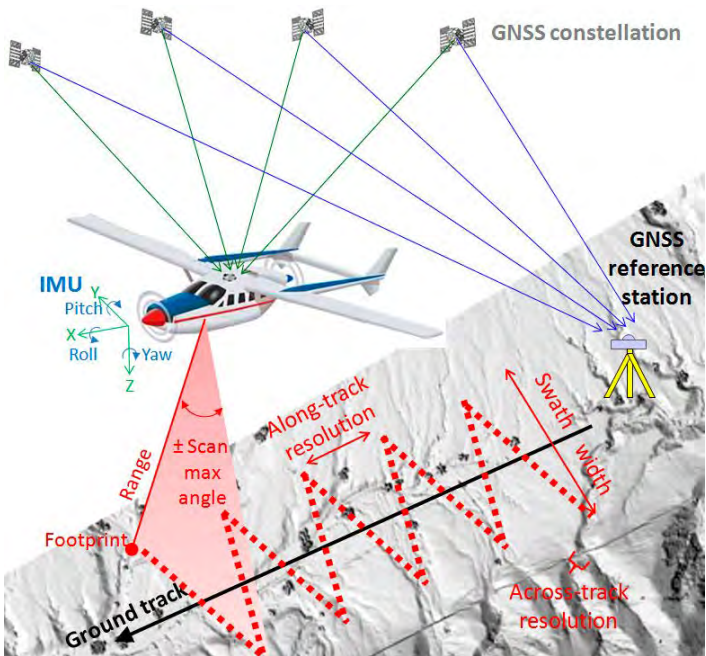
UAV camera ($\theta_v = 50^\circ$, $z_s = 140m$)



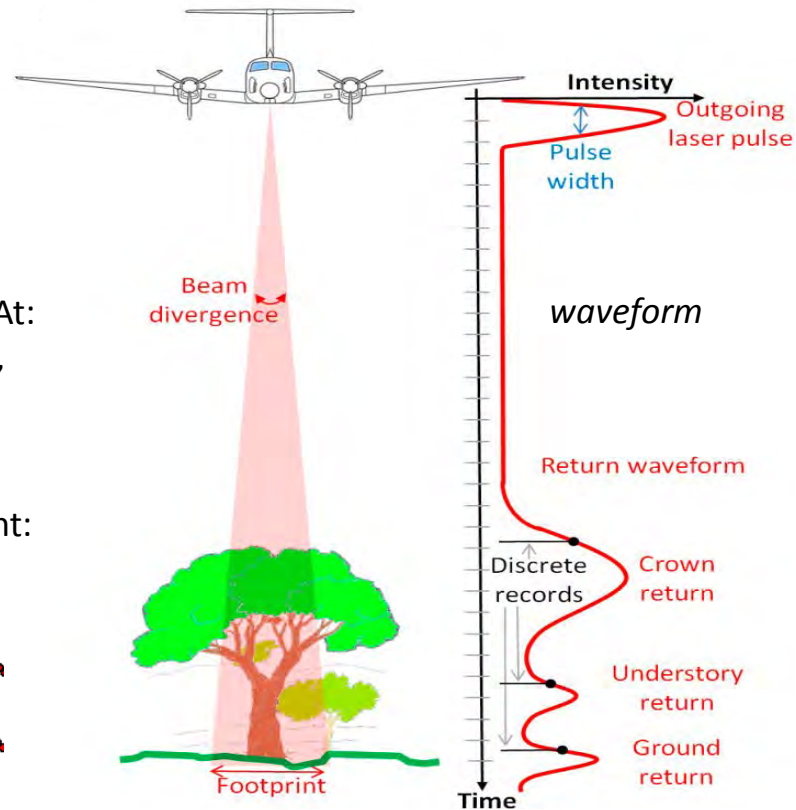
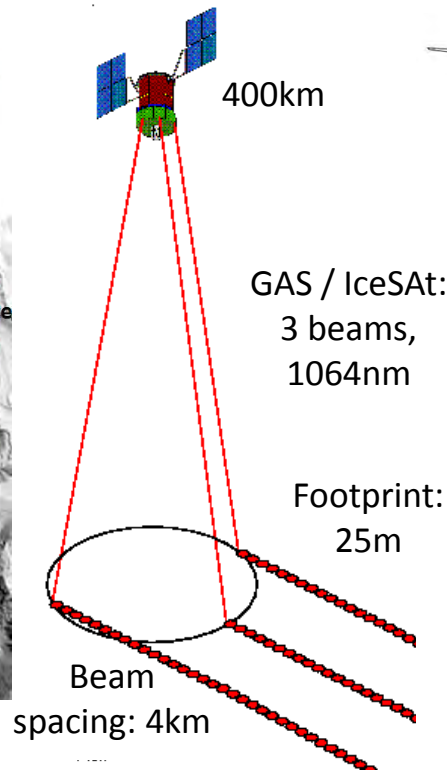
Light Detection And Ranging (LiDAR)

LiDAR emits laser pulse, and uses the time-of-flight technique for measuring distance and amplitude of return energy. Satellite, airborne and terrestrial systems

Various types: discrete-return, waveform and photon counting LiDARs.



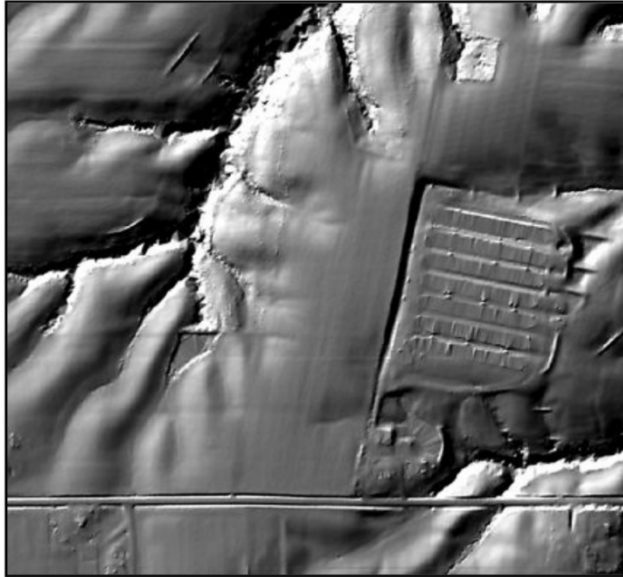
Fernandez-Diaz (Remote Sensing, 2014)



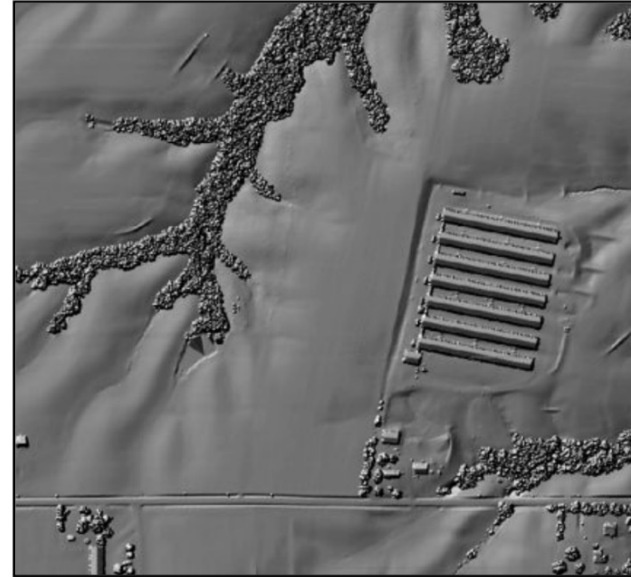
Light Detection And Ranging (LiDAR)

Application: DEM/DSM, vegetation / urban architecture & dimensions, atmosphere,...

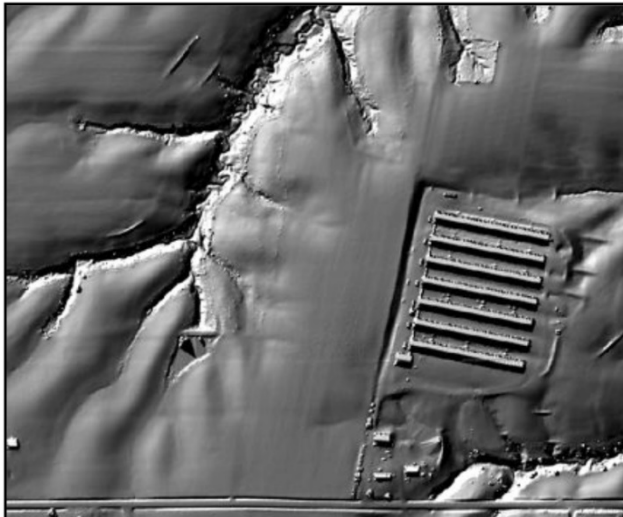
DEM



First return



Last return



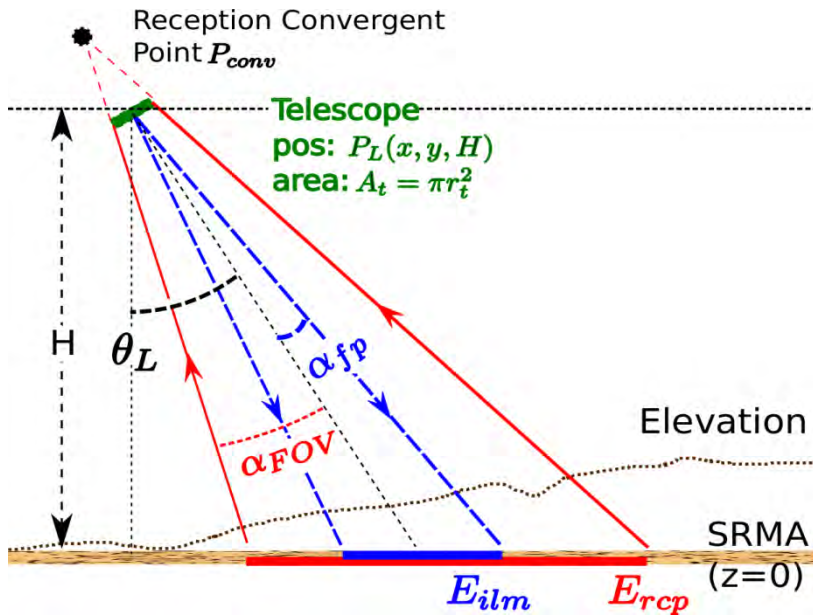
Intensity



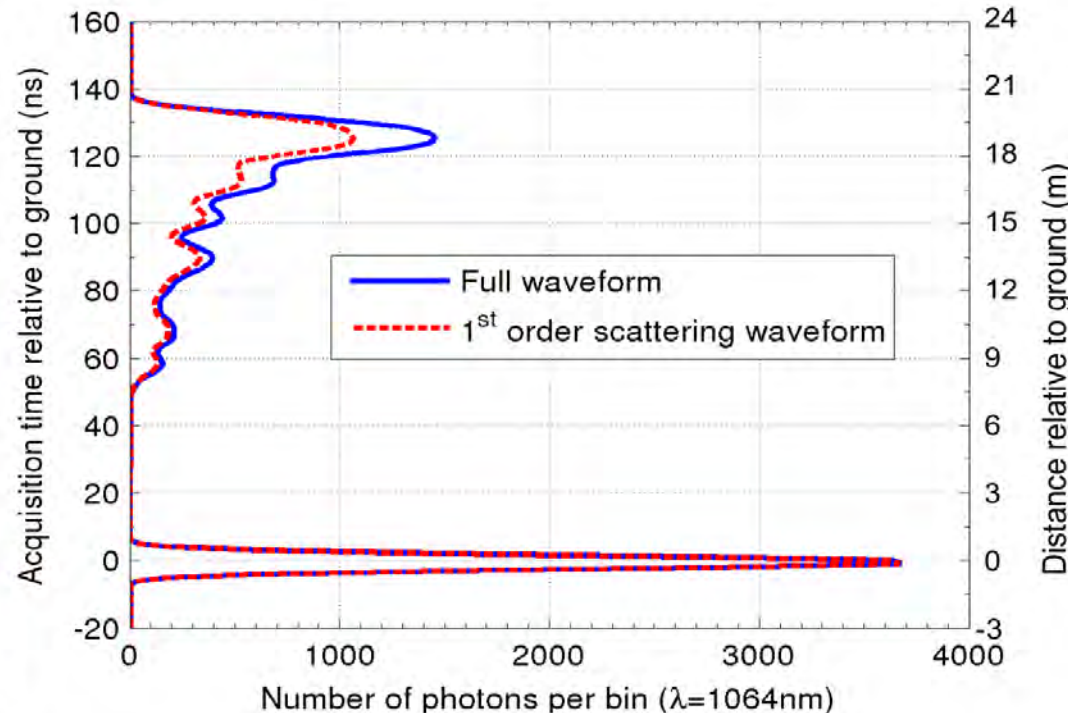
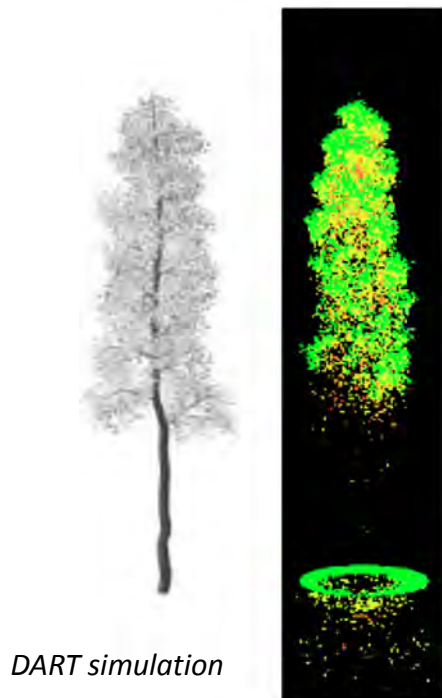
1st order LiDAR models: Geo-optical models with **hot spot** configuration.

Multiple order models: Monte-Carlo ray tracing (Flight, DELiS,...), DART (quasi-MC),...

Small footprint waveform simulation: Linden tree from RAMI-4 ($\lambda = 1064\text{nm}$, $H = 10\text{km}$)

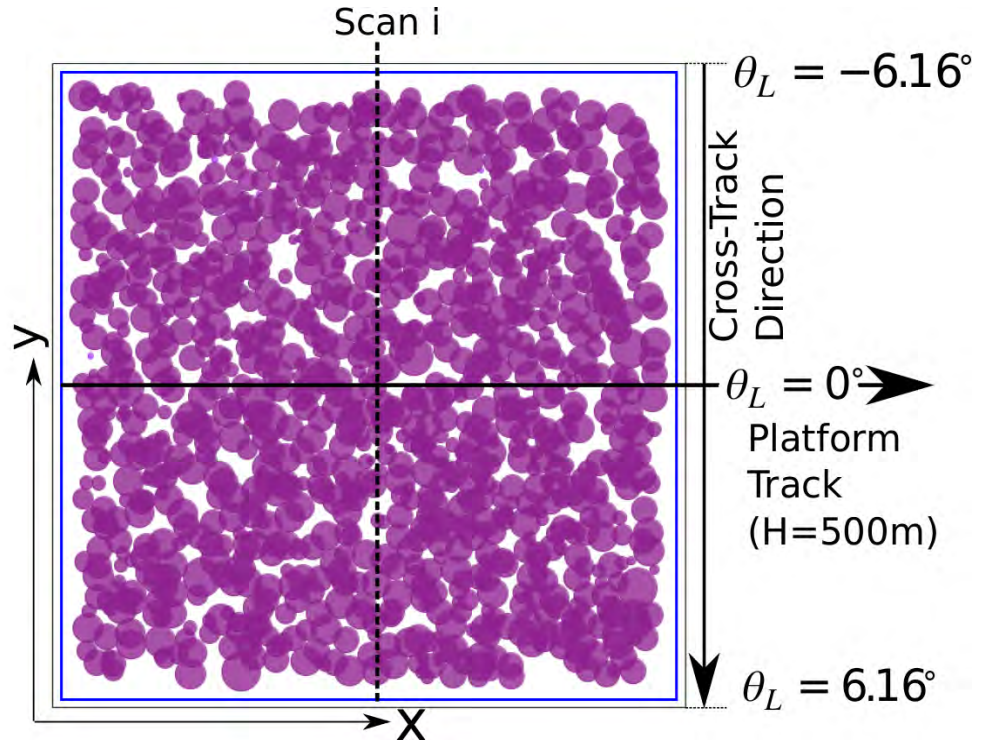


Parameters	Symbols	Values
Sensor area	A_t	0.1m^2
Time step per bin	δt_{bin}	1 ns
Footprint divergence half angle	β_{frp}	0.25 mrad
FOV divergence half angle	β_{FOV}	0.4 mrad



ALS simulation: LiDAR of CAO AtoMS system over Järvelja pine stand (RAMI-4)

Parameters	Values
Sensor area	0.1m ²
Wavelength	1064 nm
Pulse energy	1 mJ
Time step per bin	1 ns
Distance step per bin	30 cm
Footprint divergence half angle	0.25 mrad
FOV divergence half angle	0.4 mrad
Pulse Repetition Frequency	400 kHz
Scan frequency	140 Hz
Maximum look angle	32.5 °
Platform speed	49 m/s (95.24 knots)
Along-track distance step per scan	0.35 m
Look angle step per pulse	0.02275 °

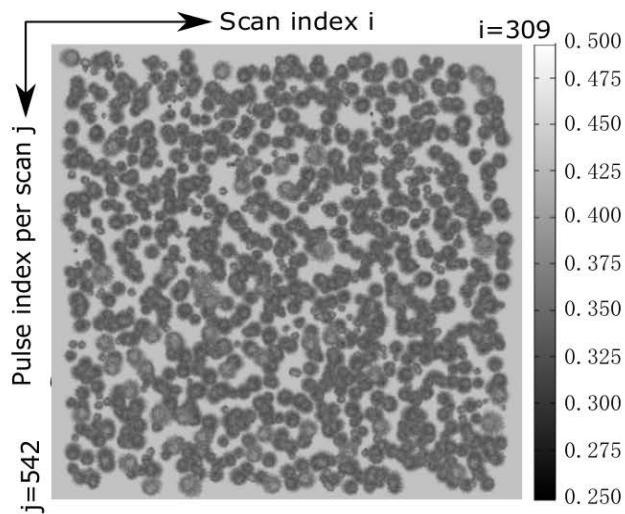


Number of pulses: 167478 (309 scans × 542 pulses per scan)

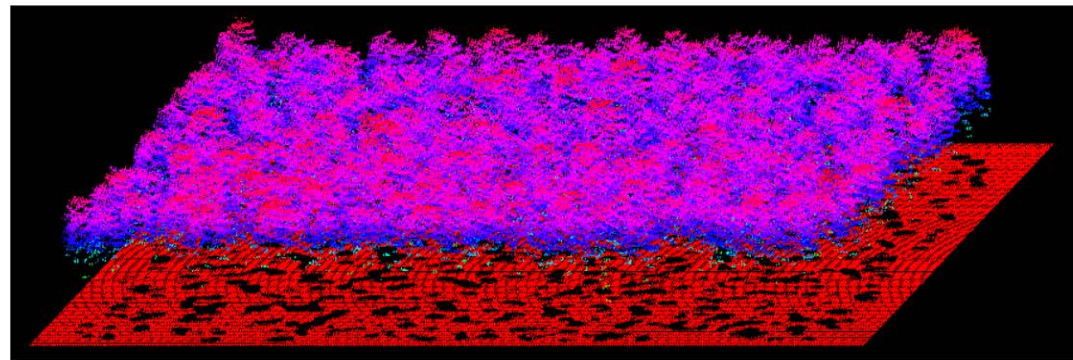
Pulse density: 14.35 /m²

5000 SPs per pulse → 0.78 seconds / pulse / thread ⇒ 110 minutes with 20 threads

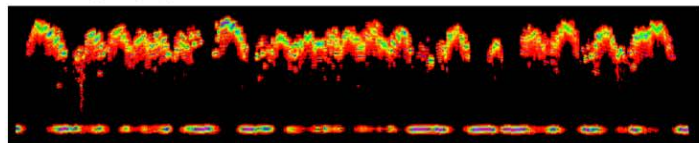
ALS simulation: LiDAR of CAO AtoMS system over Järvelja pine stand (RAMI-4)



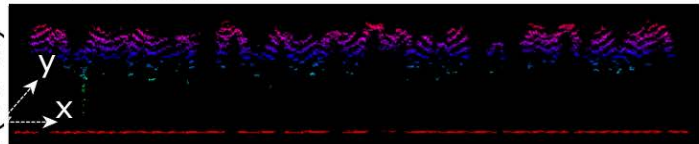
Display of DART simulations with SpDLib code
(color = altitude)



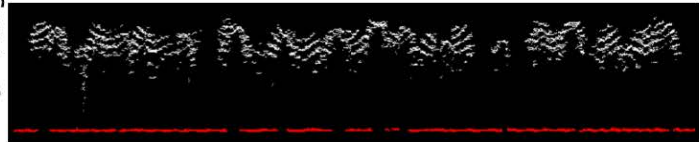
Waveform



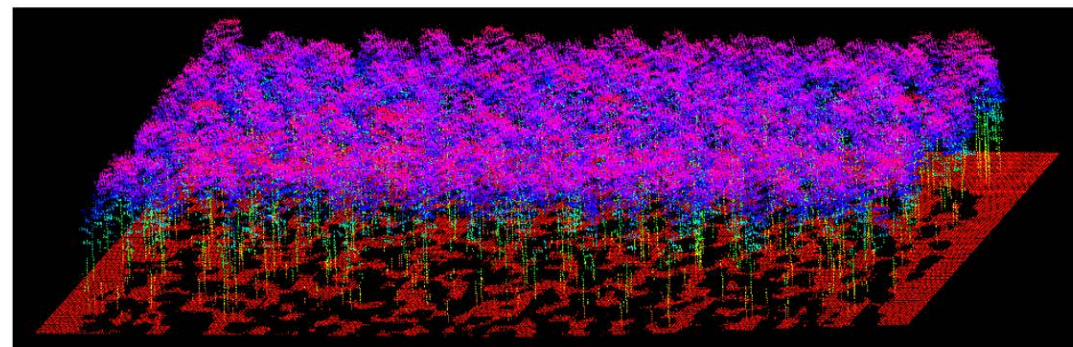
Elevation



Classification



Cross-track direction (-y axis)



$\theta_L = 45^\circ$ at the center of swath

Thank you

Questions?

DART: 3D radiative transfer model

Principles:

- Landscape: - Turbid medium (fluid, veg., atm.) + Facets
 - Repetitive or isolated
 - Imported: BD_{atm} , L.C., 3D objects,...
- Discrete ordinates (space, directions)
- Earth / Atmosphere radiative coupling
- Iterative XS flux tracking (radiometer) or photon (Lidar)
- Parallel / projective projection \Rightarrow camera, pushbroom,...

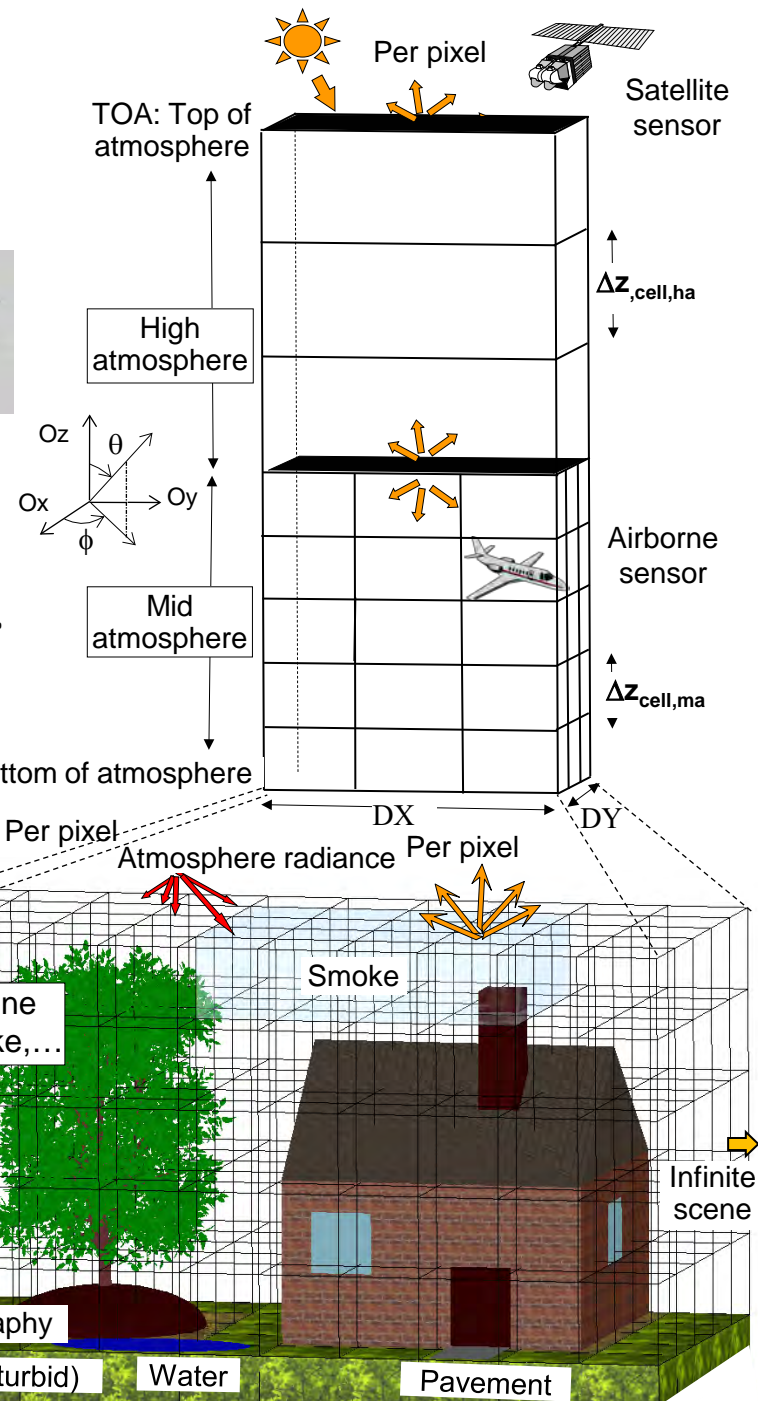


Operating modes

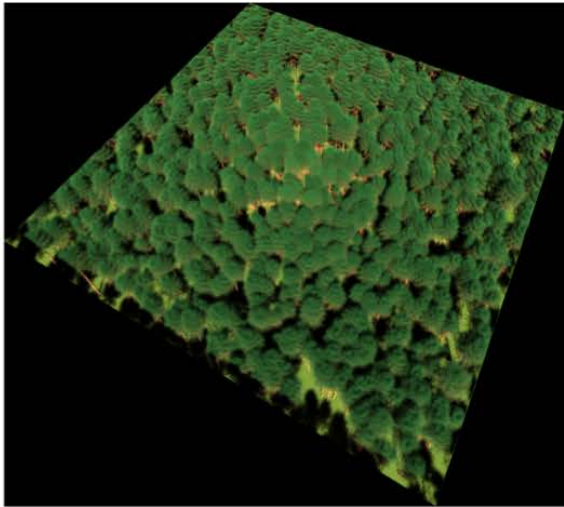
- Reflectance (R), Thermal (T) and (R+T)
- Lidar (RayCarlo: flux tracking + M. C.)
- Sequence of simulations \forall parameter (LAI, Ω_s, \dots)

Products

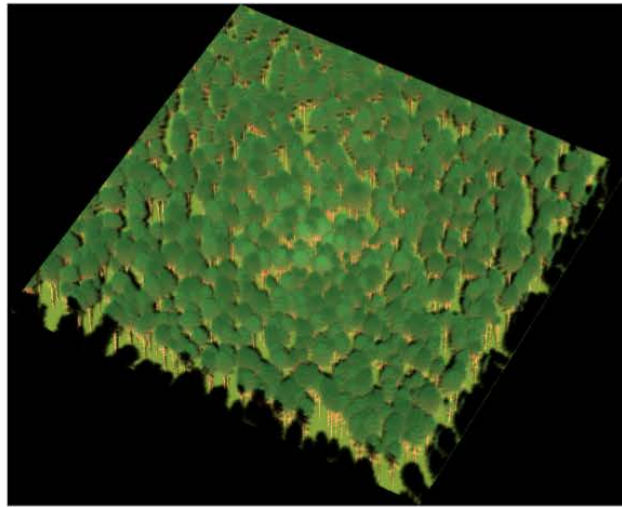
- Images $\rho_\lambda(\Omega_s, \Omega_v)$, $T_B(\Omega_s, \Omega_v)$, $L_\lambda(\Omega_s, \Omega_v) \forall \Omega_s, \Omega_v$
- Lidar waveform and photon counting
- 3D Radiative budget of Earth landscapes
- Atmosphere terms $\rho_{atm, \lambda}$, $T_{B, atm, \lambda}$, $L_{atm, \lambda}$



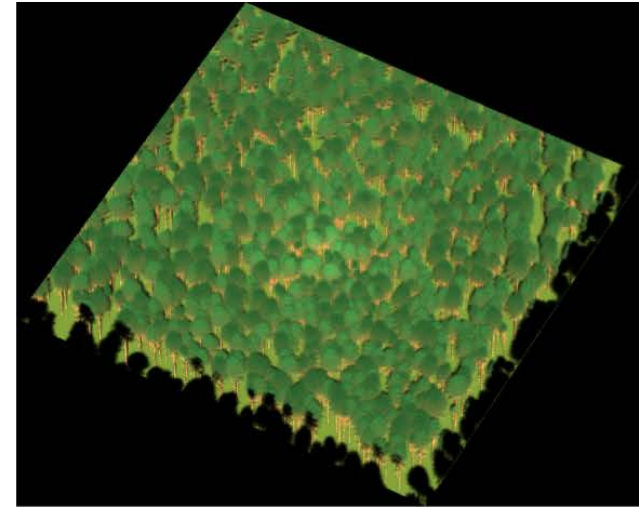
Camera hot spot effect at different altitudes



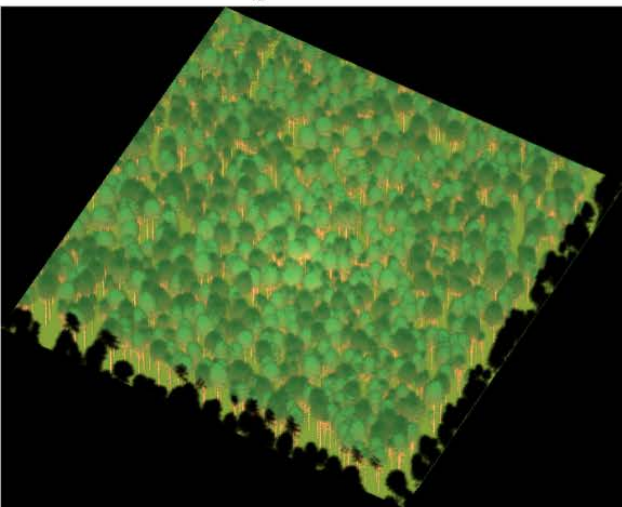
$z_S = 0.1km$



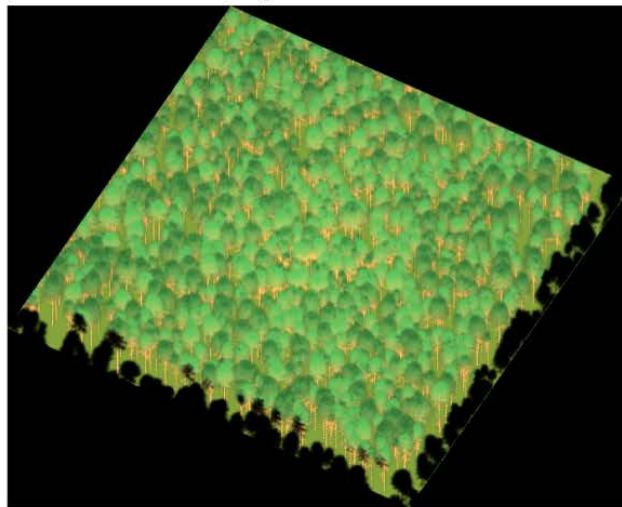
$z_S = 0.5km$



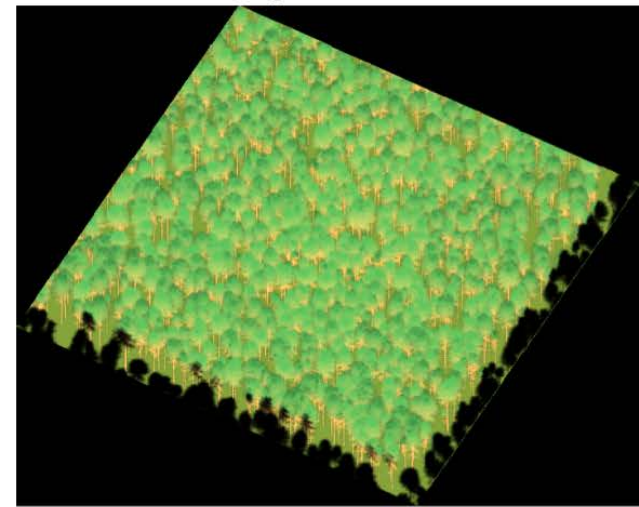
$z_S = 1km$



$z_S = 5km$



$z_S = 50km$



$z_S = 500km$